

2019

Assessment of live load distribution characteristics of press-brake-formed tub girder superstructures

Guilherme Petty
guilhermepetty@aol.com

Follow this and additional works at: <https://mds.marshall.edu/etd>



Part of the [Civil Engineering Commons](#)

Recommended Citation

Petty, Guilherme, "Assessment of live load distribution characteristics of press-brake-formed tub girder superstructures" (2019). *Theses, Dissertations and Capstones*. 1231.
<https://mds.marshall.edu/etd/1231>

This Thesis is brought to you for free and open access by Marshall Digital Scholar. It has been accepted for inclusion in Theses, Dissertations and Capstones by an authorized administrator of Marshall Digital Scholar. For more information, please contact zhangj@marshall.edu, beachgr@marshall.edu.

**ASSESSMENT OF LIVE LOAD DISTRIBUTION CHARACTERISTICS OF
PRESS-BRAKE-FORMED TUB GIRDER SUPERSTRUCTURES**

A thesis submitted to
the Graduate College of
Marshall University
In partial fulfillment of
the requirements for the degree of
Master of Science in Engineering

In
Transportation and Infrastructure Engineering
by

Guilherme de Oliveira Petty Santana

Approved by

Dr. Gregory K. Michaelson, P.E., Committee Chairperson

Dr. James M. Bryce

Dr. Isaac W. Wait, P.E.

Marshall University
May 2019

APPROVAL OF THESIS

We, the faculty supervising the work of Guilherme de Oliveira Petty Santana, affirm that the thesis, Live Load Distribution Factors Assessment of Shallow Press-Brake-Formed Steel Tub Girder Superstructures, meets the high academic standards for original scholarship and creative work established by the Master of Science in Engineering and the College of Information Technology and Engineering. This work also conforms to the editorial standards of our discipline and the Graduate College of Marshall University. With our signatures, we approve the manuscript for publication.



Dr. Gregory K. Michaelson, P.E., Committee Chairperson, Weisberg Division of Engineering
Committee Chairperson

Date 5-Apr-2019



Dr. James M. Bryce, Weisberg Division of Engineering
Committee Member

Date 5-Apr-2019



Dr. Isaac W. Wait, P.E., Weisberg Division of Engineering
Committee Member

5 April 2019

Date

© 2019
Guilherme de Oliveira Petty Santana
ALL RIGHTS RESERVED

ACKNOWLEDGMENTS

Writing a thesis is more challenging than I anticipated and more rewarding than I could have ever imagined. None of this would have been possible without my advisor, Dr. Gregory Michaelson. His encouragement, support and dedication during my time in undergraduate and graduate school are greatly appreciated. His passion for bridge engineering is inspiring, and I'm lucky to have had the opportunity to learn from him.

I would also like to thank Dr. James Bryce and Dr. Isaac Wait for serving as members of my graduate advisory committee, with a special thank you to Dr. James Bryce for taking the time to give feedback on the thesis report and formatting.

In addition, I would like to thank my beautiful wife, Erin, for her endless support and countless sacrifices made during graduate school. From reading early drafts to giving me advice during the writing process, she was as important to this thesis getting done as I was. Thank you so much, dear.

Finally, I would like to acknowledge my family and friends for their support, particularly my grandparents. I cannot express how thankful I am to have such supportive and loving grandparents. I would not be the person I am today if I hadn't had their guidance and support.

TABLE OF CONTENTS

List of Tables	ix
List of Figures	x
Abstract	xiii
Chapter 1: Introduction	1
1.1 Background	1
1.2 Project Scope & Objectives	3
1.3 Organization	4
Chapter 2: Literature Review	5
2.1 Introduction	5
2.2 History of Cold-Bent Steel Girders in Bridge Applications	5
2.2.1 Prefabricated Press-Formed Steel T-Box Girder Bridge System (Taly & Gangarao, 1979)	5
2.2.2 Composite Girders with Cold-Formed Steel U-sections (Nakamura, 2002) ..	6
2.2.3 Folded Plate Girders (Burner 2010 & Glaser 2010)	7
2.2.4 TxDOT Rapid Economical Bridge Replacement (Chandar et al., 2010)	8
2.3 Behavioral Studies on Tub Girders	9
2.3.1 Development and Feasibility Assessment (Michaelson, 2014)	9
2.3.2 Evaluation of Non-Composite Tub Girders (Kelly, 2014)	11
2.3.3 Field Performance Assessment (Gibbs, 2017)	12
2.4 Historical Development of Live Load Distribution Factors	14
2.4.1 General Overview on AASHTO Live Load Distribution Factors	14
2.5.2 Previous Studies on Live Load Distribution Factors	15

2.4.2.1	<i>Girder Spacing</i>	15
2.4.2.2	<i>Girder location</i>	16
2.4.2.3	<i>Span Length</i>	16
2.4.2.4	<i>Girder Stiffness</i>	17
2.4.2.5	<i>Continuity Conditions</i>	18
2.4.2.5	<i>Deck Thickness</i>	19
2.4.2.6	<i>Skew</i>	19
2.5	AASHTO Live Load Distribution Factors (LLDFs) for Box Girders	20
2.5.1	<i>AASHTO Empirical Approach</i>	20
2.5.2	<i>AASHTO Refined Analysis</i>	26
2.6	Conclusion	26
Chapter 3:	Finite Element Modeling Techniques	27
3.1	Introduction.....	27
3.2	Element Selection Criteria	27
3.3	Material Properties.....	28
3.4	Mesh Discretization	29
3.5	Boundary Conditions	31
3.6	Multi-Point Constraints.....	31
3.7	Load Applications.....	31
3.7.1	<i>Dead Load Applications</i>	31
3.7.2	<i>Live Load Applications</i>	32
3.9	Conclusion	33
Chapter 4:	Benchmark Experimental Study	34

4.1 Introduction.....	34
4.2 Bridge Description	34
4.3 Experimental Testing Equipment	34
4.3.1 STS-Wi-Fi Data Acquisition System	34
4.3.2 BDI Strain Transducers	36
4.3.3 Truck Specification	36
4.4 Experimental Testing Procedures	37
4.5 Data Validation	40
4.5.1 Computation of Bending Stresses at Midspan	40
4.5.2 Computation of Empirical Live Load Distribution Factors (LLDFs)	41
4.5.3 Computation of AASHTO Live Load Distribution Factors.....	43
4.5.4 Comparison of Results	44
4.6 Conclusion	52
Chapter 5: Parametric Assessment of Live Load Distribution Factors.....	53
5.1 Introduction.....	53
5.2 Description of Parametric Matrix	53
5.2.1 Girder Spacing (S) & Span Length (L) Assessment.....	54
5.2.2 Number of Girders (N_b) Assessment	55
5.3 Effect of Girder spacing (S) & Span length (L).....	55
5.4 Effect of N_b	60
5.5 Conclusion	63
Chapter 6: Summary & Concluding Remarks	65
6.1 Project Summary and Conclusions	65

6.2 Recommendations for Continued Research.....	66
References.....	67
Appendix A: Approval Letter	70
Appendix B: Results of Benchmark Analysis	71
Appendix C: Results of Parametric Assessments	108

LIST OF TABLES

Table 1: AASHTO LRDF Table 4.6.2.2.2b-1 - Distribution of Live Loads Per Lane for Moment in Interior Beams.....	21
Table 2: AASHTO LRDF Table 4.6.2.2.2b-1 - Distribution of Live Loads Per Lane for Moment in Interior Beams (Continued)	22
Table 3: AASHTO LRDF Table 4.6.2.2.2b-1 - Distribution of Live Loads Per Lane for Moment in Exterior Beams	23
Table 4: AASHTO LRDF Table 3.6.1.1.2-1 Multiple Presence Factors, m.....	25
Table 5: Finite Element Analysis Bottom Flange Bending Stress.....	45
Table 6: Gibbs, 2017 Experimental Bottom Flange Bending Stress	45
Table 7: FEA LLDFs vs Experimental LLDFs vs AASHTO LLDFs Comparison for Truck Run 3	51
Table 8: Parametric Matrix for Girder Spacing (S) Assessment	54
Table 9: Parametric Matrix for Number of Girders (Nb) Assessment.....	55
Table 10: Live Load Distribution Factors for Tub Girders (Girder Spacing of 6 feet)	63
Table 11: Live Load Distribution Factors for Tub Girders (Girder Spacing of 7 feet)	63
Table 12: Live Load Distribution Factors for Tub Girders (Girder Spacing of 8 feet)	63
Table 13: Live Load Distribution Factors for Tub Girders (Girder Spacing of 9 feet)	63
Table 14: Live Load Distribution Factors for Tub Girders (Girder Spacing of 10 feet)	64
Table 15: Live Load Distribution Factors for Tub Girders (Girder Spacing of 11 feet)	64
Table 16: Live Load Distribution Factors for Tub Girders (Girder Spacing of 12 feet)	64

LIST OF FIGURES

Figure 1: Taly and Gangarao’s Proposed Superstructure System (Taly & Gangarao, 1979).....	6
Figure 2: Nakamura’s Proposed Bridge System (Nakamura, 2002).....	7
Figure 3: Bridge System Proposed by Burner and Glasser (Burner, 2010).....	8
Figure 4: TxDOT Tub Girder Design (Chander et al., 2010).....	8
Figure 5: Michaelson’s Press-Brake-Formed Steel Tub Girder System (Michaelson, 2014)	9
Figure 6: Typical Failure mode for Composite Specimens (Michaelson, 2014).....	11
Figure 7: Photo of the Amish Sawmill Bridge (Gibbs, 2017)	12
Figure 8: Dimensional Cross-Section of Single Girder (Gibbs, 2017).....	13
Figure 9: Cross-Section of Amish Sawmill Bridge (Gibbs, 2017).....	13
Figure 10: Center-to-Center Flange Distance (AASHTO, 2014).....	25
Figure 11: Mesh Discretization (Fully Rendered Profiles).....	30
Figure 12: Nodal Distribution of Point Load (Michaelson, 2014).....	32
Figure 13: STS WiFi Base Station (Bridge Diagnostics, Inc.).....	35
Figure 14: STS WiFi 4-Channel Node (Bridge Diagnostics, Inc.).....	35
Figure 15: BDI Strain Transducer (Bridge Diagnostics, Inc.).....	36
Figure 16: Tandem-Axle Dump Truck (Gibbs, 2017).....	37
Figure 17: Gage Locations (Gibbs, 2017).....	38
Figure 18: Truck Dimensions and Wheel Loads (Gibbs, 2017).....	38
Figure 19: Live Load Truck Placements (Gibbs, 2017)	39
Figure 20: Comparison of Finite Element Analysis vs. Experimental Flange Bending Stress for Girder 1 Truck Run 3	46

Figure 21: Comparison of Finite Element Analysis vs. Experimental Flange Bending Stress for Girder 3 Truck Run 3	46
Figure 22: Comparison of Finite Element Analysis vs. Experimental Average Distribution Factors for Truck Run 3	47
Figure 23: Comparison of Finite Element Analysis vs. Experimental Distribution Factors for Truck Run 3	48
Figure 24: Comparison of Finite Element Analysis vs. Experimental Bottom Flange Stress for Two-Lane Loaded Scenario for Girder 1	49
Figure 25: Comparison of Finite Element Analysis vs. Experimental Bottom Flange Stress for Two-Lane Loaded Scenario for Girder 4.....	49
Figure 26: Distribution Factor Analysis Summary Graph (FEA vs. Experimental).....	50
Figure 27: FEA LLDFs vs Experimental LLDFs vs AASHTO LLDFs Comparison for Truck Run 3.....	51
Figure 28: Comparison of Live Load Distribution Factors with Span Length of 40 feet.....	56
Figure 29: Comparison of Live Load Distribution Factors with Span Length of 70 feet.....	57
Figure 30: Comparison of Live Load Distribution Factors with Span Length of 100 feet.....	58
Figure 31: Comparison of Live Load Distribution Factors with Girder Spacing of 6 feet.....	59
Figure 32: Comparison of Live Load Distribution Factors with Girder Spacing of 7 feet.....	59
Figure 33: Comparison of Live Load Distribution Factors with Girder Spacing of 10 feet.....	60
Figure 34: Comparison of Live Load Distribution Factors with Span Length of 40 feet and Girder Spacing of 6 feet.....	61
Figure 35: Comparison of Live Load Distribution Factors with Span Length of 40 feet and Girder Spacing of 9 feet.....	62

Figure 36: Comparison of Live Load Distribution Factors with Span Length of 40 feet and
Girder Spacing of 12 feet..... 62

ABSTRACT

The scope of this thesis project was to refine the development of live load distribution factors for tub girders. This was done in three stages. First, experimental data was gathered to assess live load distribution on the Amish Sawmill Bridge located in Fairbank, Iowa. Then, finite element analysis models were developed to benchmark against experimental data. Finally, a series of parametric studies were performed to explore the distribution factors of steel tub girders under various design conditions and to generate more accurate live load distribution factors. Results drawn from this research project demonstrate that press-brake-formed steel tub girders exhibit consistent performance and are a practical option in short span bridge construction. In addition, it was found that the current AASHTO LRFD Bridge Design Specifications can overestimate distribution factors for interior girders and fails to estimate distribution factors for exterior girders depending on girder spacing and length of bridge.

CHAPTER 1: INTRODUCTION

1.1 BACKGROUND

Press-brake-formed tub girder superstructures are a new technology and consist of modular galvanized shallow trapezoidal boxes, fabricated from cold-bent structural steel plate(s). In 2009, the Federal Highway Administration (FHWA) and the North American steel industry decided to develop a cost-effective short span steel bridge, up to 140 feet in length, with modular components that could be installed in a short period of time. Early investigation on press-brake-formed steel tub girders began in October 2011 (Michaelson, 2014). Since then, more and more studies have been performed to improve: 1. Design, 2. Applications, 3. Constructability and 4. Evaluation of the steel tub girder system.

There have been increased efforts to determine a design solution to utilize steel in short-span bridge applications. Previous research has been conducted to try and utilize numerous tub girder designs in bridge applications. Researchers have found the steel tub girder design to be practical and cost-effective. The noteworthy advantage is that 95% of the girder system can be fabricated off-site and then transported to the bridge construction site. By using a press-brake to cold form the tub girders, manufacture costs are reduced significantly when compared to traditional fabrication processes for box girders. In addition, the bridge superstructure is lightweight, allowing low capacity equipment to be used during its construction (Taly and Gangarao, 1979; Nakamura, 2002; Michaelson, 2014; Kelly 2014; Gibbs, 2017).

The American Association of State Highway and Transportation Officials (AASHTO) holds the current standards and specifications for bridge construction. A recent study performed at West Virginia University has shown that, although AASHTO standards for box girders work for designing press-brake-formed steel tub girders, the computation of LLDFs needs to be further

optimized (Gibbs, 2017). There are many different types of girders with different shapes constructed with either concrete or steel. All shapes contained in the Section 4: Structural Analysis and Evaluation Chapter of AASHTO LRFD Bridge Design Specifications Manual have different live load distribution factor models based on exterior beams or interior beams, except for steel tub girders which have one equation for either type of girder based on number of beams and number of designed lane (AASHTO, 2014). Assessment studies on the subject and experimental data suggest that even though AASHTO distribution factors may be able to design tub girder superstructures, they end up overestimating sections and therefore make the design project more expensive than it could be.

The findings of the study in this thesis will propose an original contribution for this growing body of literature on tub girder superstructures by improving live load distribution factors for press-brake-formed steel tub girder systems. Furthermore, providing recommendations of practical value for the design of the system is expected to be beneficial for engineers, manufacturers and the public.

1.2 PROJECT SCOPE & OBJECTIVES

The work presented in this thesis was to assess and refine AASHTO live load distribution factors for tub girders and evaluate its effectiveness and drawbacks in order to propose more accurate distribution factors for its computation and design. The objectives of this work were achieved in the following manner:

- Assessment of AASHTO specifications for box section flexural members (tub girders), as well as the computation of live load distribution factors (LLDFs) using AASHTO standards.
- Finite element analysis of Amish Sawmill Bridge, located in Fairbank, Iowa, to benchmark against experimental data in order to generate analytical live load distribution factors.
- Field performance assessment of Amish Sawmill Bridge and strain data collection from Gibbs (2017) to validate finite element model presented in this study as well as description of experimental investigation and testing procedures conducted by Gibbs (2017).
- Comparison of analytical and experimental LLDFs using AASHTO specifications.
- Parametric study to understand which parameters affect the computation LLDFs for steel tub girders and to compute more accurate LLDFs for AASHTO limit state evaluations.

1.3 ORGANIZATION

- Chapter 2: Literature Review
 - This chapter summarizes previous studies on LLDFs, AASHTO distribution factors as well as previous research performed on cold-bent tub girder applications.
- Chapter 3: Finite Element Modeling Techniques
 - This chapter outlines the finite element modeling techniques utilized for this research project.
- Chapter 4: Benchmark Experimental Study
 - This chapter summarizes the Amish Sawmill Bridge field test procedures to assess LLDFs. Additionally, data validation is described in this chapter which was performed to benchmark experimental data against finite element model.
- Chapter 5: Parametric Assessment of Live Load Distribution Factors
 - This chapter describes the matrices of parametric assessments along with both constant and varied parameters. The results and achievements of this study are also discussed in this chapter.
- Chapter 6: Summary & Concluding Remarks
 - This chapter provides a summary of the scope of work and objectives of this project as well as suggestions for future research in LLDFs for tub girders.

CHAPTER 2: LITERATURE REVIEW

2.1 INTRODUCTION

Assessment studies on tub girders and experimental data on tub girder live load distribution factors suggest that even though AASHTO distribution factors are functional for the design tub girder superstructures, the specifications result in overestimating computation of LLDFs (Gibbs, 2017). This overestimation results in a design project that is more expensive and not maximally cost effective. These findings indicate the need for a review of current methods and discussion of possible improvements to current AASHTO specifications. The following literature review discusses the history and investigative research findings of steel-tub girders and leads us to discussion of future areas of research.

2.2 HISTORY OF COLD-BENT STEEL GIRDERS IN BRIDGE APPLICATIONS

2.2.1 Prefabricated Press-Formed Steel T-Box Girder Bridge System (Taly & Gangarao, 1979)

The steel-tub girder design originated when Taly and Gangarao (1979) proposed a press-brake to bend an A36 3/8-inch steel plate to form a tub girder in a short-span modular bridge system. Since this design was innovative, the AASHTO manual did not provide specifications for bridge members using a press-brake cold form in the shape of tub girders. To account for various bridge widths, without AASHTO specifications, the researchers proposed that several prefabricated tub girder units should be placed adjacent to one another and joined with a longitudinal closure placement. The ends of the tub girder beams were closed off with a 3/8-inch thick steel plate diaphragm that was completely welded around the perimeter of the tub girder. To provide additional support, bearing stiffeners were provided at the tub girder ends along with the 3/8-inch thick diaphragm as shown in the following figure.

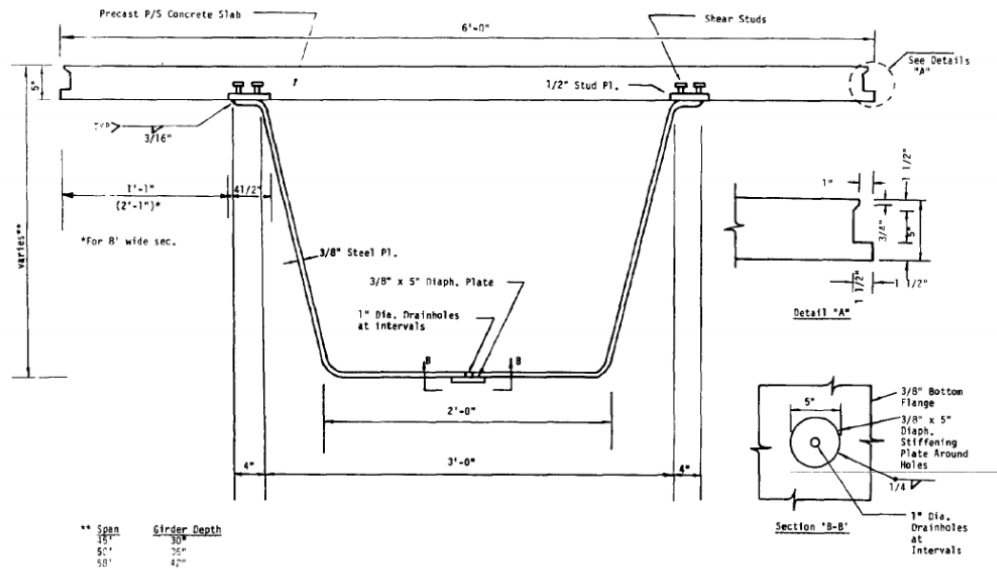


Figure 1: Taly and Gangarao's Proposed Superstructure System (Taly & Gangarao, 1979)

Ultimately, Taly and Gangarao (1979) estimated that 95% of the bridge, using press-brake cold bent girders, could be fabricated off site. Bridge fabrication costs could be significantly reduced in comparison to traditional fabrication processes for tub girders. Although that was a breakthrough and promising design, AASHTO still had not developed specifications for such a design to make the technology standardized and usable.

2.2.2 Composite Girders with Cold-Formed Steel U-sections (Nakamura, 2002)

Like Taly's and Gangarao's proposed design, Nakamura (2002) proposed a bridge superstructure system that exploited a press-brake to cold form steel tub girders shown in Figure 2. Nakamura (2002) proposed a continuous superstructure system with multiple intermediate piers to support the deck. The researcher designed the tub girders to be filled with concrete and bars to compensate for the possible buckling of the bottom flange at pier locations, resulting in an increased required strength against buckling at the support locations.

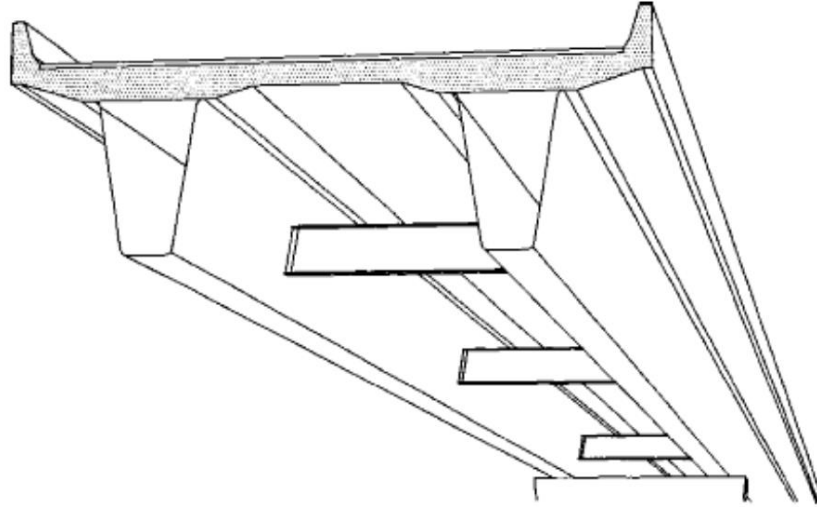


Figure 2: Nakamura's Proposed Bridge System (Nakamura, 2002)

Nakamura (2002) performed several bending tests and concluded that the tub girder behaved as a composite beam at the center span, making the system feasible due to its adequate bending strength and deflection capacity. The main drawback to Nakamura's design was that the tub girders required additional steel compared to conventional plate girders. However, Nakamura suggested that the costs could be offset if decreased fabrication costs were achieved, thus resulting in a more economical design.

2.2.3 Folded Plate Girders (Burner 2010 & Glaser 2010)

Burner (2010) and Glaser (2010) also researched cold-bent steel girders and the proposed system utilizes an inverted tub girder where the flanges of the girder are bent inwards (See Figure 3). The concrete deck is then cast on the wider center flange as opposed to previously developed systems, where the deck is cast on the two smaller exterior flanges. The main advantages of this system include ease of inspection, easier maintenance of the folded plate girder, and safe work area during construction due to the wider flange being the top surface.

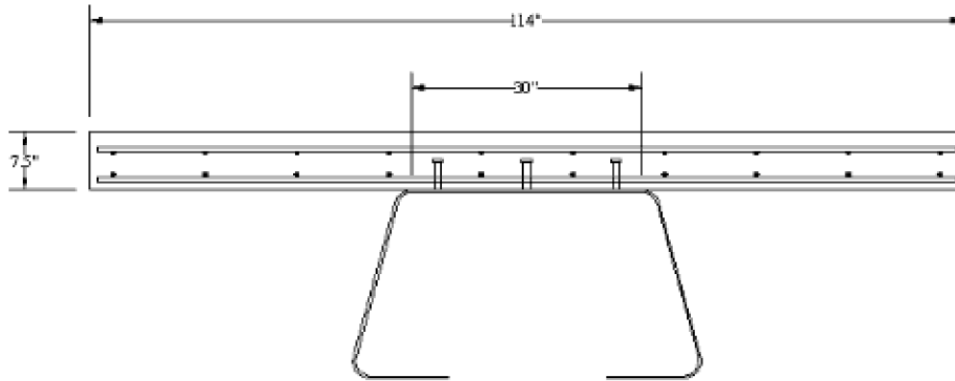


Figure 3: Bridge System Proposed by Burner and Glasser (Burner, 2010)

2.2.4 TxDOT Rapid Economical Bridge Replacement (Chandar et al., 2010)

Alternatively, the Texas Department of Transportation (TxDOT) developed a tub girder bridge design which consisted of a 5-foot-wide bottom flange with a 3-foot-deep web, as shown in Figure 4. The proposed bridge system has a shallower bridge superstructure with shallow steel tub girders, shear studs welded to the top flanges and reinforced concrete deck casted on top (Chandar et al., 2010).

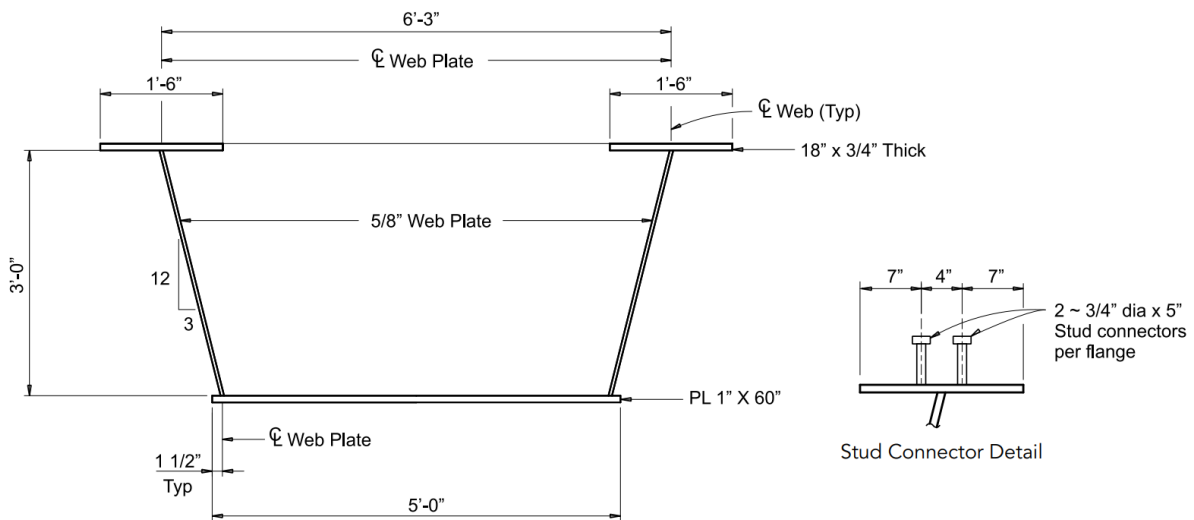


Figure 4: TxDOT Tub Girder Design (Chander et al., 2010)

The designed displayed in Figure 4 was developed to construct a bridge located 75 miles north of Austin on I-35. The main goal of the project was to create an aesthetically pleasing design as well as provide a rapidly constructible and cost-efficient structure. It is important to be noted that the girder system employed conventionally fabricated tub girders as opposed to cold-bent steel tub girders.

2.3 BEHAVIORAL STUDIES ON TUB GIRDERS

2.3.1 Development and Feasibility Assessment (Michaelson, 2014)

The innovative publication that combines press-brake-formed manufacturing techniques with steel tub girders, while creating a set of standards for its use, originates from Michaelson (2014). Michaelson produced a set of standardized press-brake-formed tub girder designs which would be fabricated from commonly sized steel plates that mills produce regularly. The focal concept was that the construction of such girders would be feasible and economic. The author performed a series of laboratory experiments that tested the tub girders both compositely and non-compositely.

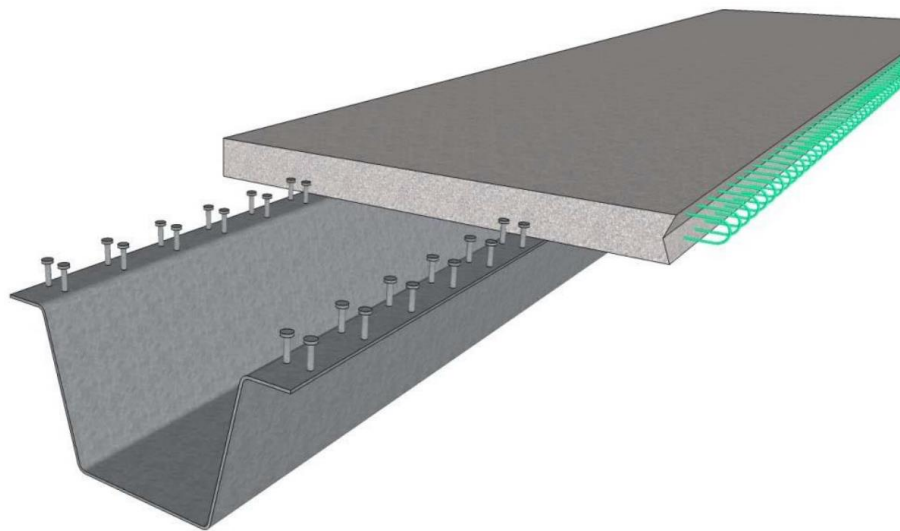


Figure 5: Michaelson's Press-Brake-Formed Steel Tub Girder System (Michaelson, 2014)

Michaelson (2014) performed several studies assessing the behavior of the composite systems. The objective of these studies was to compare the testing results to the AASHTO LRFD specifications to determine if the specifications were reasonably applicable to this new design. It was discovered that the AASHTO LRFD specifications were conservative in computing the nominal capacity of the modular composite specimens. Following this data collection, Michaelson (2014) derived an improved, simplified expression to compute the nominal capacity of the proposed system which is shown below:

$$M_n = \begin{cases} M_p & D_p \leq 0.1 D_t \\ M_p \left(1.025 - 0.25 \frac{D_p}{D_t} \right) & 0.1 D_t < D_p \leq 0.42 D_t \end{cases}$$

Equation 1: Nominal Capacity Equation (Michaelson, 2014)

Where,

M_n is the nominal flexural resistance

M_p is the plastic moment of the composite section

D_p is a distance from the top of the concrete deck to the neutral axis of the composite section at the plastic moment

D_t is a total depth of the composite section

After the performance of the proposed system was fully evaluated, a feasibility analysis was performed on different tub girder sizes against traditional analysis, such as steel rolled beams, to determine if the tub girders could be a viable design solution for superstructures using steel in short span bridge applications. Michaelson's specimens were able to withhold greater loads than the non-composite specifies. That outcome was achieved due to the specimens being governed by the section's ductility. The average of the maximum applied load on specimens tested by the researcher was of 304 kips with maximum deflection of 3.1 inches at failure during his lab tests.



Figure 6: Typical Failure mode for Composite Specimens (Michaelson, 2014)

Michaelson (2014) discovered that tub girder systems employing a 120" x 5/8" plate worked for spans up to 80 feet, exceling in performance, and competitive with other construction solutions, especially in applications with span lengths 60 feet and less. Michaelson (2014) advises that while AASHTO standards for tub girders conservatively estimates live load distribution, the economic competitiveness of the proposed system is maximized. An increased accuracy in determining live load distribution factors would result in increased span applicability of Michaelson's proposed system.

2.3.2 Evaluation of Non-Composite Tub Girders (Kelly, 2014)

In addition to the work detailed in Michaelson (2014), further studies and testing were completed to develop a complete understanding of the stability and torsional behavior of the non-composite press-brake-formed steel tub girders. Kelly (2014) included destructive flexural testing of two non-composite girders to physically validate their buckling capacity and behavior, as well as developing finite element models to simulate the behavior of the specimens to compare with the experimental data.

The goal of the study in Kelly (2014) was to use the experimental data along with the finite element analysis results to determine a need for bracing options and develop recommendations for future research. Moreover, Kelly concluded that initial imperfections and other second-order effects can greatly contribute to the loss of capacity for the specimens.

2.3.3 Field Performance Assessment (Gibbs, 2017)

More recently, Gibbs (2017) performed a field test and assessment of the performance of press-brake-formed steel tub girders of the Amish Sawmill Bridge in Buchanan County, Iowa, and compared it to analytical testing completed through finite element modeling. The Amish Sawmill Bridge is a 52-foot long, single span press-brake-formed steel tub girder bridge. Construction on the bridge initiated late in the summer of 2015 and was finished in December 2015, Figure 7.



Figure 7: Photo of the Amish Sawmill Bridge (Gibbs, 2017)

The press-brake-formed tub girders are made of galvanized steel and have the following dimensions:

- 96-inch-wide by ½-inch thick steel plates
- 7 ½-foot-spacing girders
- 6 steel diaphragms, two between each girder, with 17 ½ feet from each end
- 31-foot-3-inch-wide concrete deck with thickness of 8 ½ inches

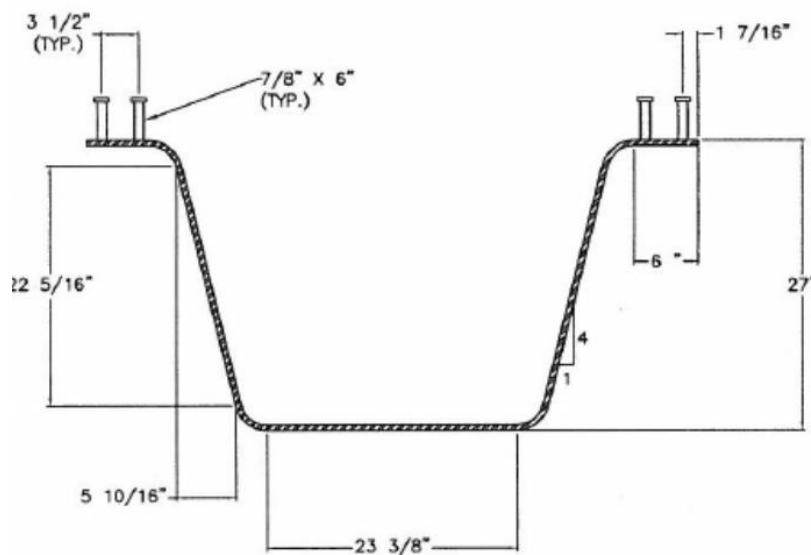


Figure 8: Dimensional Cross-Section of Single Girder (Gibbs, 2017)

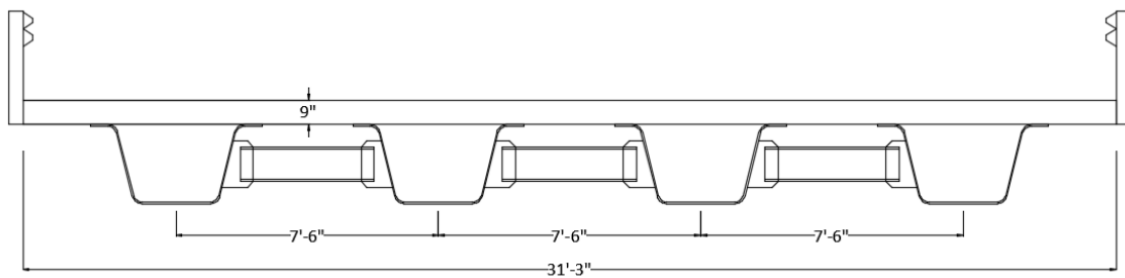


Figure 9: Cross-Section of Amish Sawmill Bridge (Gibbs, 2017)

Gibbs (2017) discovered that the magnitude of bottom flange bending stress varied between the FEA and field test due to the difference in boundary conditions between the finite element model and the field; the two sets of results exhibited correlated behavior. Additionally, Gibbs' work aimed to compare LLDFs calculated from the experimental and analytical testing to LLDFs calculated using AASHTO specifications. The study concluded that AASHTO specifications for calculating LLDFs for tub girders can safely be applied to press-brake-formed tub girders, but are very conservative, resulting in an over-estimation of the materials to be used.

2.4 HISTORICAL DEVELOPMENT OF LIVE LOAD DISTRIBUTION FACTORS

2.4.1 General Overview on AASHTO Live Load Distribution Factors

LLDFs have been introduced to American bridge codes in the first edition of AASHTO at the time, in 1931. In 1994, AASHTO adopted the LRFD Bridge Design Specifications, which contain a new procedure for computation of distribution factors that embodied the first major change to these equations since 1931.

Even though the provisions of the AASHTO Standard Specifications allow for more detailed analyses of various bridge systems, the use of simplified methods to determine bridge load response were employed. These simplified methods involved the use of wheel load distribution factors. Specifically, these factors are used in combination with a line-girder analysis to determine the maximum number of wheels that would be resisted by a given girder.

Most of the distribution factors empirical equations have the following form:

$$g = \frac{S}{D}$$

Equation 2: General LLDFs Computation

Where,

g is the distribution factor

S is the center-to-center girder spacing

D is a constant varying with the bridge type and number of loaded lanes

2.5.2 Previous Studies on Live Load Distribution Factors

It has been discovered that different parameters, such as girder spacing, girder location, span length and girder stiffness affect the computation of live load distribution in slab-and-beam bridges. Other parameters are noted to have influence in distribution factors; however, their effect is considered negligible. In addition, it is important to mention that studies performed in the past, regarding live load distribution, are based on I-girder bridges due to their popular shape. (Eom & Nowak, 2001; Kim & Nowak, 1997; Mabsout, Tarhini, Fredrick & Kobrosly, 1997; Newmark and Siess, 1942; Newmark, 1949; Nutt, Schamber, Zokaie, 1988; Tarhini and Frederick, 1992; Tarhini, Mabsout, Kobrosly, 1996; Walker, 1987; Zokaie, 2000).

2.4.2.1 Girder Spacing

Girder spacing has been determined to be the most influential parameter affecting live load distribution since early work by Newmark (1938). Newmark and Siess (1942) developed simple, empirical equations expressing distribution factors as a function of girder spacing, span length, and girder stiffness. Later, the effects of span length and girder stiffness were neglected, and the distribution factors were derived solely as a linear function of girder spacing (Newmark, 1949). These relationships are still incorporated in the AASHTO LRFD Bridge Design Specification with some modifications since their implementation.

In addition, sensitivity studies presented in NCHRP Project 12-26 (Nutt et al., 1988) and analytical studies by Tarhini and Frederick (1992) have shown that, whereas girder spacing significantly affects live load distribution characteristics, the relationship is not linear as implied by the Equation 2, and consequently does not correlate accurately with the AASHTO Standard Specifications. The S/D factor consistently overestimates the actual live load distribution factors.

2.4.2.2 Girder location

Interior and exterior girders have an influence on live-load distribution factors, according to Walker (1987). Walker's distribution factors were used to calculate an equivalent value of D (as used in the S/D formulas) that would have produced the same distribution factor. Results confirmed that the S/D factors overestimated actual distribution to a reduced magnitude in exterior girders. Additionally, for bridges with five equally spaced girders, the calculated value of D was greater for the center girder than the value for the first interior girder. In addition, Zokaie (2000) discovered that exterior girders are more sensitive to truck placement than interior girders. In order to overcome the issue, a combination of these two methods is incorporated into the LRFD Specifications. The lever rule is used for cases involving one traffic lane and a correction factor is used for two or more traffic lanes.

2.4.2.3 Span Length

Span length has been determined to share a non-linear relationship with girder distribution factors (Nutt et al., 1988; Tarhini and Frederick, 1992). The study conducted by Nutt et al. (1988) revealed that the non-linear nature of this relationship was consistently most evident in interior girders compared to exterior girders, throughout the span lengths tested. Tarhini and Frederick (1992) discovered that, accounting for the increased potential number of vehicles with a larger span length, there was a quadratic increase in the distribution factor. With finding this relationship, they proposed a function of girder spacing (S) and span length (L) be used to compute distribution factors:

$$DF = 0.00013 L^2 - 0.021 L + 1.25\sqrt{S} - \frac{(S + 7)}{10}$$

Equation 3: Distribution Factor Equation (Tarhini and Frederick, 1992)

Where,

DF is the distribution factor

S is the center-to-center girder spacing

L is the length of the bridge

2.4.2.4 Girder Stiffness

Various studies have indicated that relative stiffness has a negligible effect on live load distribution (Newmark & Siess, 1942; Nutt et al., 1988; Tarhini & Frederick, 1992). In the reviewed studies, different parameters of stiffness were assessed, but findings were comparable.

Earlier works of Newmark and Seiss (1942) expressed the amount of live load distributed across individual bridge girders by discussing relative stiffness of the girder compared to the stiffness of the slab, expressed by the dimensionless parameter H .

$$H = \frac{E_b I_b}{aEI}$$

Equation 4: Distribution Factor Equation (Newmark and Seiss, 1942)

Where,

E_b is the modulus of elasticity of the material of the beam

I_b is the moment of inertia of the cross section of the beam

a is the span length

E is the modulus of elasticity of the slab material

I is the moment of inertia per unit of width of the cross section of the slab

Results, using parameter H , revealed that this relative stiffness did have a small effect on live load distribution. In sequential literature produced by Newmark and Siess (1942), it was clarified that the range of H for a particular type of bridge is small enough that this variable can usually be neglected.

Nutt et al. (1988) used a different parameter to define girder stiffness with similar results. In this study, girder stiffness was defined by parameter K_g :

$$K_g = I + Ae^2$$

Equation 5: Parameter K Equation (Nutt et al., 1988)

Where,

I is the moment of inertia of the cross section of the beam

A is the area of the girder cross section

e is distance between centers of gravity of the slab and beam

In order to confirm that this was an acceptable means of quantifying girder stiffness, individual values of moment of inertia, area, and eccentricity were varied, while maintaining a constant value of K_g . Findings exhibited that if K_g was held constant, varying individual parameters was relatively inconsequential, with only 1.5% difference noted. By defining girder stiffness in this manner, Nutt et al. (1988) found there was a significant relationship between girder stiffness and live load distribution. However, the effect of increasing the distribution factor by increasing girder stiffness was largely reduced when increasing the span length, as increasing the span length decreases the distribution factor. Since the girders used in longer span bridges often possess larger stiffness values, the two parameters were reduced. The effects of varying torsional stiffness were also evaluated in this study with results showing this parameter caused only a 3% difference on girder distribution factors.

In more recent studies, Tarhini & Frederick (1992) studied the impact of changes in moment of inertia of the cross section. Changes, such as doubling the cross-sectional area of the girder and altering the thickness of the slab, resulted in approximately a 5% variance in comparison to the initial design, which was considered to be an insignificant effect.

2.4.2.5 Continuity Conditions

Nutt et al. (1988) examined the difference in distribution factors between simple span and two-span continuous bridges. The two-span bridges that were analyzed had two equal length spans, five girders, and were not skewed. The results exhibited that the distribution factors obtained for the two-span bridges were

up to 11% higher than the distribution factors that resulted from the corresponding simple-span bridges. By examining the average increase in distribution factor between simply- supported and two-span continuous bridges, Nutt et al. (1988) recommended that a distribution factor of 1.10 be used for all bending moments.

Zokaie (2000) also researched the continuity conditions effect on live load distribution factors. The author states that there is a 5% variance between positive moments and 10% variance between negative moments for simple span versus continuous bridges, though, it is assumed that moment redistribution will cancel this effect and no correction factor is recommended. The formulas for distribution factors are therefore considered to be directly applicable to continuous span bridges and it is recommended that the average length of the adjacent spans be used in the formulas.

2.4.2.5 Deck Thickness

There are conflicting research findings regarding the relationship of concrete deck thickness and live load distribution. An earlier article by Newmark (1949) reported that since deck thickness directly influences relative stiffness, there will be a resulting impact on wheel load distribution. However, Tarhini & Frederick researched varying concrete slab thicknesses, from 5.5 in. to 11.5 in., where analyses indicated varying thickness levels had a negligible influence on live load distribution (1992). Nutt et al. (1988) also researched varying concrete slab thicknesses, 6 in. and 9 in., and determined the 10% difference to be a small difference, but they did include this parameter in the recommended distribution factor equations contained in NCHRP Project 12-26.

2.4.2.6 Skew

A singular study by Nutt et al. (1988) has investigated the impact of skew on live load distribution. Findings indicated skew did impact live load distribution by decreasing the wheel load distribution for moment as well as increasing the shear force dispersed to the obtuse corner of the bridge. They also

discovered this effect to be non-linear and stated the effect would be larger for increasing skew. As a result of their sensitivity studies, two correction factors for skewed bridges were developed. One suggested correction factor is to be used for moment and the second is to be applied to the distribution factor for shear in the obtuse corner of the bridge. These correction factors are a function of girder spacing, span length, slab thickness, transformed moment of inertia of the girder, transformed area of the girder, girder eccentricity, and skew angle.

2.5 AASHTO LIVE LOAD DISTRIBUTION FACTORS (LLDFs) FOR BOX GIRDERS

2.5.1 AASHTO Empirical Approach

AASHTO LRFD Design Specifications includes live load distribution factors for several girder shapes. These factors provide distributed moment along a girder, which are needed for designing bridges. The parameters contained on AASHTO specifications for box girders are unknown and thereby unfeasible and overestimating. Furthermore, AASHTO model for tub girders utilizes only one equation to determine distribution factors on interior and exterior girders.

Table 1 through Table 3 present the distribution factors in the AASHTO Bridge Design Specifications 2014 organized based on bridge type.

Type of Beams	Applicable Cross-Section from Table – 4.6.2.2.1-1	Distribution Factors	Range of Applicability
Wood Deck on Wood or Steel Beams	a, l	See Table 4.6.2.2.2a-1	
Concrete Deck on Wood Beams	l	Once Design Lane Loaded: $S/12.0$ Two or More Design Lanes Loaded: $S/10.0$	$S \leq 6.0$
Concrete Deck, Filled Grid, Partially Filled Grid or Unfilled Grid Deck Composite with Reinforced Concrete Slab on Steel or Concrete Beams; Concrete T-Beams, T- and Double T-Sections	a, e, k and also i, j if sufficiently connected to act as a unit	One Design Lane Loaded: $0.06 + \left(\frac{S}{14}\right)^{0.4} \left(\frac{S}{L}\right)^{0.3} \left(\frac{K_g}{12.0Lt_s^3}\right)^{0.1}$ Two or More Design Lanes Loaded: $0.075 + \left(\frac{S}{9.5}\right)^{0.6} \left(\frac{S}{L}\right)^{0.2} \left(\frac{K_g}{12.0Lt_s^3}\right)^{0.1}$	$3.5 \leq S \leq 16.0$ $4.5 \leq t_s \leq 12.0$ $20 \leq L \leq 240$ $N_b \geq 4$ $10,000 \leq K_g \leq 7,000,000$
		Use lesser of the values obtained from the equation above with $N_b = 3$ or the lever rule.	$N_b = 3$
Cast-in-Place Concrete Multicell Box	d	One Design Lane Loaded: $\left(1.75 + \frac{S}{3.6}\right) \left(\frac{1}{L}\right)^{0.35} \left(\frac{1}{N_c}\right)^{0.45}$ Two or More Design Lanes Loaded: $\left(\frac{13}{N_c}\right)^{0.3} \left(\frac{S}{5.8}\right) \left(\frac{1}{L}\right)^{0.25}$	$7.0 \leq S \leq 13.0$ $60 \leq L \leq 240$ $N_c \geq 3$ If $N_c > 8$ use $N_c = 8$
Concrete Deck on Concrete Spread Box Beams	b, c	One Design Lane Loaded: $\left(\frac{S}{3.0}\right)^{0.35} \left(\frac{Sd}{12.0L^2}\right)^{0.25}$ Two ore More Design Lanes Loaded: $\left(\frac{S}{6.3}\right)^{0.6} \left(\frac{Sd}{12.0L^2}\right)^{0.125}$	$6.0 \leq S \leq 18.0$ $20 \leq L \leq 140$ $18 \leq d \leq 65$ $N_b \geq 3$
		Use Lever Rule	$S > 18.0$

Table 1: AASHTO LRDF Table 4.6.2.2.2b-1 - Distribution of Live Loads Per Lane for Moment in Interior Beams

Type of Beams	Applicable Cross-Section from Table – 4.6.2.2.1-1	Distribution Factors	Range of Applicability												
Concrete Beams Used in Multi-Beam Decks	f	One Design Lane Loaded: $k \left(\frac{b}{33.3L} \right)^{0.5} \left(\frac{I}{J} \right)^{0.25}$	$35 \leq b \leq 60$ $20 \leq L \leq 120$ $5 \leq N_b \leq 20$												
	g if sufficiently connected to act as a unit	where: $k = 2.5 (N_b)^{-0.2} \geq 1.5$ Two or More Design Lanes Loaded: $k \left(\frac{b}{305} \right)^{0.6} \left(\frac{b}{12.0L} \right)^{0.2} \left(\frac{I}{J} \right)^{0.06}$													
	h	Regardless of Number of Loaded Lanes: S/D where: $C = K (W/L)$ $D = 11.5 - N_L + 1.4 N_L (1 - 0.2C)^2$ when $C \leq 5$ $D = 11.5 - N_L$ when $C > 5$ $K = \sqrt{\frac{(1 + \mu)I}{J}}$	Skew $\leq 45^\circ$ $N_L \leq 6$												
	g, i, j if connected only enough to prevent relative vertical displacement at the interface	for preliminary design, the following value of K may be used: <table style="width: 100%; border-collapse: collapse;"> <thead> <tr> <th style="text-align: left;"><u>Beam Type</u></th> <th style="text-align: left;"><u>K</u></th> </tr> </thead> <tbody> <tr> <td>Nonvoided rectangular beams</td> <td>0.7</td> </tr> <tr> <td>Rectangular beams with circular voids:</td> <td>0.8</td> </tr> <tr> <td>Box section beams</td> <td>1.0</td> </tr> <tr> <td>Channel beams</td> <td>2.2</td> </tr> <tr> <td>T-Beam</td> <td>2.0</td> </tr> <tr> <td>Double T-Beam</td> <td>2.0</td> </tr> </tbody> </table>		<u>Beam Type</u>	<u>K</u>	Nonvoided rectangular beams	0.7	Rectangular beams with circular voids:	0.8	Box section beams	1.0	Channel beams	2.2	T-Beam	2.0
<u>Beam Type</u>	<u>K</u>														
Nonvoided rectangular beams	0.7														
Rectangular beams with circular voids:	0.8														
Box section beams	1.0														
Channel beams	2.2														
T-Beam	2.0														
Double T-Beam	2.0														
Open Steel Gird Deck on Steel Beams	a	One Design Lane Loaded: $S/7.5$ if $t_g < 4.0$ IN $S/10.0$ if $t_g \geq 4.0$ IN Two or More Design Lanes Loaded: $S/8.0$ if $t_g < 4.0$ IN $S/10.0$ if $t_g \geq 4.0$ IN	$S \leq 6.0$ FT $S \leq 10.5$ FT												
Concrete deck on Multiple Steel Box Girders	b, c	Regardless of Number of Loaded Lanes: $0.05 + 0.85 \frac{N_L}{N_b} + \frac{0.425}{N_L}$	$0.5 \leq \frac{N_L}{N_b} \leq 1.5$												

Table 2: AASHTO LRFD Table 4.6.2.2.2b-1 - Distribution of Live Loads Per Lane for Moment in Interior Beams (Continued)

Type of Superstructure	Applicable Cross-Section from Table 4.6.2.2.1-1	One Design Lane Loaded	Two or More Design Lanes Loaded	Range of Applicability
Wood Deck on Wood or Steel Beams	a, l	Lever Rule	Lever Rule	N/A
Concrete Deck on Wood	l	Lever Rule	Lever Rule	N/A
Concrete Deck, Filled Grid, Partially Filled Grid, or Unfilled Grid Deck Composite with Reinforced Concrete Slab on Steel or Concrete Beams; Concrete T-Beams, T and Double T sections	a, e, k and also i, j if sufficiently connected to act as a unit	Lever Rule	$g = e g_{interior}$ $e = 0.77 + \frac{d_e}{9.1}$	$-1.0 \leq d_e \leq 5.5$
			Use lesser of the values obtained from the equation above with $N_b = 3$ or the lever rule.	$N_b = 3$
Cast-in-Place Concrete Multi Cell Box	d	$g = \frac{W_e}{14}$	$g = \frac{W_e}{14}$	$W_e \leq S$
		Or the provisions for a whole-width design specified in Article 4.6.2.2.1		
Concrete Deck on Concrete Spread Box Beams	b, c	Lever Rule	$g = e g_{interior}$ $e = 0.97 + \frac{d_e}{28.5}$	$0 \leq d_e \leq 4.5$ $6.0 < S \leq 18.0$
			Use Lever Rule	$S > 18.0$
Concrete Box Beams Used in Multi-Beam Decks	f, g	Lever Rule	$g = e g_{interior}$ $e = 1.04 + \frac{d_e}{25}$	$-1.0 \leq d_e \leq 2.0$
Concrete Beams other than Box Beams Used in Multi-Beam Decks	h	Lever Rule	Lever Rule	N/A
	i, j if connected only enough to prevent relative vertical displacement at the interface			
Open Steel Gird Deck on Steel Beams	a	Lever Rule	Lever Rule	N/A
Concrete Deck on Multiple Steel Box Girders	b, c	As specified in Table 4.6.2.2.2b-1		

Table 3: AASHTO LRFD Table 4.6.2.2.2b-1 - Distribution of Live Loads Per Lane for Moment in Exterior Beams

The current AASHTO model, used for computing LLDFs for tub girders, is shown as well as its set of assumptions and constraints. The following equation can be found on *AASHTO LRFD Bridge Design Specifications Manual, Chapter 4* and showed in the previous tables.

$$DF = 0.05 + 0.85 \frac{N_L}{N_b} + \frac{0.0425}{N_L}$$

Equation 6: Concrete deck on Multiple Steel Box Girders LLDFs Equation (AASHTO, 2014)

Where,

DF is the *live load distribution factor*

N_L is the *number of design lanes as specified in Table 4.6.2.2.2b-1*

N_b is the *number of girders*

- **Assumption 1.** Bearing lines shall not be skewed.
- **Assumption 2.** Inclination of the web plates to a plane normal to the bottom flange shall not exceed a 1 to 4 slope.
- **Assumption 3.** The cantilever overhang of the concrete deck, including the curb and parapet, shall not be greater than either 60 percent of the average distance between the centers of the top steel flanges of adjacent box sections (see Figure 10) or 6.0 feet.
- **Assumption 4.** The distance taken at midspan shall neither be greater than 120 percent nor less than 80 percent of the distance center-to-center of the flanges of each adjacent box (see Figure 10).
- **Assumption 5.** If nonparallel box sections are used, the distance center-to-center of the flanges of each adjacent tub girders shall neither be greater than 135 percent nor less than 65 percent.

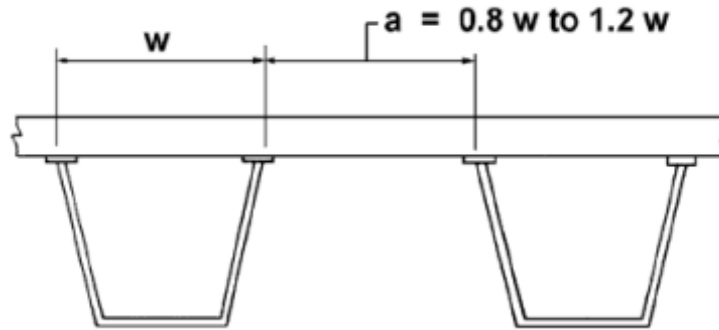


Figure 10: Center-to-Center Flange Distance (AASHTO, 2014)

- **Constraint 1.** AASHTO specifies the range of applicability of the live load distribution equation for Concrete Deck on Multiple Steel Box Girders, as follows:

$$0.5 \leq \frac{N_L}{N_b} \leq 1.5$$

Where,

N_L is the number of design lanes as specified in Table 4.6.2.2.2b-1

N_b is the number of girders

Furthermore, AASHTO specifications make use of multiple presence factors to account for multiple lanes loading simultaneously on the bridge (See Table 4). It is important to mention that the multiple presence factors are not to be used when evaluating fatigue, so that one design truck is used, regardless of the number of design lanes.

Number of Loaded Lanes	Multiple Presence Factors, m
1	1.20
2	1.00
3	0.85
>3	0.65

Table 4: AASHTO LRDF Table 3.6.1.1.2-1 Multiple Presence Factors, m

2.5.2 AASHTO Refined Analysis

Although the utilization of the empirical models described in this chapter is the most common method of determining distribution factors, AASHTO LRFD specifications allow the use of more refined analysis techniques to determine the transverse distribution of wheel loads in a bridge superstructure.

The first level of refined analysis permitted in the AASHTO LRFD specifications is the utilization of computer aided techniques in order to determine appropriate wheel load distribution factors. More specifically, computer software which simplifies bridge behavior using influence surface or influence section concepts, which are then used to determine distribution factors. Detailed computer analysis may be used for bridges that do not meet the AASHTO geometric limitations required for the use of simplified distribution factors. In this case, the actual forces occurring in the superstructure are calculated making the use of distribution factors unnecessary.

It is worth mentioning that if either method is used, it is the designer's responsibility to determine live loads critical locations.

2.6 CONCLUSION

Based on the results and conclusions drawn from this literature review, press-brake-formed steel tub girders are expected to exhibit consistent performance and are a practical option in the short span bridge industry, that prove to be reliable. However, more accurate specifications and mathematical models for live load distribution factor calculations need to be developed for the optimization of tub girder design. Assuming a more optimized design is developed, press-brake-formed steel tub girder bridges are expected to become even more cost-beneficial, faster to fabricate and section-material-saving due to its efficient design.

CHAPTER 3: FINITE ELEMENT MODELING TECHNIQUES

3.1 INTRODUCTION

This chapter outlines the finite element modeling techniques used for the research project. Details such as element type and material type, mesh discretization, boundary conditions used, and load applications are discussed in this chapter. In addition, the methods used to compute deflections and distribution factors can be found in this chapter. Finite element analysis was performed in this project using the commercial finite element software suite ABAQUS/CAE 6.14 by Dassault Systèmes. Modeling results from ABAQUS were benchmarked against experimental data from the Amish Sawmill bridge located in Fairbank, Iowa, (Gibbs, 2017) to evaluate their validity and accuracy in Chapter 4 of this thesis.

3.2 ELEMENT SELECTION CRITERIA

ABAQUS provides a large elements library for three-dimensional stress analysis such as T2D2, S4R and C3D8R amongst others. It is crucial to define the suitability of the selected element type for the given research model, steel plate girders. According to Michaelson (2014), S4R shell elements are accurate in modeling the physical behavior of steel plate girders. S4R elements were used to simulate the girder, deck and bearing stiffeners in all finite elements model for this research project. The S4R element is a 4-node multi-purpose shell element designed to provide accurate solutions for both thin and thick shells, using classical shell theory (Kirchoff) for thin shells as well as thick shell theory (Mindlin). In addition, S4R employ reduced integration schemes; only one Gauss integration point is used to form the element stiffness matrix, therefore, yielding advantage over traditional shell elements due to its reduced computing time and storage requirements.

Although the S4R proves to be an efficient element for modeling physical behavior of both noncomposite and composite steel plate girders (Yang, 2004; Roberts, 2004; Righman, 2005), the primary disadvantage of using S4R and its reduced integration is that the deformation modes may cause no strain at integration points, leading to inaccurate results if these no-strain modes propagate through the structure. This phenomenon is known as hourglassing, and though this issue might seem detrimental to the results, it can be easily prevented by the user adding artificial stiffness associated with no strain deformation modes under the “Section Controls” on ABAQUS. In order to model the composite interaction between the steel girders and the concrete deck, node-to-node multiple point constraints (MPC) were used. MPC allowed the degrees of freedom between the deck nodes and the girder nodes to be restrained.

3.3 MATERIAL PROPERTIES

In structural analysis, strain is a phenomenon with nonlinear behavior. Although this phenomenon can be simply observed as nonlinear, the incorporation of such behavior to predict strain values and live load distributions can be difficult if stresses exceed the material yield point. In order to overcome the issue, Eom and Nowak (2001) tested 17 steel I-girder bridges in Michigan and concluded that girders under the application of live load presented linear, elastic, and isotropic behavior throughout their study when maximum stress values, for both steel and concrete, are below the yield stress of steel and the compressive strength of concrete. Therefore, it was assumed that the model created for this research project followed such material properties.

Details of the material properties as follows:

For reinforced concrete, which was taken to have a compressive strength of 4.0 ksi, according to the provisions of AASHTO LRFD Section 5.4.2.4, the modulus of elasticity of concrete was determined to be 3640ksi. In addition, according to AASHTO LRFD Section 5.4.2.5, and Poisson's ratio to be 0.2.

For steel, which was taken to have a yield strength of 50ksi, according to the provisions of AASHTO LRFD Section 6.4.1, the modulus of elasticity of steel was taken to be 29000 ksi and Poison's ratio to be 0.3.

3.4 MESH DISCRETIZATION

AASHTO LRFD Section 4.6.3.3 describes specifications that should be followed when modeling beam-slab bridges. The AASHTO guidelines states that the aspect ratio of finite elements mesh measure should not exceed 5.0. In addition to such restriction in mesh proportion, the mesh elements should not have abrupt changes in its shape and size. In addition, it should be mentioned that research by Michaelson (2014) has demonstrated that these mesh densities precisely represent the composite steel bridge load response as well as attaining accurate results while adhering to AASHTO LRFD specifications.

For the model of the Amish Sawmill Bridge in this study, the mesh discretization dimensions utilized can be found as follows:

- 210 elements along the length of the bridge
- 116 elements along the width
- Each deck element is approximately 3 inches by 3 inches
- 2 elements along the widths of the top flanges
- 2 elements along the widths of the top flanges
- 3 elements along the bend region
- 7 elements along the flat portions of the webs
- 7 elements along the flat portions of bottom flanges
- Steel channel diaphragms were discretized through trial and error method until desired mesh achieved
- Connection plates were discretized to match each girder mesh

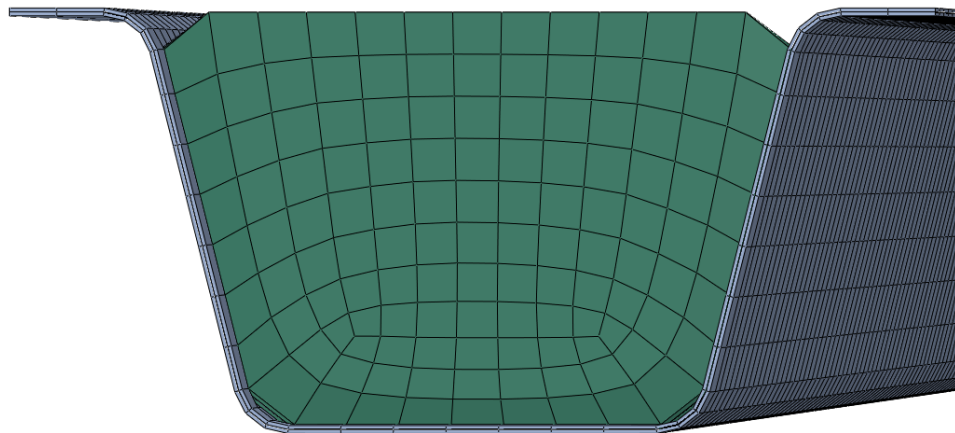


Figure 11: Mesh Discretization (Fully Rendered Profiles)

3.5 BOUNDARY CONDITIONS

In order to satisfy the boundary conditions for the problem, the hinge-roller conditions were applied, due to its continuous span. In addition, the girder ends were also restrained from lateral movement so that the bridge does not “slide off” its supports. These restrictions were applied at the nodes along the edges of the bottom flange of each girder.

3.6 MULTI-POINT CONSTRAINTS

As previously mentioned in this chapter, MPCs were used in order to create the composite action between the steel girders and the concrete deck. In ABAQUS, MPC is a tool which relates to degrees of freedom between multiple geometries within the bridge model. If MPCs are not used, ABAQUS would not be able to transfer the live loads from the concrete deck to the steel girder, as the software would process that the concrete deck would be “hovering” on top of the girders with no interaction between such structures.

The MPCs were placed at every node between the concrete deck and top flanges of each girder, where both structures are connected to one another. In addition, MPCs were placed at nodes between the steel channel diaphragms and their respective connection plates

3.7 LOAD APPLICATIONS

3.7.1 Dead Load Applications

The dead load of the system can be interpreted as the self-weight of the system, also known as gravity load. In order to compute dead loads, gravity was assumed to be 32.2 ft/s^2 . The unit weight of each material was defined as density. Therefore, in order to compute the weight of each element, the multiplication of density, volume and gravity was performed.

The following parameters were utilized in order to assess dead load applications for the Amish Sawmill Bridge model:

- Normal weight of concrete was taken to be 0.150 kip/ft³ throughout the deck
- Unit weight of steel was taken to be 0.490 kip/ft³ for the girders

3.7.2 Live Load Applications

Live load deflection characteristics and truck placement need to be assessed in order to compute live load distributions. This assessment and computation will be further discussed in Chapter 4 of this thesis. With the truck placement positions determined from the experimental test performed by Gibbs (2017), the wheel point load elements were linearly distributed amongst the 4 neighboring nodes in Figure 12.

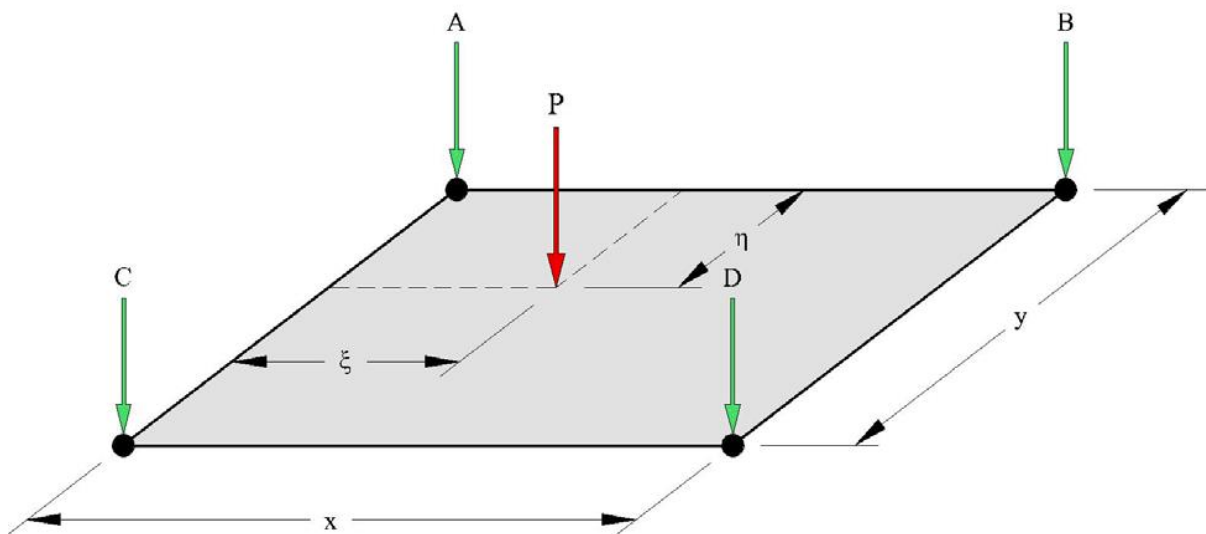


Figure 12: Nodal Distribution of Point Load (Michaelson, 2014)

Furthermore, AASHTO LRFD Section 4.6.3.3.1 states that nodal loads must be statically equivalent to the actual point load applied. Therefore, in order to fulfill the requirement, the equations to compute the nodal loads are listed as follows.

$$A = P \left(1 - \frac{\xi}{x}\right) \left(1 - \frac{\eta}{y}\right)$$

Equation 7: Nodal Computation A

$$B = P \left(\frac{\xi}{x} \right) \left(1 - \frac{\eta}{y} \right)$$

Equation 8: Nodal Computation B

$$C = P \left(1 - \frac{\xi}{x} \right) \left(\frac{\eta}{y} \right)$$

Equation 9: Nodal Computation C

$$D = P \left(\frac{\xi}{x} \right) \left(\frac{\eta}{y} \right)$$

Equation 10: Nodal Computation D

3.9 CONCLUSION

The preceding chapter describes the finite element modeling techniques used for this thesis, specifically, element type and material type, mesh discretization, boundary conditions used, and load applications. In addition, the methods used to compute deflections and distribution factors can be found in this chapter. Finite element analysis was performed in this thesis using the commercial finite element software suite ABAQUS/CAE 6.14 by Dassault Systèmes.

The results obtained by the finite element analysis are utilized in the following chapter to investigate the accuracy and validity of the AASHTO live load distribution factor mathematical model and propose an alternate, more optimized computation method.

CHAPTER 4: BENCHMARK EXPERIMENTAL STUDY

4.1 INTRODUCTION

The following chapter discusses the research method used to assess experimental data of the Amish Sawmill Bridge obtained by Gibbs (2017). This chapter also includes a summary of the bridge design, testing equipment, and testing procedures. The strain data obtained from Gibbs (2017) will be used for the data validation and comparison of the actual LLDFs and the FEA LLDFs generated by the bridge's model on ABAQUS presented in Section 4.5 of this thesis.

4.2 BRIDGE DESCRIPTION

As discussed in Section 2.3.3 of this report, the Amish Sawmill Bridge is a 52-foot long, single span press-brake-formed steel tub girder bridge. More details on the bridge specifications can be found in Section 2.3.3. Construction on the bridge initiated late in the summer of 2015 and was finished in December 2015.

4.3 EXPERIMENTAL TESTING EQUIPMENT

4.3.1 STS-Wi-Fi Data Acquisition System

The Bridge Diagnostics, Inc. (BDI) Data Acquisition System includes a series of wireless nodes, which can each accommodate up to four BDI strain transducers and a wireless base station. It is important to note that a mobile device running full Windows is necessary in order to run BDI Data Acquisition Software. The instruments used for Gibbs' (2017) field test were BDI strain transducers. Each instrument used was equipped with BDI's "Intelliducer" chip, giving the equipment the advantage to identify itself in BDI's software. The benefit of such capabilities is that it makes data collection and data organization distinguishable from different gauges during the post-processing phase.

The primary physical components of the system used consist of a wireless base station (Figure 13) and multiple 4-channel nodes (Figure 14). The base station obtains data by monitoring real-time wireless broadband signals that are transmitted from the 4-channel nodes. The base station can take readings of up to 500 samples per second and can monitor a vast number of devices on 4 to 128 channels.



Figure 13: STW WiFi Base Station (Bridge Diagnostics, Inc.)



Figure 14: STW WiFi 4-Channel Node (Bridge Diagnostics, Inc.)

The base station and 4-channel nodes are powered by rechargeable 9.6V Makita Nickel-Metal Hydride batteries that can last up to six hours under continuous use. Additionally, having wireless equipment allows for much easier data acquisition when testing location is difficult to access.

4.3.2 BDI Strain Transducers

Gibbs (2017) used BDI's re-usable strain transducers as the strain gages to be utilized during the bridge field testing (See Figure 15). Each strain gage has a range of $\pm 2,000 \mu\epsilon$ with an accuracy of ± 2 percent. The gages have a temperature range of -60°F to $+250^{\circ}\text{F}$ and require minimal surface preparation and effort to install. The gages are attached to the girder by two re-usable mounting tabs provided by BDI. The mounting tabs fit through two holes on each end of the gage and the gage is tightened snug with two 7/16-in. nuts. Each tab is placed into a slotted BDI jig during the installation process to ensure proper alignment and spacing.



Figure 15: BDI Strain Transducer (Bridge Diagnostics, Inc.)

4.3.3 Truck Specification

Gibbs (2017) described the live load for the field test was produced by a fully loaded tandem-axle dump truck provided by the Buchanan County Secondary Roads Department, which is shown in Figure 18. The weight of each axle was taken preceding the arrival of the truck at the bridge location shown in Figure 18.



Figure 16: Tandem-Axle Dump Truck (Gibbs, 2017)

4.4 EXPERIMENTAL TESTING PROCEDURES

The field test of the Amish Sawmill Bridge was completed in three days, per Gibbs (2017). A total of 16 gage locations were utilized for Gibbs' field test. Each girder was equipped with a minimum of three gages on the bottom flange at midspan. Girders 1 and 2 were equipped with two additional gages each at midspan; one on each web of each girder, three inches above the bend in the girders. The bottom flange gages were spaced six inches apart along quarter points across the width of the bottom flange. The gage arrangement is shown in Figure 17. The following steps were completed to set up the gages for completion of the experimental data collection:

1. Measurements were taken and locations were marked for every strain gage location on the tub girders.
2. Surface roughness of girders was reduced by using disk grinders to ensure proper surface adherence with gage tabs.
3. Gages were tightened on each set of tabs and plugged into wireless nodes.
4. Girders were labeled 1 through 4 from left to right, looking north, as shown in Figure 17.

5. Data collection was performed.

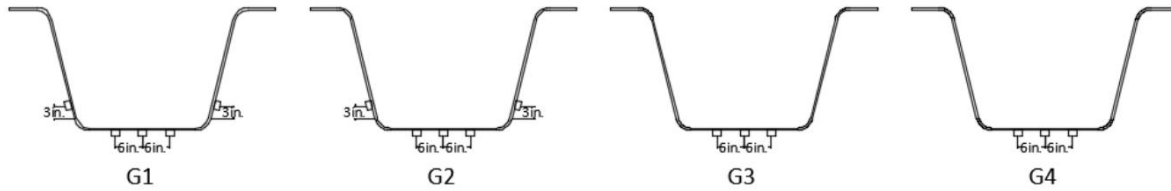


Figure 17: Gage Locations (Gibbs, 2017)

Axle measurements of the tandem-axle dump truck were taken upon its arrival to the bridge site. The dimensions, as well as the wheel weights are shown in Figure 18. Gibbs (2017) concluded the truck was considered appropriate for the field test due to its similarity to the AASHTO HS-20 design load truck.

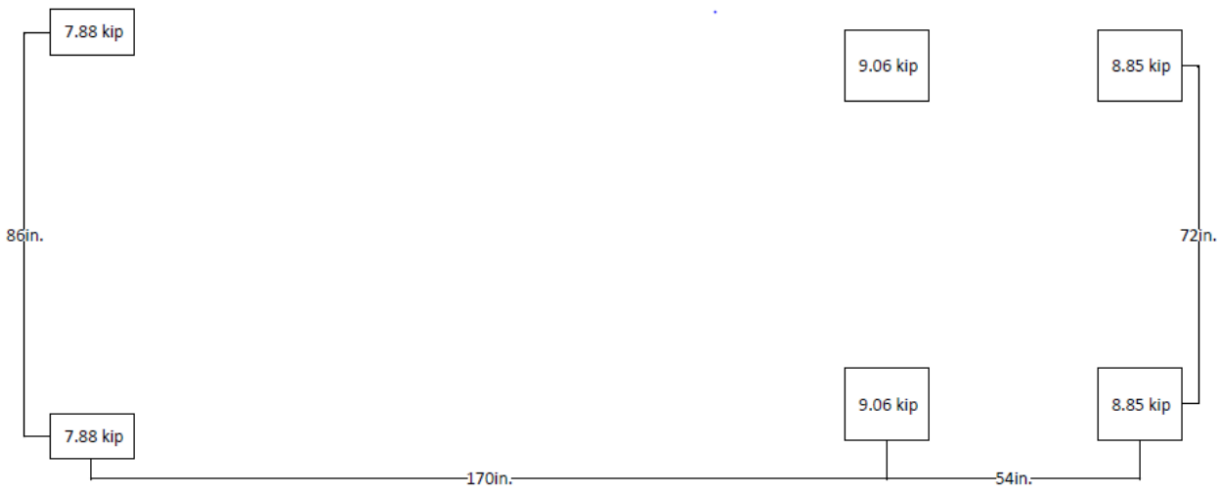


Figure 18: Truck Dimensions and Wheel Loads (Gibbs, 2017)

A total of five truck runs were mapped out onto the bridge deck using chalk at each tenth point along the length of the bridge. Considering the bridge is symmetric and not skewed, only five truck runs were needed to complete the field test. For each run, the truck was directed to stop with the center axle resting at each tenth point on the previously marked spots. Upon moving to each new spot, time was taken to let vibration in the girders end so that the data results

would be as accurate as possible. Measurements for each truck run were taken from the west guard rail to the center line of the front tire closest to the guard rail (See Figure 19).

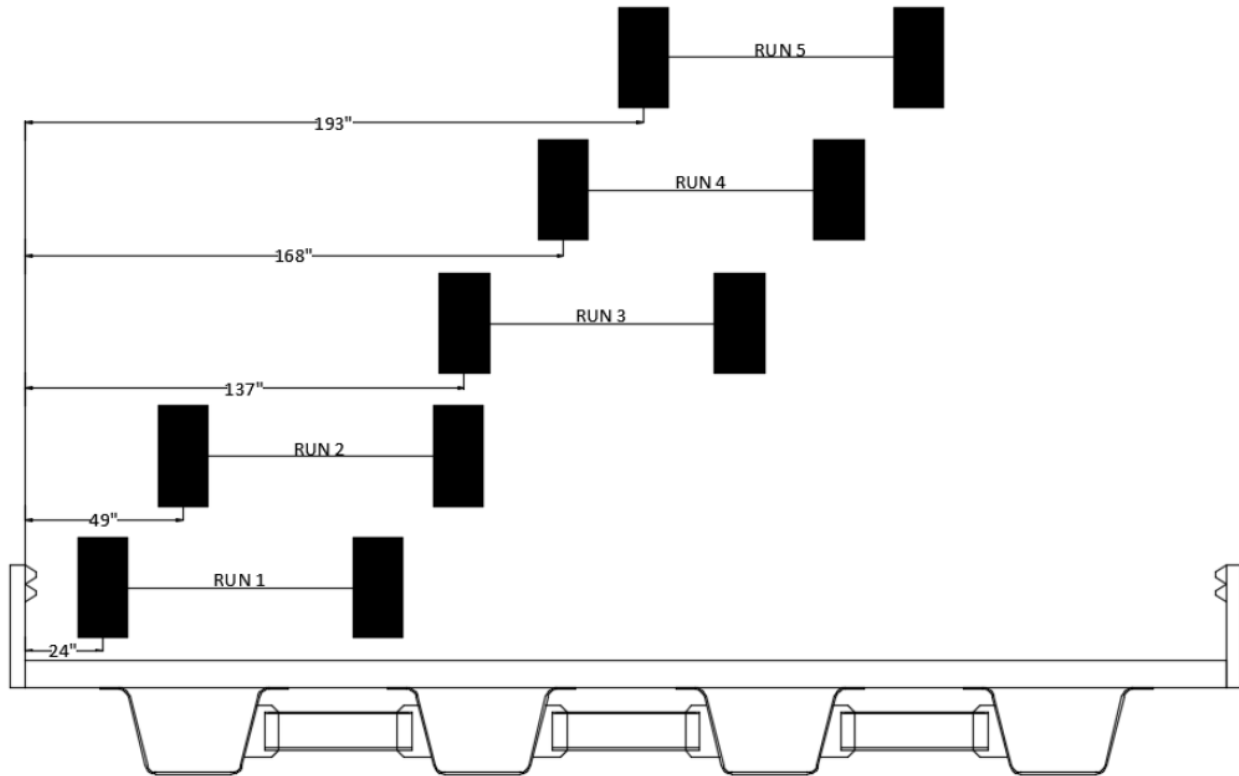


Figure 19: Live Load Truck Placements (Gibbs, 2017)

Truck Run 1 was placed two feet from the guard rail following AASHTO 2014 Section 3.6 specifications which states that such distance accounts for the worst-case loading scenario for an exterior girder. Truck Run 2 was placed so that one-wheel line was directly above Girder 2 to maximize load effects on the interior girder. Truck Run 3 was placed in the center of the bridge to detect if symmetrical results were produced. Truck Run 4 was placed 12 feet from Truck Run 1, and Truck Run 5 was placed 12 feet from Truck Run 2. The standard lane width is equal to 12 feet according to AASHTO Section 3.6. Consequently, Truck Runs 4 and 5 were placed 12 feet from Truck Runs 1 and 2, respectively, thus the results for two-lane loading scenarios could be calculated. The combination of Truck Runs 1 and 4 maximized load effects on the exterior

girder, while the combination of Truck Runs 2 and 5 maximized load effects on the interior girder.

4.5 DATA VALIDATION

This subsection will summarize Gibbs' (2017) experimental results in comparison to the analytical results achieved for this study. Results include flange stresses at midspan and LLDFs. This comparison is necessary to benchmark the FEA model and proceed with sensitivity and parametric studies (Chapter 5) in order to generate a more optimized LLDFs computation model.

4.5.1 Computation of Bending Stresses at Midspan

The following procedure was used to calculate the bending stresses at midspans. These calculations were performed for all five truck runs with the experimental strain data gathered by Gibbs (2017). In order to obtain midspan bending stresses, the strain values were divided by 1,000,000, due to the fact that the gages report the values in microstrain. After the unit conversion, the values were multiplied by the steel Young's Modulus of 29,000 ksi to obtain stresses.

1. Average Strain Reading Value By Using The Equation:

$$\varepsilon_{avg} = \frac{\sum \varepsilon}{\text{number of strains per girder}}$$

Equation 11: Computation of Average Strain

Where,

ε_{avg} is the average bottom flange strain i^{th} girder

$\sum \varepsilon$ is the summation of bottom flange strain generated by i^{th} girder

2. Strain to Bending Stress Conversion:

$$\sigma = \frac{\varepsilon_{avg}}{1,000,000} \times E_s$$

Equation 12: Bending Stress Computation

Where,

σ is the bottom flange bending stress of i^{th} girder

ε_{avg} is the average bottom flange strain of i^{th} girder

E_s is Young's Modulus of steel

4.5.2 Computation of Empirical Live Load Distribution Factors (LLDFs)

LLDFs are based on the average strain values for each girder as shown in Equation 11. To calculate LLDFs for each panel point, the strain for each girder was divided by the total strain in the system at that respective panel point. This process was repeated for each panel point at a given truck run with a total of 5 truck runs. In order to obtain the average distribution factor for each girder per truck run, the distribution factor obtained per panel point was averaged. Finally, the distribution factor values obtained were compared to AASHTO LLDFs in order to determine their validity.

$$g_i = \frac{n\varepsilon_i}{\sum_{j=1}^k \varepsilon_j} \times m$$

Equation 13: Empirical Computation of LLDFs

Where,

g_i is the distribution factor for the i^{th} girder

ε_i is the bottom flange static strain at the i^{th} girder

n is the number of applied design trucks

k is the number of girders

m is the AASHTO multiple presence factor

In addition, live load distribution factors were calculated where two lanes were loaded simultaneously in the respective order:

- Truck Run #1 and Truck Run #4
- Truck Run #2 and Truck Run #5

Example calculations of live load distribution factors containing single-lane and two-lane loaded are shown on the following page:

4.5.2.1 Computation of Live Load Distribution Factors for Single-Lane Loading

LLDF Calculation of Girder i^{th} During Truck Run j^{th}

$$LLDF_{i-j} = \frac{\varepsilon_{Gi}}{\sum_{j=1}^k \varepsilon_j} m$$

Equation 14: LLDFs Computation for Single-Lane Loading

Where,

$LLDF_{i-j}$ is the distribution factor for the i^{th} girder at j^{th} panel point

ε_{Gi} is the bottom flange static strain at the i^{th} girder

$\sum_{j=1}^k \varepsilon_j$ is the summation of average strain of all girders

m is the AASHTO multiple presence factor

4.5.2.2 Computation of Live Load Distribution Factors for Two-Lane Loading

LLDF Calculation of Girder i^{th} During Truck Run j^{th}

1. Average Strain Values for Girder i^{th} , Truck Runs i & j

$$\varepsilon_{Gi} = \varepsilon_{Gi_{avg}} + \varepsilon_{Gj_{avg}}$$

Equation 15: Total Average Strain Computation

Where,

ε_{Gi} is the bottom flange static strain at the i^{th} girder

$\varepsilon_{Gi_{avg}}$ is the average strain for Truck Run i

$\varepsilon_{Gj_{avg}}$ is the average strain for Truck Run j

Then,

2. Average LLDFs for Girder i^{th} , Truck Runs i & j

$$LLDF_i = \frac{\sum G_i LLDFs}{\text{Total Panel Points}}$$

Equation 16: : LLDFs Computation for Two-Lane Loading

Where,

$LLDF_{i-j}$ is the distribution factor for the i^{th}

$\sum G_i LLDFs$ is the summation of average live load distribution factors for girder i^{th}

4.5.3 Computation of AASHTO Live Load Distribution Factors

In order to benchmark and compare experimental data and analytical data to AASHTO specifications, live load distribution factors were calculated using AASHTO's methodology found on AASHTO LRFD Bridge Design Specification Chapter 4 and discussed in this thesis in Section 2.6.1. Therefore,

$$DF = 0.05 + 0.85 \frac{N_L}{N_b} + \frac{0.0425}{N_L}$$

Equation 6: Concrete deck on Multiple Steel Box Girders LLDFs Equation (AASHTO, 2014)

Where,

DF is the live load distribution factor

N_L is the number of design lanes as specified in Table 4.6.2.2.2b-1

N_b is the number of girders

And,

$$0.5 \leq \frac{N_L}{N_b} \leq 1.5$$

N_L is the number of design lanes as specified in Table 4.6.2.2.2b-1

N_b is the number of girders

4.5.4 Comparison of Results

This subsection will further discuss the results and comparisons between analytical LLDFs, Gibbs' experimental live load distribution factors and AASHTO live load distribution factors. Section 4.5.3.1 will compare the similarities and differences between the analytical results generated by finite elements modeling techniques and Gibbs' experimental results. Section 4.5.3.2 will demonstrate that AASHTO live load distribution factors are overestimated when compared to analytical and experimental data.

4.5.4.1 Analytical Data vs. Gibbs' Experimental Data

The primary observation when calculating average stresses for the superstructures was that the stresses on the finite elements model were considerably higher than the experimental results. It is also notable that the Amish Sawmill Bridge had integral abutments. Integral abutments are when the end of the girders are completely encased by concrete, which makes the structure much stiffer than the conventional simply-supported boundary conditions (high-roller). Table 5 and Table 6 provide the FEA and Gibbs' results, respectively.

Truck Run 3, Bending Stress					
Panel Points		Average Stress (ksi)			
x (ft)	x/L	G1	G2	G3	G4
0	0	0	0	0	0
5.2	0.1	0.76	0.92	0.92	0.77
10.4	0.2	1.18	1.56	1.57	1.20
15.6	0.3	1.49	1.92	1.93	1.51
20.8	0.4	1.64	2.17	2.18	1.67
26	0.5	1.64	2.50	2.52	1.67
31.2	0.6	1.47	2.27	2.29	1.50
36.4	0.7	1.17	1.58	1.58	1.19
41.6	0.8	0.87	1.00	1.01	0.88
46.8	0.9	0.54	0.57	0.56	0.54
52	1	0	0	0	0

Table 5: Finite Element Analysis Bottom Flange Bending Stress

Truck Run 3, Bending Stress					
Panel Points		Average Stress (ksi)			
x (ft)	x/L	G1	G2	G3	G4
0	0	0	0	0	0
5.2	0.1	0.33	0.37	0.37	0.29
10.4	0.2	0.49	0.70	0.71	0.45
15.6	0.3	0.63	0.79	0.79	0.60
20.8	0.4	0.74	0.97	0.94	0.70
26	0.5	0.76	1.32	1.25	0.76
31.2	0.6	0.65	1.19	1.10	0.66
36.4	0.7	0.46	0.62	0.58	0.45
41.6	0.8	0.26	0.28	0.27	0.32
46.8	0.9	0.12	0.13	0.13	0.20
52	1	0	0	0	0

Table 6: Gibbs, 2017 Experimental Bottom Flange Bending Stress

Integral abutment as boundary conditions was not used in the finite element model due to its controversy in the structural engineering community. In addition, there is no conventional technique to create integral abutment and replicate such boundary conditions on finite element modeling software. Figure 20 and Figure 21 demonstrate that, even though the boundary conditions differ between finite modeling techniques and actual bridge boundary conditions, the

behaviors correlated. The following figures show such correlation in Girder 1 and Girder 3 during the same truck run.

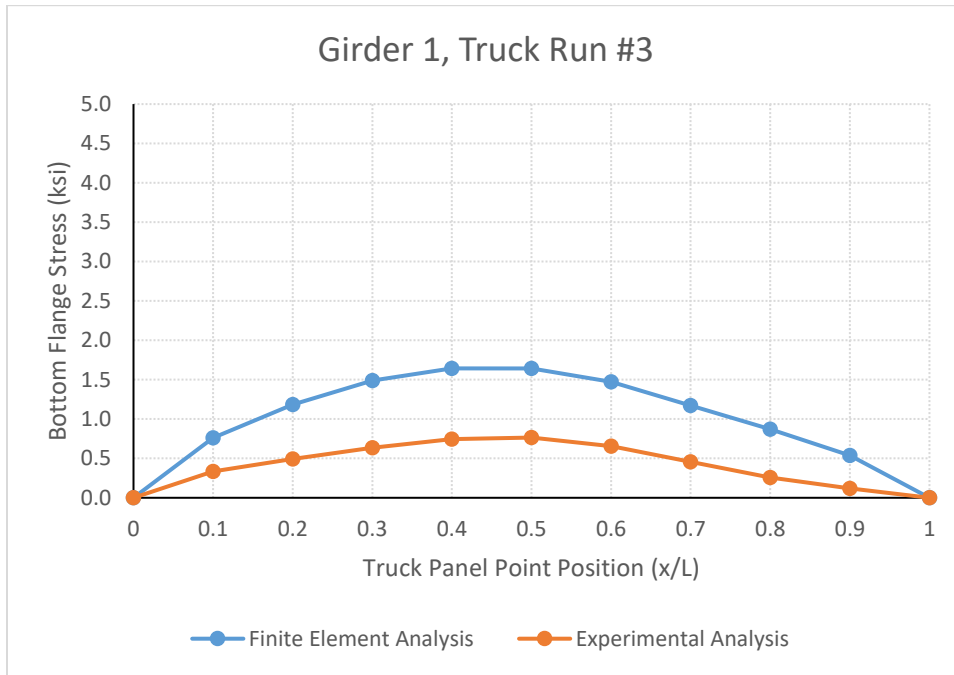


Figure 20: Comparison of Finite Element Analysis vs. Experimental Flange Bending Stress for Girder 1 Truck Run 3

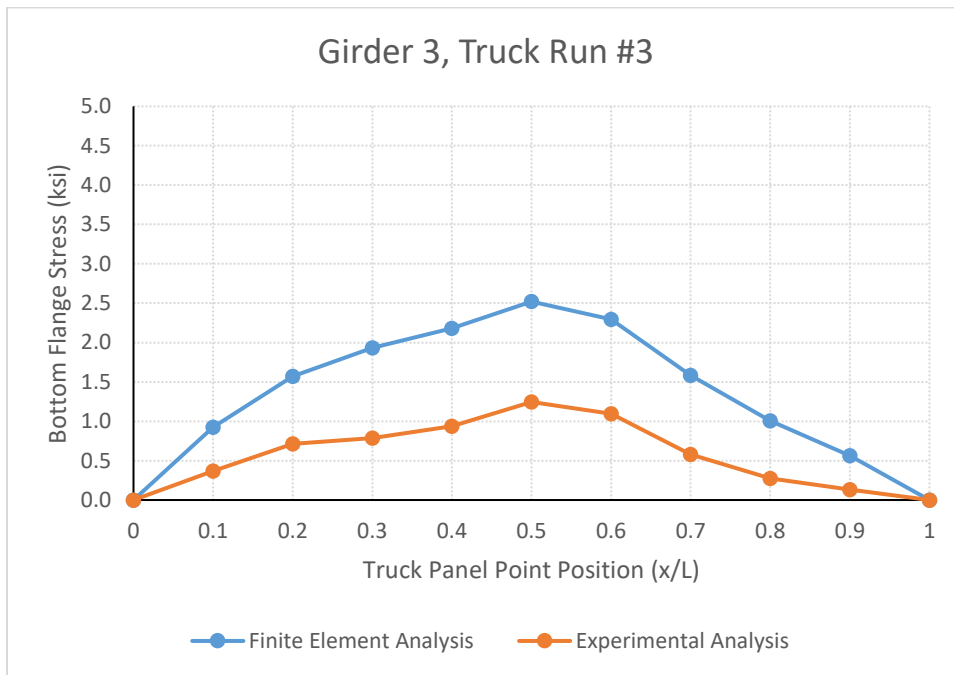


Figure 21: Comparison of Finite Element Analysis vs. Experimental Flange Bending Stress for Girder 3 Truck Run 3

Figure 22 and Figure 23 show the distribution factors for Truck Run 3 are approximately the same values for both the finite element analysis model results and the experimental data results. For this specific truck run, each graph is showing that Girders 2 and 3 supported most of the truck load, while Girders 1 and 4 supported a lesser portion of the load.

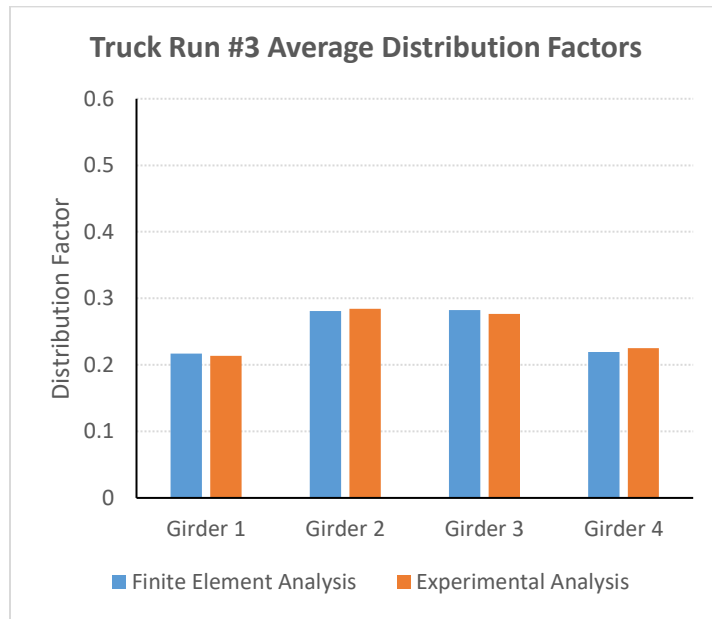


Figure 22: Comparison of Finite Element Analysis vs. Experimental Average Distribution Factors for Truck Run 3

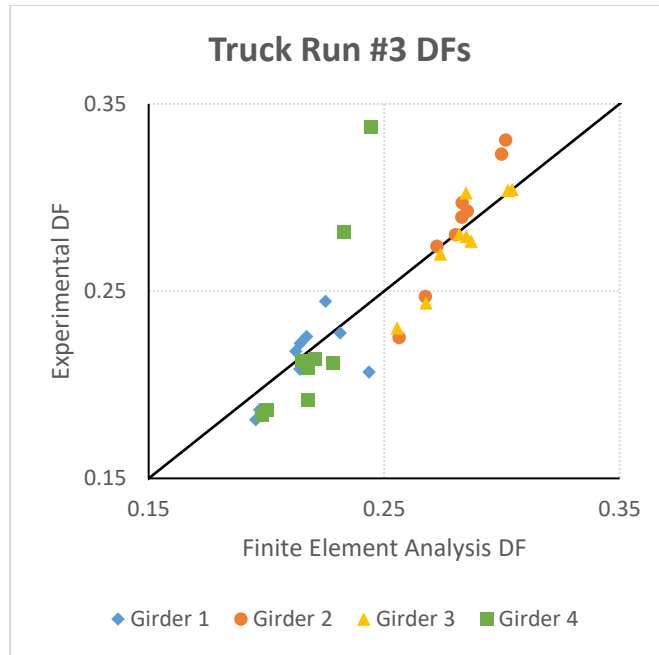


Figure 23: Comparison of Finite Element Analysis vs. Experimental Distribution Factors for Truck Run 3

Additionally, further analyses were performed to calculate the distribution factors for the scenario in which two of the load trucks were simultaneously on the bridge. To simulate the two-lane loaded scenario, data resulted in the combination of Truck Runs 1 and 4, and the combination of Truck Runs 2 and 5. The run combination was performed for two separate scenarios; the combination of the bottom flange stresses of Girder 1 and Girder 4 for the combined loading scenario of Truck Runs 1 and 4 (See Figure 24 and Figure 25). The finite element model still resulted in higher stresses than the field, which is expected to be due to the difference in integral abutments previously discussed.

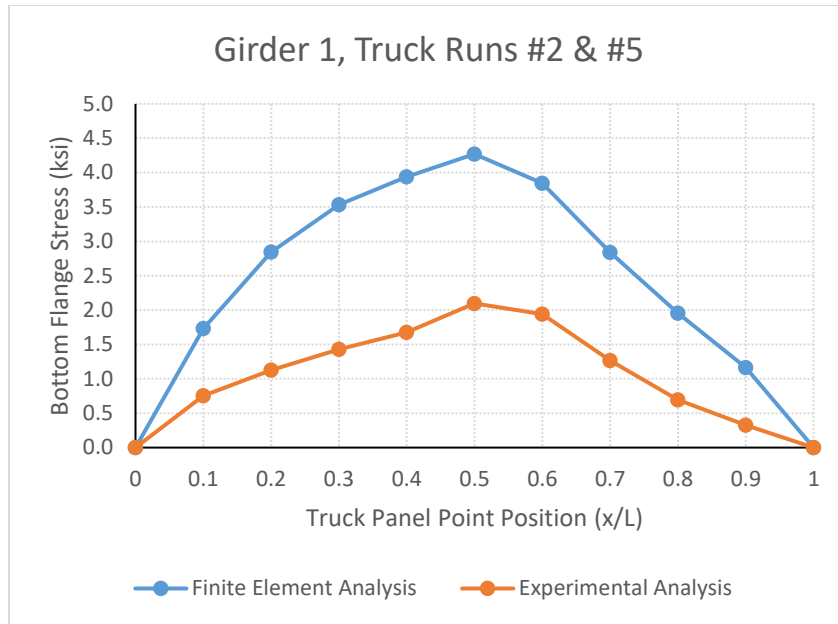


Figure 24: Comparison of Finite Element Analysis vs. Experimental Bottom Flange Stress for Two-Lane Loaded Scenario for Girder 1

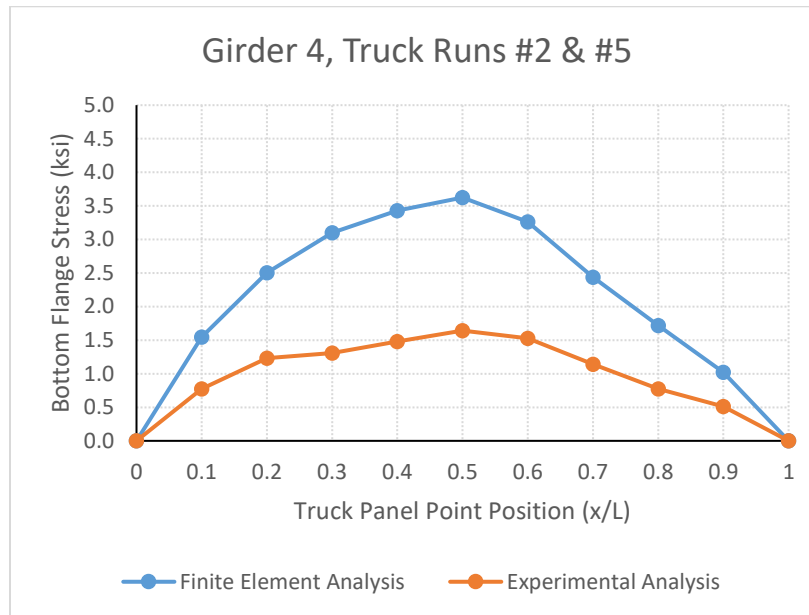


Figure 25: Comparison of Finite Element Analysis vs. Experimental Bottom Flange Stress for Two-Lane Loaded Scenario for Girder 4

To summarize the remaining distribution factor data between the finite element analysis model and experimental results, Figure 26 displays a quantile-quantile (Q-Q) plot containing all the calculated average distribution factors for each truck run in both the one-lane-loaded scenario as well as the two-lane-loaded scenario. Figure 26 also shows the correlation between the FEA

distribution factors and the experimental distribution factors with a R^2 of 0.9433 or roughly 94% correlation. Appendix B includes a complete collection of tables, graphs, and diagrams that summarize the data results from every truck run.

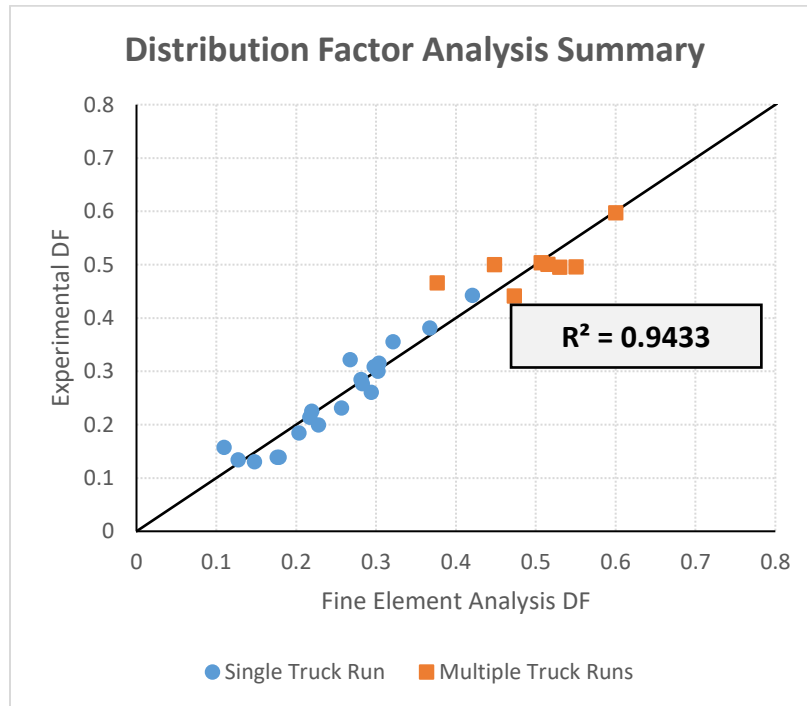


Figure 26: Distribution Factor Analysis Summary Graph (FEA vs. Experimental)

4.5.4.2 Comparison of Live Load Distribution Factors

Both finite element analysis and experimental live load distribution factors are very similar. Both analyses are well correlated and have the same magnitude of variance between interior and exterior girders. However, live load distribution factors computed by using AASHTO specifications are significantly higher than the other LLDFs computation method studied in this project. Table 7 and Figure 29 demonstrate the discrepancies between AASHTO distribution factors and FEA/experimental distribution factors.

Truck Run 3, Average Live Load Distribution Factors				
Analysis/Girder	G1	G2	G3	G4
FEA	0.217	0.281	0.283	0.220
Experimental	0.213	0.284	0.277	0.225
AASHTO	0.688	0.688	0.688	0.688

Table 7: FEA LLDFs vs Experimental LLDFs vs AASHTO LLDFs Comparison for Truck Run 3

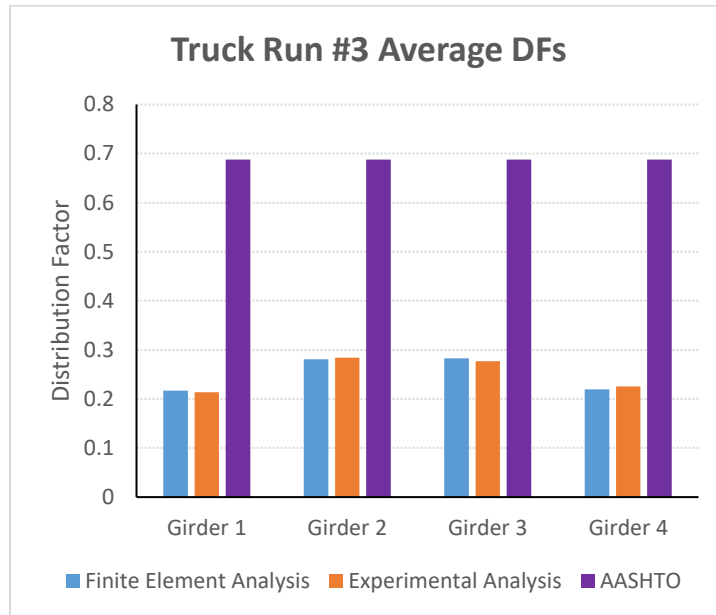


Figure 27: FEA LLDFs vs Experimental LLDFs vs AASHTO LLDFs Comparison for Truck Run 3

Per the findings of this data collection, AASHTO specifications were very conservative when computing distribution factors for the studied superstructure. In certain girders, the AASHTO Specifications predict a live load distribution factor three times higher than it should.

4.6 CONCLUSION

This chapter included a full benchmark experimental study of the field test performed by Gibbs on the Amish Sawmill Bridge, and finite element analysis (FEA) model. The data analyzed included bottom flange stresses at midspan and live load distribution factors for each girder in both one-lane-loaded and two-lanes-loaded scenarios. It has been found that the FEA model and the experimental data from field tests correlate very closely when compared to each other. On the contrary, AASHTO distribution factors tend to overestimate live load distribution factors due to its computation method being based solely on number of lanes and number of beams.

CHAPTER 5: PARAMETRIC ASSESSMENT OF LIVE LOAD DISTRIBUTION FACTORS

5.1 INTRODUCTION

A series of parametric studies were performed using the finite element modeling techniques discussed in Chapter 3. For each of these studies, a custom MATLAB script was written that would generate finite element models of the proposed composite bridge system based on desired input. The primary goal of these analyses was to explore the distribution factors of press-brake-formed steel tub girders under various design conditions and to generate more accurate live load distribution factors.

In order to evaluate the distribution factors under different design conditions, girder spacing (S), number of girders (N_b) and span length (L) were analyzed and described in the following sections in order to determine which parameter has influence in the live load distribution factor. The parametric matrices used in order to evaluate those parameters are described in the following sections.

5.2 DESCRIPTION OF PARAMETRIC MATRIX

As previously mentioned, MATLAB R2018b was used to perform the parametric study. A script was written that would generate “n” numbers of finite element models of the proposed bridge system. This script was then looped to generate a model for each increment of desired span length. For each of these studies, span lengths from 40 ft to 100 ft, in 5 ft increments were investigated in order to determine the maximum span range given AASHTO performance limits. The parametric assessment performed in this study did not investigate effects of skew, stiffness or deck thickness on live load distribution factors for press-brake tub girders. The main goals of these studies were to:

1. Understand which of the following parameters affect the computation of live load distribution factors for press-brake-formed steel tub girders: girder spacing (S), number of girders (N_b) and span length (L)
2. Compute more accurate live load distribution factors for AASHTO limit state evaluations

To assess and generate such distribution factors, the following sub sections of this thesis describe the parametric matrices that were developed.

5.2.1 Girder Spacing (S) & Span Length (L) Assessment

For this assessment, 91 analyses were performed. The following parameters were used to form the parametric matrix:

- Span length, L: [40ft to 100ft] in 5ft increments
- Girder spacing, S: [6ft to 12ft] in 1ft increments
- Overhang equals to girder spacing divided by two

Span Length [ft.]	40	45	50	55	60	65	70	75	80	85	90	95	100
Girder Spacing [ft.]	6	6	6	6	6	6	6	6	6	6	6	6	6
	7	7	7	7	7	7	7	7	7	7	7	7	7
	8	8	8	8	8	8	8	8	8	8	8	8	8
	9	9	9	9	9	9	9	9	9	9	9	9	9
	10	10	10	10	10	10	10	10	10	10	10	10	10
	11	11	11	11	11	11	11	11	11	11	11	11	11
	12	12	12	12	12	12	12	12	12	12	12	12	12

Table 8: Parametric Matrix for Girder Spacing (S) Assessment

The goal of this parametric analysis was to evaluate how girder spacing influences the computation of live load distribution given difference in span length. In addition, for each increment of span length in combination with each girder spacing increment, four separate analyses were performed with the following goals:

- Maximizing live load deflection to the exterior girder with one lane loaded
- Maximizing live load deflection to the exterior girder with two lanes loaded
- Maximizing live load deflection to the interior girder with one lane loaded
- Maximizing live load deflection to the interior girder with two lanes loaded

5.2.2 Number of Girders (N_b) Assessment

For this assessment, 105 analyses were performed. The following parameters were used to form the parametric matrix:

- Span length, L: [40ft, 70ft, 100ft]
- Girder spacing, S: [6ft, 9ft, 12ft]
- Number of beams, N_b : [4 to 8]
- Overhang equals to girder spacing divided by two

Number of Beams, N_b	4			5			6			7			8		
Span Length [ft.]	40	70	100	40	70	100	40	70	100	40	70	100	40	70	100
Girder Spacing [ft.]	6	6	6	6	6	6	6	6	6	6	6	6	6	6	6
	7	7	7	7	7	7	7	7	7	7	7	7	7	7	7
	8	8	8	8	8	8	8	8	8	8	8	8	8	8	8
	9	9	9	9	9	9	9	9	9	9	9	9	9	9	9
	10	10	10	10	10	10	10	10	10	10	10	10	10	10	10
	11	11	11	11	11	11	11	11	11	11	11	11	11	11	11
	12	12	12	12	12	12	12	12	12	12	12	12	12	12	12

Table 9: Parametric Matrix for Number of Girders (N_b) Assessment

5.3 EFFECT OF GIRDER SPACING (S) & SPAN LENGTH (L)

Using the methods described in Section 5.2.1 for the parametric study and the truck loading methodologies described in Chapter 4 of this report, analyses were performed using MATLAB R2018b to determine the live load distribution factors. The distribution factors (Y-axis) were plotted against the girder spacing (X-axis) as shown in Figure 28.

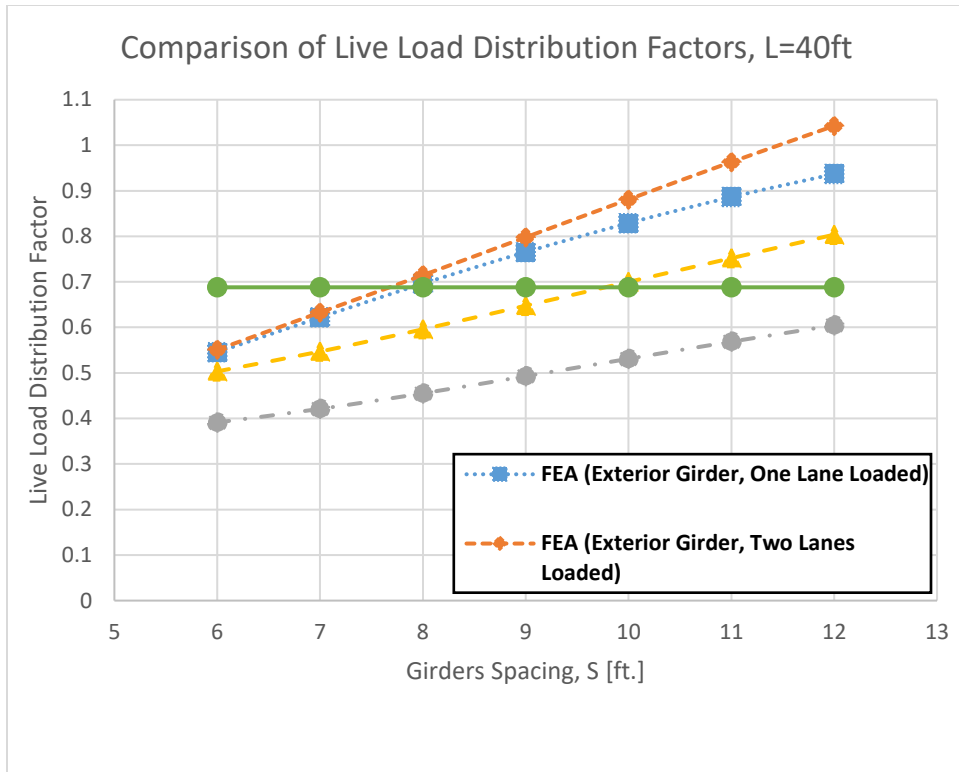


Figure 28: Comparison of Live Load Distribution Factors with Span Length of 40 feet

As shown in Figure 28, live load distribution factors for the exterior girders were higher than those for the interior girders. This difference in magnitude is primarily due to the ability of finite element analysis software (ABAQUS) to consider three-dimensional effects (i.e., twisting of the exterior girders due to transverse eccentricity of truck loading). In addition, according to Figure 28, AASHTO LRFD Distribution Factor seems to be only reliable if girder spacing is roughly kept less than 7.5 feet. It is important to reaffirm that AASHTO Distribution Factors calculations for box girders are based only on the number of loaded designed lanes and numbers of beams on a given bridge. AASHTO equation does not differentiate interior or exterior beam when distribution factors are analyzed. Figure 29 and Figure 30 show that AASHTO LRFD Distribution Factor for box girder fails to estimate distribution factors when girder spacing exceeds approximately 9 feet for bridge span length of 70 feet and girder spacing of 10.5 feet for bridge span length of 100 feet.

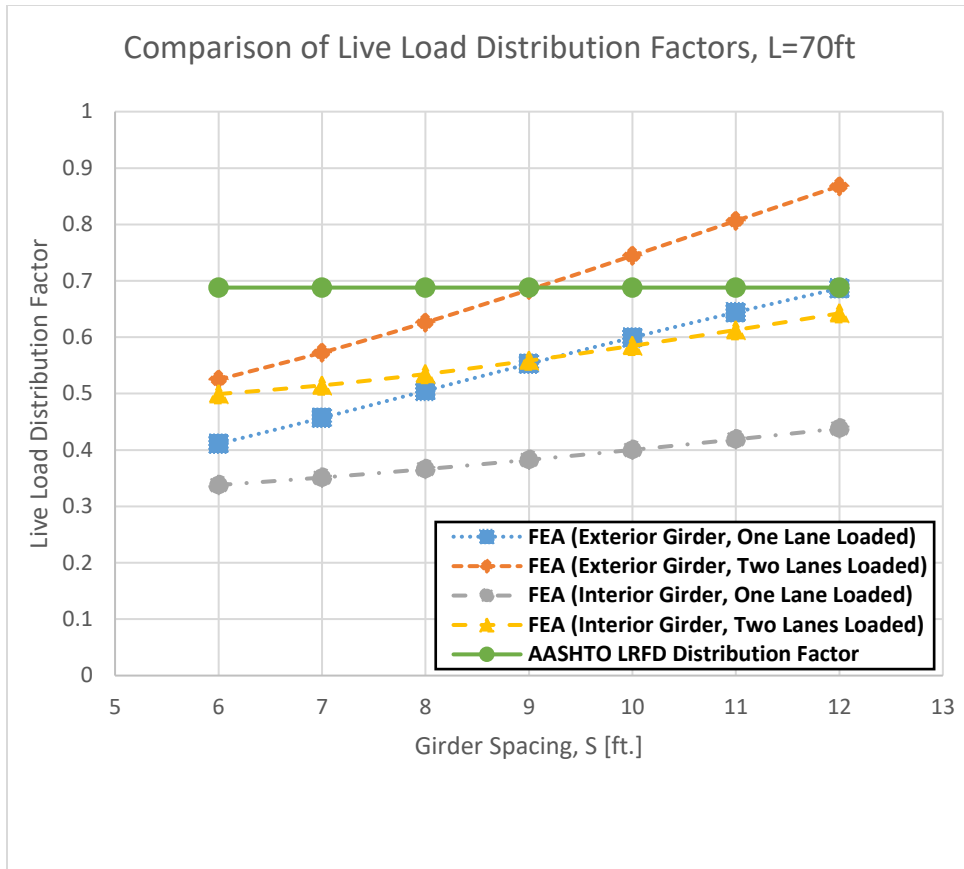


Figure 29: Comparison of Live Load Distribution Factors with Span Length of 70 feet

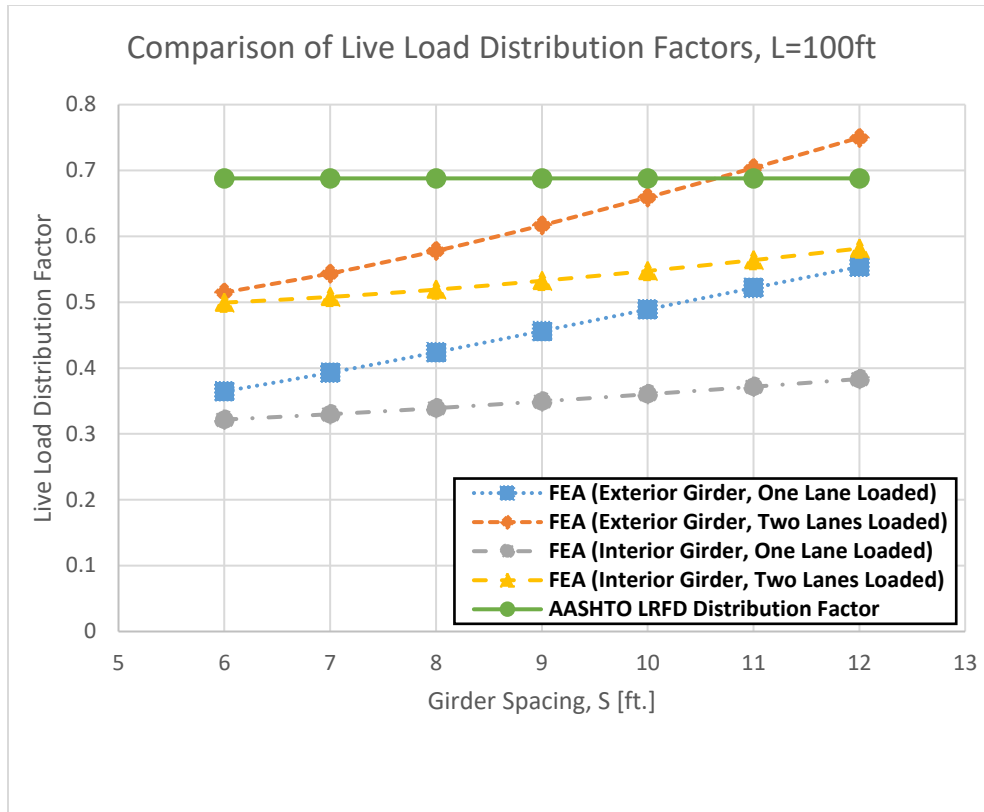


Figure 30: Comparison of Live Load Distribution Factors with Span Length of 100 feet

The same discrepancy could be found using AASHTO LRFD Distribution Factor calculations when a fixed girder spacing is kept and span length was variable. When girder spacing was kept below 7 feet, AASHTO LRFD Distribution Factor tended to overestimate the results for every tub girder length, see Figure 31 and Figure 32.

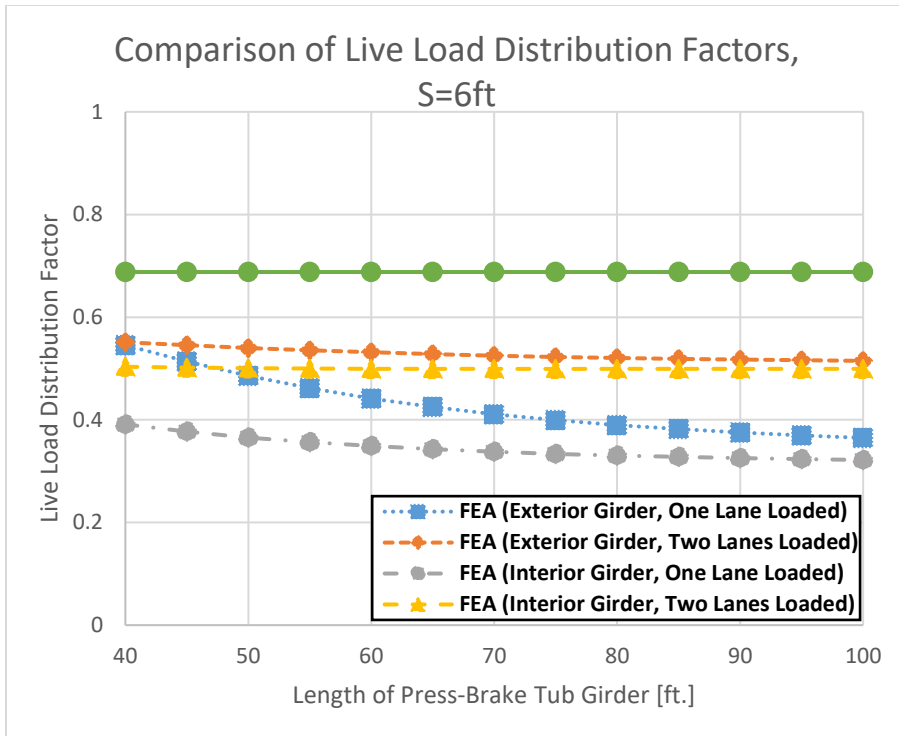


Figure 31: Comparison of Live Load Distribution Factors with Girder Spacing of 6 feet

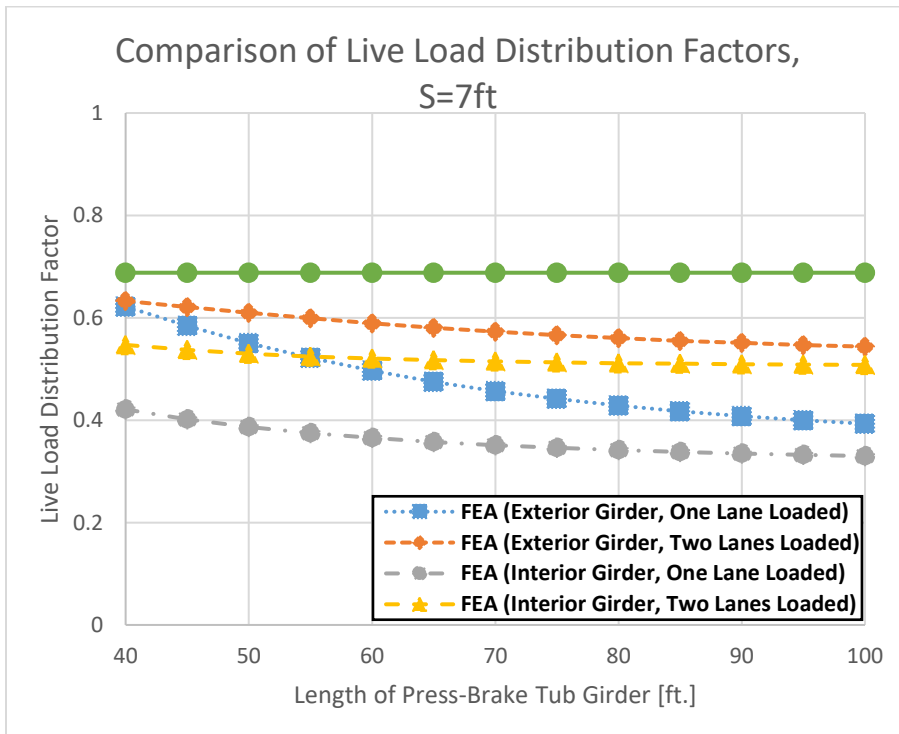


Figure 32: Comparison of Live Load Distribution Factors with Girder Spacing of 7 feet

However, when girder spacing was increased over 7 feet, AASHTO Live Load Distribution computations tended to overestimate its results for certain girders as well as

underestimate its results for others. For example, in Figure 33, AASHTO LLDF computations overestimated results for exterior girders spaced at 10 feet apart and up to 70 feet of length. This pattern repeated for any over 9 feet of girder spacing.

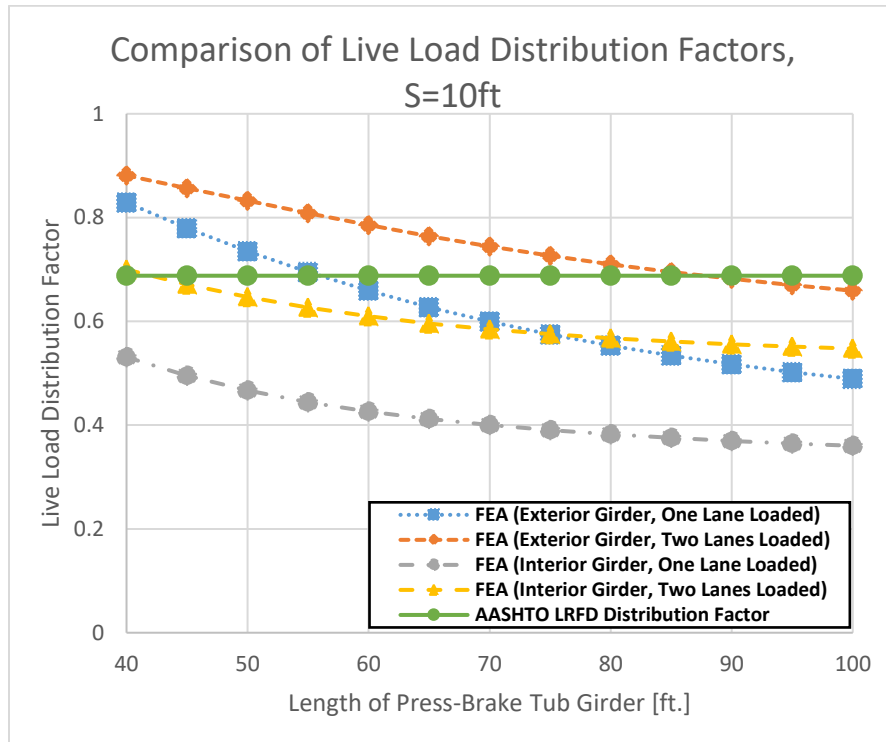


Figure 33: Comparison of Live Load Distribution Factors with Girder Spacing of 10 feet

All the other live load distribution comparisons, varying girder spacing, and span length contained in the S & L parametric matrix (Table 8) can be found in Appendix C.

5.4 EFFECT OF N_B

Using the methods described in Section 5.2.2 for the parametric study and the truck loading methodologies described in Chapter 4 of this report, analyses were performed using MATLAB R2018b to determine the live load distribution factors. The distribution factors (Y-axis) were plotted against the number of beams (X-axis) as shown in Figure 34.

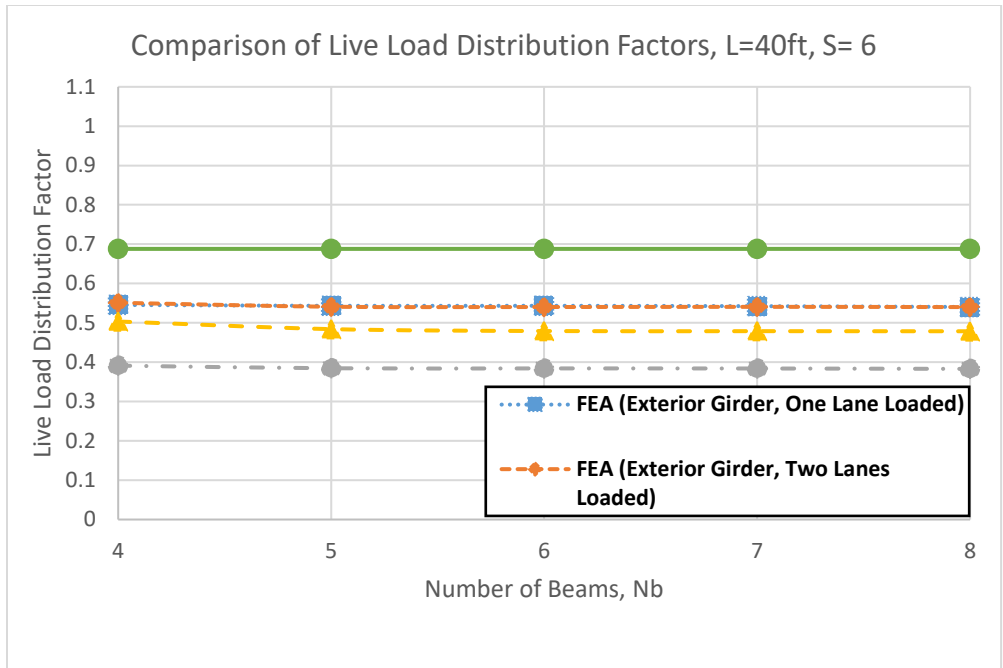


Figure 34: Comparison of Live Load Distribution Factors with Span Length of 40 feet and Girder Spacing of 6 feet

As shown in the previous figure, live load distribution factors remain nearly constant when compared against the number of beams. In addition, the same behavior is apparent when girder spacing is increased as shown in Figure 35 and Figure 36.

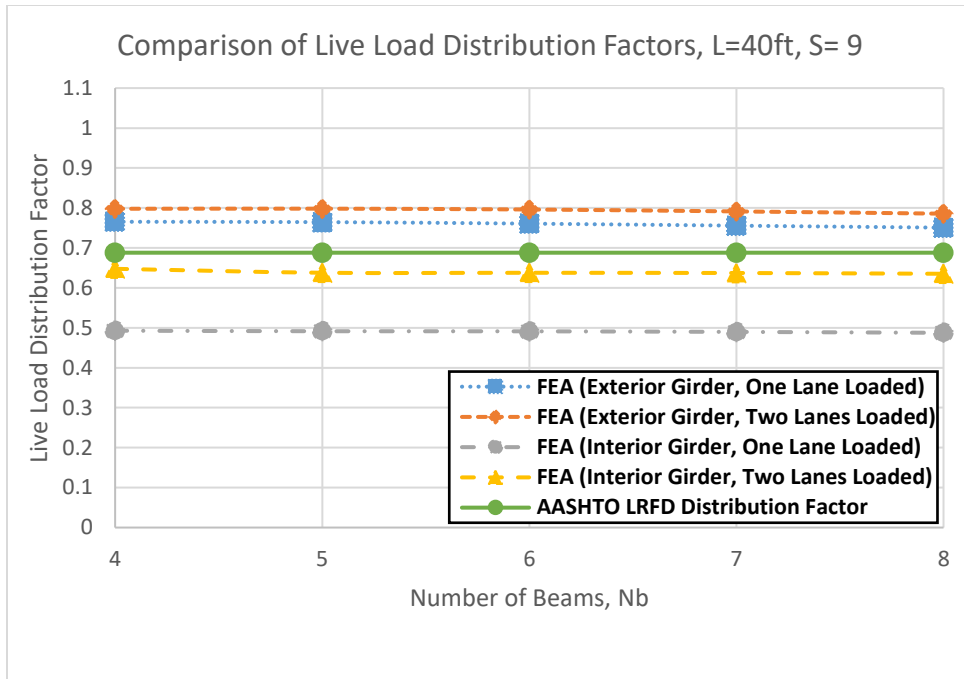


Figure 35: Comparison of Live Load Distribution Factors with Span Length of 40 feet and Girder Spacing of 9 feet

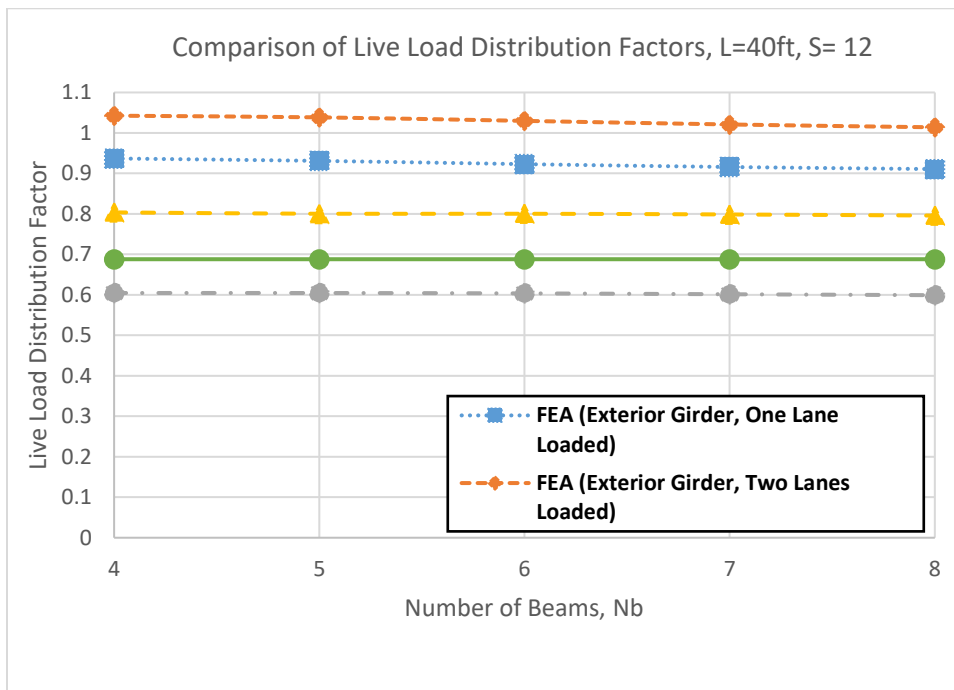


Figure 36: Comparison of Live Load Distribution Factors with Span Length of 40 feet and Girder Spacing of 12 feet

All the other live load distribution comparisons varying number of beams contained in the parametric matrix (Table 9) can be found in Appendix C.

5.5 CONCLUSION

This chapter detailed the results of a comprehensive suite of 196 finite element analyses. From these analyses, essential data were queried; these data points were used to create tabulated results, which have been provided in the appendices of this report. The proposed live load distribution factors tables for steel tub girders are presented in Table 10 through Table 16.

Girder Location	Girder Spacing of 6 Feet												
	Length of Girders, [feet]												
	40	45	50	55	60	65	70	75	80	85	90	95	100
Exterior Girder, One Lane Loaded	0.545	0.514	0.486	0.462	0.442	0.425	0.411	0.399	0.390	0.382	0.375	0.370	0.365
Exterior Girder, Two Lanes Loaded	0.551	0.545	0.540	0.536	0.531	0.528	0.525	0.523	0.520	0.519	0.517	0.516	0.515
Interior Girder, One Lane Loaded	0.391	0.377	0.366	0.356	0.349	0.343	0.338	0.334	0.330	0.328	0.325	0.323	0.322
Interior Girder, Two Lanes Loaded	0.503	0.502	0.501	0.500	0.500	0.499	0.499	0.499	0.499	0.499	0.499	0.499	0.499

Table 10: Live Load Distribution Factors for Tub Girders (Girder Spacing of 6 feet)

Girder Location	Girder Spacing of 7 Feet												
	Length of Girders, [feet]												
	40	45	50	55	60	65	70	75	80	85	90	95	100
Exterior Girder, One Lane Loaded	0.622	0.584	0.551	0.522	0.496	0.475	0.457	0.442	0.429	0.418	0.408	0.400	0.393
Exterior Girder, Two Lanes Loaded	0.633	0.621	0.610	0.599	0.589	0.580	0.573	0.566	0.560	0.555	0.551	0.547	0.544
Interior Girder, One Lane Loaded	0.421	0.402	0.387	0.375	0.365	0.358	0.351	0.346	0.342	0.338	0.335	0.332	0.330
Interior Girder, Two Lanes Loaded	0.547	0.537	0.530	0.524	0.520	0.517	0.515	0.513	0.511	0.510	0.509	0.509	0.508

Table 11: Live Load Distribution Factors for Tub Girders (Girder Spacing of 7 feet)

Girder Location	Girder Spacing of 8 Feet												
	Length of Girders, [feet]												
	40	45	50	55	60	65	70	75	80	85	90	95	100
Exterior Girder, One Lane Loaded	0.696	0.653	0.615	0.582	0.552	0.527	0.505	0.486	0.470	0.456	0.444	0.433	0.424
Exterior Girder, Two Lanes Loaded	0.715	0.698	0.682	0.666	0.652	0.638	0.626	0.615	0.606	0.598	0.590	0.584	0.578
Interior Girder, One Lane Loaded	0.455	0.430	0.411	0.396	0.384	0.374	0.366	0.360	0.354	0.349	0.346	0.342	0.339
Interior Girder, Two Lanes Loaded	0.596	0.579	0.566	0.555	0.547	0.540	0.535	0.531	0.527	0.525	0.522	0.521	0.519

Table 12: Live Load Distribution Factors for Tub Girders (Girder Spacing of 8 feet)

Girder Location	Girder Spacing of 9 Feet												
	Length of Girders, [feet]												
	40	45	50	55	60	65	70	75	80	85	90	95	100
Exterior Girder, One Lane Loaded	0.765	0.719	0.677	0.640	0.607	0.578	0.553	0.531	0.512	0.495	0.480	0.468	0.456
Exterior Girder, Two Lanes Loaded	0.798	0.777	0.756	0.736	0.718	0.700	0.684	0.669	0.656	0.645	0.634	0.625	0.617
Interior Girder, One Lane Loaded	0.493	0.462	0.438	0.419	0.404	0.392	0.383	0.375	0.368	0.362	0.357	0.353	0.349
Interior Girder, Two Lanes Loaded	0.648	0.625	0.606	0.590	0.577	0.567	0.558	0.552	0.546	0.542	0.538	0.535	0.533

Table 13: Live Load Distribution Factors for Tub Girders (Girder Spacing of 9 feet)

Girder Location	Girder Spacing of 10 Feet												
	Length of Girders, [feet]												
	40	45	50	55	60	65	70	75	80	85	90	95	100
Exterior Girder, One Lane Loaded	0.829	0.780	0.735	0.695	0.659	0.627	0.599	0.575	0.553	0.534	0.517	0.502	0.489
Exterior Girder, Two Lanes Loaded	0.881	0.857	0.832	0.808	0.786	0.764	0.745	0.727	0.710	0.695	0.682	0.670	0.659
Interior Girder, One Lane Loaded	0.531	0.495	0.467	0.444	0.426	0.412	0.400	0.391	0.382	0.376	0.370	0.365	0.360
Interior Girder, Two Lanes Loaded	0.700	0.671	0.647	0.627	0.610	0.596	0.585	0.575	0.568	0.561	0.556	0.551	0.547

Table 14: Live Load Distribution Factors for Tub Girders (Girder Spacing of 10 feet)

Girder Location	Girder Spacing of 11 Feet												
	Length of Girders, [feet]												
	40	45	50	55	60	65	70	75	80	85	90	95	100
Exterior Girder, One Lane Loaded	0.886	0.835	0.789	0.747	0.709	0.675	0.644	0.617	0.593	0.572	0.553	0.537	0.522
Exterior Girder, Two Lanes Loaded	0.963	0.936	0.908	0.881	0.854	0.830	0.806	0.785	0.766	0.748	0.732	0.717	0.704
Interior Girder, One Lane Loaded	0.569	0.529	0.497	0.471	0.450	0.433	0.419	0.407	0.398	0.390	0.383	0.377	0.372
Interior Girder, Two Lanes Loaded	0.752	0.719	0.690	0.665	0.645	0.627	0.613	0.601	0.591	0.582	0.575	0.569	0.564

Table 15: Live Load Distribution Factors for Tub Girders (Girder Spacing of 11 feet)

Girder Location	Girder Spacing of 12 Feet												
	Length of Girders, [feet]												
	40	45	50	55	60	65	70	75	80	85	90	95	100
Exterior Girder, One Lane Loaded	0.937	0.885	0.838	0.794	0.755	0.719	0.687	0.658	0.632	0.609	0.589	0.570	0.554
Exterior Girder, Two Lanes Loaded	1.043	1.012	0.982	0.951	0.922	0.894	0.868	0.844	0.822	0.801	0.782	0.765	0.750
Interior Girder, One Lane Loaded	0.605	0.562	0.526	0.497	0.474	0.454	0.438	0.425	0.414	0.404	0.396	0.389	0.383
Interior Girder, Two Lanes Loaded	0.804	0.766	0.733	0.705	0.680	0.660	0.642	0.628	0.615	0.605	0.596	0.588	0.582

Table 16: Live Load Distribution Factors for Tub Girders (Girder Spacing of 12 feet)

CHAPTER 6: SUMMARY & CONCLUDING REMARKS

6.1 PROJECT SUMMARY AND CONCLUSIONS

The scope of this thesis was to develop more accurate live load distribution factors for exterior and interior girders in press-brake-formed steel tub girder superstructures. As mentioned in Section 1.2, the objectives of this thesis were as follows:

- Assessment and discussion of AASHTO specifications for box section flexural members (tub girders), as well as the computation of live LLDFs using AASHTO standards.
- Finite element analysis of Amish Sawmill Bridge to benchmark against experimental data in order to generate analytical live load distribution factors.
- Field performance assessment of Amish Sawmill Bridge to validate finite element model as well as a description of experimental investigation and testing procedures conducted by Gibbs, 2017.
- Comparison of analytical and experimental LLDFs using AASHTO specifications.
- Parametric study to understand which parameters affect the computation of live load distribution factors for steel tub girders and to compute more accurate live load distribution factors for AASHTO limit state evaluations.

Based on the results drawn from this study, press-brake-formed steel tub girders exhibit consistent performance and are a practical option in short span bridge construction. However, the current AASHTO LRFD Specifications can overestimate distribution factors for interior girders and fail to estimate distribution factors for exterior girders depending on girder spacing and length of bridge.

6.2 RECOMMENDATIONS FOR CONTINUED RESEARCH

The author recommends the following tasks for future work:

- Expand parametric matrices in this project to include more parameters to verify proposed live load distribution factors.
- Investigate other parameters to determine their effect on live load distribution factor, such as:
 - Skew
 - Deck thickness
 - Girder stiffness
- Assess and develop specifications to more accurately calculate the distribution of live load shear.
- Determine if the live load distribution factors proposed in this study can be safely used for different types of box girders.

REFERENCES

- American Association of State Highway and Transportation Officials (2014). *AASHTO LRFD Bridge Design Specifications, Seventh Edition*. Washington, DC, AASHTO.
- American Association of State Highway Officials. (1931). *AASHTO Standard Specifications for Highway Bridges, First Edition*. Washington, DC.
- Barth, K. E., Michaelson G. K., Barker, M. G., (2015). Development and Experimental Validation of Composite Press Brake-Formed Modular Steel Tub Girders for Short-Span Bridges. *ASCE Journal of Bridge Engineering*, 20 (11).
- Bridge Diagnostics, Inc. (n.d.). STS-WiFi Operations Manual. Boulder, CO.
- Burner, K. A. (2010). *Experimental Investigation of Folded Plate Girders and Slab Joints Used in Modular Construction*. Department of Civil Engineering. Lincoln, NE, University of Nebraska-Lincoln. Master of Science.
- Chandar, G., Hyzak, M. D., et al. (2010). *Rapid Economical Bridge Replacement. Modern Steel Construction*. Chicago, IL, National Steel Bridge Alliance. 2010.
- Dassault-Systèmes (2010). Abaqus/CAE. Providence, RI, Dassault Systèmes Simulia Corp.
- Eom, J., & Nowak, A. S. (2001). Live Load Distribution for Steel Girder Bridges. *ASCE Journal of Bridge Engineering*, 489-4
- Gibbs, C. L. (2017). *Field Performance Assessment of Press-Brake-Formed Steel Tub Girder Superstructures*. Department of Civil & Environmental Engineering. Morgantown, WV, West Virginia University. Master of Science.
- Glaser, L. A. (2010). *Constructability Testing of Folded Plate Girders*. Department of Civil Engineering. Lincoln, NE, University of Nebraska-Lincoln. Master of Science.
- Kelly, L. T. (2014). *Experimental Evaluation of Non-Composite Shallow Press-Brake-Formed Steel Tub Girders*. Department of Civil & Environmental Engineering. Morgantown, WV, West Virginia University. Master of Science.
- Kim, S., & Nowak, A. S. (1997). Load Distribution and Impact Factors for I-Girders. *ASCE Journal of Bridge Engineering*, 97-104.
- Mabsout, M. E., Tarhini, K. M., Frederick, G. R., & Kobrosly, M. (1997). Influence of Sidewalks and Railings on Wheel Load Distribution in Steel Girder Bridges. *ASCE Journal of Bridge Engineering*, 88-96

- Michaelson, G. K. (2014). *Development and Feasibility Assessment of Shallow Press-Brake-Formed Steel Tub Girders for Short-Span Bridge Applications*. Department of Civil & Environmental Engineering. Morgantown, WV, West Virginia University. Doctor of Philosophy.
- Nakamura, S. (2002). Bending Behavior of Composite Girders with Cold Formed Steel U Section. *ASCE Journal of Structural Engineering* 128 (9): 8
- Newmark, N. M. (1938). A Distribution Procedure for the Analysis of Slabs Continuous over Flexible Girders. *University of Illinois, Engineering Experiment Station Bulletin No. 304*, 7-118
- Newmark N. M. (1949). Design of I-Beam Bridges, *Bridge Floors*.
- Newmark, N. M., & Siess, C. P. (1942). Moments in I-beam Bridges. University of Illinois, *Engineering Experiment Station Bulletin No. 336, Volume XXXIX*, 1-148.
- Nutt, R. V., Schamber, R. A. & Zokaie, T. (1988). Distribution of Wheel Loads on Highway Bridges, *NCHRP Final Report 12-26*.
- Righman, J. E. (2005). *Rotation Compatibility Approach to Moment Redistribution for Design and Rating of Steel I-Girders*. Department of Civil & Environmental Engineering. Morgantown, WV, West Virginia University. Doctor of Philosophy.
- Roberts, N. R. (2004). *Evaluation of the Ductility of Composite Steel I-Girders in Positive Bending*. Department of Civil & Environmental Engineering. Morgantown, WV, West Virginia University. Master of Science
- Short Span Steel Bridge Alliance (2016). *Amish Sawmill Bridge: An Innovative Steel Solution for Short Span Bridge Design*. <http://www.shortspansteelbridges.org/case-studies/casestudies-folder/amish-sawmill-bridge---an-innovative-steel-solution.aspx>.
- Taly, N. and Gangarao, H. (1979). Prefabricated Press-Formed Steel T-Box Girder Bridge System. *AISC Engineering Journal* 16 (3):9.
- Tarhini, K. M. & Frederick, G. R. (1992). Wheel Load Distribution in I-Girder Highway Bridges, *ASCE Journal of Structural Engineering*, 118(5).
- Tarhini, K. M., Mabsout, M. & Kobrosly, M. (1996). Effect of Sidewalks and Railings on Wheel Load Distribution in Steel Girder Bridges, *3rd ASCE Computing in Engineering Congress*.
- Walker, W. H. (1987). Lateral Load Distribution in Multi-girder Bridges, *AISC Engineering Journal, First Quarter*.

Yang, L. (2004). *Evaluation of Moment Redistribution for Hybrid HPS 70W Bridge Girders*. Department of Civil & Environmental Engineering. Morgantown, WV, West Virginia University. Master of Science.

Zokaie, T. (2000). AASHTO-LRFD Live Load Distribution Specifications, *ASCE Journal of Bridge Engineering*, 5(2).

APPENDIX A: APPROVAL LETTER



Office of Research Integrity

April 11, 2019

Guilherme De Oliveira Petty Santana
1408 6th Ave, Apt 9
Huntington, WV 25701

Dear Guilherme:

This letter is in response to the submitted thesis abstract entitled "*Assessment of Live Load Distribution Characteristics of Press-Brake-Formed Tub Girder Superstructures.*" After assessing the abstract, it has been deemed not to be human subject research and therefore exempt from oversight of the Marshall University Institutional Review Board (IRB). The Code of Federal Regulations (45CFR46) has set forth the criteria utilized in making this determination. Since the information in this study does not involve human subjects as defined in the above referenced instruction, it is not considered human subject research. If there are any changes to the abstract you provided then you would need to resubmit that information to the Office of Research Integrity for review and a determination.

I appreciate your willingness to submit the abstract for determination. Please feel free to contact the Office of Research Integrity if you have any questions regarding future protocols that may require IRB review.

Sincerely,

Bruce F. Day, ThD, CIP
Director

WE ARE... MARSHALL.

One John Marshall Drive • Huntington, West Virginia 25755 • Tel 304/696-4303
A State University of West Virginia • An Affirmative Action/Equal Opportunity Employer

APPENDIX B: RESULTS OF BENCHMARK ANALYSIS

This appendix contains the complete collection of tabulated data, graphs and diagrams utilized for the benchmark analysis.

Truck Run 1, Distribution Factors (Finite Element Analysis)									
Panel Points		Averages				Distribution Factors			
x (ft)	x/L	G1	G2	G3	G4	G1	G2	G3	G4
0	0	0	0	0	0	---	---	---	---
5.2	0.1	47.32	33.68	21.64	14.29	0.405	0.288	0.185	0.122
10.4	0.2	79.11	56.38	33.73	22.19	0.413	0.295	0.176	0.116
15.6	0.3	98.49	69.50	42.23	27.13	0.415	0.293	0.178	0.114
20.8	0.4	112.36	77.75	46.35	29.09	0.423	0.293	0.175	0.110
26	0.5	128.92	86.70	45.88	28.27	0.445	0.299	0.158	0.098
31.2	0.6	116.89	78.36	40.93	24.87	0.448	0.300	0.157	0.095
36.4	0.7	84.79	57.98	33.46	20.15	0.432	0.295	0.170	0.103
41.6	0.8	53.37	38.01	24.47	14.56	0.409	0.292	0.188	0.112
46.8	0.9	30.26	22.20	15.22	9.04	0.394	0.289	0.198	0.118
52	1	0	0	0	0	---	---	---	---
					Average	0.420	0.294	0.176	0.110
					St. Dev.	0.018	0.004	0.013	0.009

Truck Run 2, Distribution Factors (Finite Element Analysis)									
Panel Points		Averages				Distribution Factors			
x (ft)	x/L	G1	G2	G3	G4	G1	G2	G3	G4
0	0	0	0	0	0	---	---	---	---
5.2	0.1	40.91	34.04	24.76	16.89	0.351	0.292	0.212	0.145
10.4	0.2	69.22	57.82	38.32	25.50	0.363	0.303	0.201	0.134
15.6	0.3	86.18	71.17	48.20	31.14	0.364	0.301	0.204	0.132
20.8	0.4	97.36	80.58	53.48	33.47	0.368	0.304	0.202	0.126
26	0.5	109.47	93.11	53.99	32.61	0.379	0.322	0.187	0.113
31.2	0.6	99.17	84.28	48.41	28.71	0.381	0.323	0.186	0.110
36.4	0.7	71.25	58.66	38.24	22.66	0.373	0.307	0.200	0.119
41.6	0.8	47.49	37.59	27.89	16.94	0.366	0.289	0.215	0.130
46.8	0.9	27.59	21.33	17.07	10.44	0.361	0.279	0.223	0.137
52	1	0	0	0	0	---	---	---	---
					Average	0.367	0.302	0.203	0.127
					St. Dev.	0.009	0.014	0.012	0.011

Truck Run 3, Distribution Factors (Finite Element Analysis)									
Panel Points		Averages				Distribution Factors			
x (ft)	x/L	G1	G2	G3	G4	G1	G2	G3	G4
0	0	0	0	0	0	---	---	---	---
5.2	0.1	26.20	31.70	31.88	26.58	0.225	0.272	0.274	0.228
10.4	0.2	40.80	53.90	54.22	41.45	0.214	0.283	0.285	0.218
15.6	0.3	51.34	66.26	66.65	52.14	0.217	0.280	0.282	0.221
20.8	0.4	56.62	74.74	75.26	57.49	0.214	0.283	0.285	0.218
26	0.5	56.64	86.12	86.91	57.55	0.197	0.300	0.303	0.200
31.2	0.6	50.84	78.42	79.12	51.59	0.196	0.302	0.304	0.198
36.4	0.7	40.44	54.31	54.64	40.95	0.212	0.285	0.287	0.215
41.6	0.8	29.97	34.64	34.67	30.19	0.231	0.268	0.268	0.233
46.8	0.9	18.54	19.51	19.45	18.60	0.244	0.256	0.256	0.244
52	1	0	0	0	0	---	---	---	---
				Average		0.217	0.281	0.283	0.220
				St. Dev.		0.015	0.014	0.016	0.015

Truck Run 4, Distribution Factors (Finite Element Analysis)									
Panel Points		Averages				Distribution Factors			
x (ft)	x/L	G1	G2	G3	G4	G1	G2	G3	G4
0	0	0	0	0	0	---	---	---	---
5.2	0.1	22.02	29.43	33.36	31.48	0.189	0.253	0.287	0.271
10.4	0.2	34.28	49.33	56.63	50.33	0.180	0.259	0.297	0.264
15.6	0.3	42.76	60.82	69.66	63.16	0.181	0.257	0.295	0.267
20.8	0.4	46.68	67.73	79.56	70.11	0.177	0.256	0.301	0.265
26	0.5	46.02	74.77	93.76	72.70	0.160	0.260	0.326	0.253
31.2	0.6	40.98	67.84	85.41	65.64	0.158	0.261	0.329	0.253
36.4	0.7	32.62	49.10	57.96	50.77	0.171	0.258	0.304	0.267
41.6	0.8	24.60	32.88	35.87	36.20	0.190	0.254	0.277	0.279
46.8	0.9	15.33	19.10	19.82	21.85	0.201	0.251	0.260	0.287
52	1	0	0	0	0	---	---	---	---
				Average		0.179	0.257	0.297	0.267
				St. Dev.		0.014	0.003	0.022	0.011

Truck Run 5, Distribution Factors (Finite Element Analysis)									
Panel Points		Averages				Distribution Factors			
x (ft)	x/L	G1	G2	G3	G4	G1	G2	G3	G4
0	0	0	0	0	0	---	---	---	---
5.2	0.1	18.82	27.12	34.08	36.35	0.162	0.233	0.293	0.312
10.4	0.2	28.91	43.08	57.81	60.90	0.152	0.226	0.303	0.319
15.6	0.3	35.65	53.96	71.16	75.76	0.151	0.228	0.301	0.320
20.8	0.4	38.54	59.90	81.26	84.70	0.146	0.227	0.307	0.320
26	0.5	37.77	62.10	95.30	92.34	0.131	0.216	0.331	0.321
31.2	0.6	33.47	56.08	86.84	83.82	0.129	0.216	0.334	0.322
36.4	0.7	26.67	43.31	59.14	61.45	0.140	0.227	0.310	0.322
41.6	0.8	19.99	30.55	36.87	42.30	0.154	0.236	0.284	0.326
46.8	0.9	12.55	18.39	20.46	24.86	0.165	0.241	0.268	0.326
52	1	0	0	0	0	---	---	---	---
					Average	0.148	0.228	0.304	0.321
					St. Dev.	0.012	0.008	0.021	0.004

Panel Points		Averages				Distribution Factors			
x (ft)	x/L	G1	G2	G3	G4	G1	G2	G3	G4
0	0	0	0	0	0	---	---	---	---
5.2	0.1	69.34	63.12	54.99	45.77	0.595	0.541	0.472	0.392
10.4	0.2	113.38	105.71	90.35	72.52	0.594	0.554	0.473	0.380
15.6	0.3	141.25	130.33	111.89	90.29	0.596	0.550	0.472	0.381
20.8	0.4	159.04	145.48	125.91	99.20	0.601	0.549	0.475	0.375
26	0.5	174.94	161.47	139.64	100.96	0.606	0.560	0.484	0.350
31.2	0.6	157.88	146.20	126.34	90.50	0.606	0.561	0.485	0.347
36.4	0.7	117.41	107.08	91.42	70.92	0.607	0.554	0.473	0.367
41.6	0.8	77.97	70.90	60.34	50.76	0.600	0.545	0.464	0.391
46.8	0.9	45.59	41.30	35.04	30.89	0.597	0.541	0.459	0.404
52	1	0	0	0	0	---	---	---	---
					Average	0.600	0.551	0.473	0.376
					St. Dev.	0.005	0.007	0.008	0.019

Truck Runs 2 & 5, Distribution Factors (Finite Element Analysis)									
Panel Points		Averages				Distribution Factors			
x (ft)	x/L	G1	G2	G3	G4	G1	G2	G3	G4
0	0	0	0	0	0	---	---	---	---
5.2	0.1	59.73	61.17	58.83	53.25	0.513	0.525	0.505	0.457
10.4	0.2	98.13	100.90	96.13	86.40	0.514	0.529	0.504	0.453
15.6	0.3	121.84	125.12	119.36	106.90	0.515	0.529	0.504	0.452
20.8	0.4	135.89	140.48	134.74	118.17	0.513	0.531	0.509	0.447
26	0.5	147.24	155.20	149.29	124.95	0.511	0.538	0.518	0.433
31.2	0.6	132.64	140.35	135.25	112.53	0.509	0.539	0.519	0.432
36.4	0.7	97.91	101.98	97.38	84.11	0.513	0.535	0.511	0.441
41.6	0.8	67.48	68.14	64.76	59.24	0.520	0.525	0.499	0.456
46.8	0.9	40.14	39.72	37.53	35.30	0.526	0.520	0.492	0.462
52	1	0	0	0	0	---	---	---	---
					Average	0.515	0.530	0.507	0.448
					St. Dev.	0.005	0.006	0.009	0.011

Truck Run 1, Bending Stress (FEA)					
Panel Points		Average Stress (ksi)			
x (ft)	x/L	G1	G2	G3	G4
0	0	0	0	0	0
5.2	0.1	1.37	0.98	0.63	0.41
10.4	0.2	2.29	1.63	0.98	0.64
15.6	0.3	2.86	2.02	1.22	0.79
20.8	0.4	3.26	2.25	1.34	0.84
26	0.5	3.74	2.51	1.33	0.82
31.2	0.6	3.39	2.27	1.19	0.72
36.4	0.7	2.46	1.68	0.97	0.58
41.6	0.8	1.55	1.10	0.71	0.42
46.8	0.9	0.88	0.64	0.44	0.26
52	1	0	0	0	0

Truck Run 2, Bending Stress (FEA)					
Panel Points		Average Stress (ksi)			
x (ft)	x/L	G1	G2	G3	G4
0	0	0	0	0	0
5.2	0.1	1.19	0.99	0.72	0.49
10.4	0.2	2.01	1.68	1.11	0.74
15.6	0.3	2.50	2.06	1.40	0.90
20.8	0.4	2.82	2.34	1.55	0.97
26	0.5	3.17	2.70	1.57	0.95
31.2	0.6	2.88	2.44	1.40	0.83
36.4	0.7	2.07	1.70	1.11	0.66
41.6	0.8	1.38	1.09	0.81	0.49
46.8	0.9	0.80	0.62	0.49	0.30
52	1	0	0	0	0

Truck Run 3, Bending Stress (FEA)					
Panel Points		Average Stress (ksi)			
x (ft)	x/L	G1	G2	G3	G4
0	0	0	0	0	0
5.2	0.1	0.76	0.92	0.92	0.77
10.4	0.2	1.18	1.56	1.57	1.20
15.6	0.3	1.49	1.92	1.93	1.51
20.8	0.4	1.64	2.17	2.18	1.67
26	0.5	1.64	2.50	2.52	1.67
31.2	0.6	1.47	2.27	2.29	1.50
36.4	0.7	1.17	1.58	1.58	1.19
41.6	0.8	0.87	1.00	1.01	0.88
46.8	0.9	0.54	0.57	0.56	0.54
52	1	0	0	0	0

Truck Run 4, Bending Stress (FEA)					
Panel Points		Average Stress (ksi)			
x (ft)	x/L	G1	G2	G3	G4
0	0	0	0	0	0
5.2	0.1	0.64	0.85	0.97	0.91
10.4	0.2	0.99	1.43	1.64	1.46
15.6	0.3	1.24	1.76	2.02	1.83
20.8	0.4	1.35	1.96	2.31	2.03
26	0.5	1.33	2.17	2.72	2.11
31.2	0.6	1.19	1.97	2.48	1.90
36.4	0.7	0.95	1.42	1.68	1.47
41.6	0.8	0.71	0.95	1.04	1.05
46.8	0.9	0.44	0.55	0.57	0.63
52	1	0	0	0	0

Truck Run 5, Bending Stress (FEA)					
Panel Points		Average Stress (ksi)			
x (ft)	x/L	G1	G2	G3	G4
0	0	0	0	0	0
5.2	0.1	0.55	0.79	0.99	1.05
10.4	0.2	0.84	1.25	1.68	1.77
15.6	0.3	1.03	1.56	2.06	2.20
20.8	0.4	1.12	1.74	2.36	2.46
26	0.5	1.10	1.80	2.76	2.68
31.2	0.6	0.97	1.63	2.52	2.43
36.4	0.7	0.77	1.26	1.71	1.78
41.6	0.8	0.58	0.89	1.07	1.23
46.8	0.9	0.36	0.53	0.59	0.72
52	1	0	0	0	0

Truck Runs 1 & 4, Bending Stress (FEA)					
Panel Points		Average Stress (ksi)			
x (ft)	x/L	G1	G2	G3	G4
0	0	0	0	0	0
5.2	0.1	2.01	1.83	1.59	1.33
10.4	0.2	3.29	3.07	2.62	2.10
15.6	0.3	4.10	3.78	3.24	2.62
20.8	0.4	4.61	4.22	3.65	2.88
26	0.5	5.07	4.68	4.05	2.93
31.2	0.6	4.58	4.24	3.66	2.62
36.4	0.7	3.40	3.11	2.65	2.06
41.6	0.8	2.26	2.06	1.75	1.47
46.8	0.9	1.32	1.20	1.02	0.90
52	1	0	0	0	0

Truck Runs 2 & 5, Bending Stress (FEA)					
Panel Points		Average Stress (ksi)			
x (ft)	x/L	G1	G2	G3	G4
0	0	0	0	0	0
5.2	0.1	1.73	1.77	1.71	1.54
10.4	0.2	2.85	2.93	2.79	2.51
15.6	0.3	3.53	3.63	3.46	3.10
20.8	0.4	3.94	4.07	3.91	3.43
26	0.5	4.27	4.50	4.33	3.62
31.2	0.6	3.85	4.07	3.92	3.26
36.4	0.7	2.84	2.96	2.82	2.44
41.6	0.8	1.96	1.98	1.88	1.72
46.8	0.9	1.16	1.15	1.09	1.02
52	1	0	0	0	0

Truck Run 1, Distribution Factors (Experimental)									
Panel Points		Averages				Distribution Factors			
x (ft)	x/L	G1	G2	G3	G4	G1	G2	G3	G4
0	0	0	0	0	0	---	---	---	---
5.2	0.1	19.78	13.54	8.45	5.75	0.416	0.285	0.178	0.121
10.4	0.2	36.33	24.33	12.12	7.32	0.454	0.304	0.151	0.091
15.6	0.3	42.28	26.90	14.46	10.24	0.450	0.287	0.154	0.109
20.8	0.4	49.14	29.48	15.71	12.28	0.461	0.277	0.147	0.115
26	0.5	65.10	36.80	16.05	12.70	0.498	0.282	0.123	0.097
31.2	0.6	59.81	32.46	13.38	11.89	0.509	0.276	0.114	0.101
36.4	0.7	33.12	18.66	9.63	9.41	0.468	0.263	0.136	0.133
41.6	0.8	15.55	8.72	5.77	9.16	0.397	0.222	0.147	0.234
46.8	0.9	3.08	1.41	0.93	3.87	0.331	0.152	0.100	0.417
52	1	0	0	0	0	---	---	---	---
					Average	0.443	0.261	0.139	0.158
					St. Dev.	0.055	0.047	0.024	0.106

Truck Run 2, Distribution Factors (Experimental)									
Panel Points		Averages				Distribution Factors			
x (ft)	x/L	G1	G2	G3	G4	G1	G2	G3	G4
0	0	0	0	0	0	---	---	---	---
5.2	0.1	16.48	12.99	9.36	7.27	0.357	0.282	0.203	0.158
10.4	0.2	31.44	25.97	14.85	11.02	0.378	0.312	0.178	0.132
15.6	0.3	37.33	29.02	18.12	12.22	0.386	0.300	0.187	0.126
20.8	0.4	43.56	34.07	21.25	13.86	0.386	0.302	0.188	0.123
26	0.5	56.68	45.54	21.16	13.93	0.413	0.332	0.154	0.101
31.2	0.6	52.10	40.47	18.52	12.39	0.422	0.328	0.150	0.100
36.4	0.7	30.64	23.08	13.81	8.56	0.403	0.303	0.182	0.113
41.6	0.8	15.95	11.90	8.68	6.69	0.369	0.275	0.201	0.155
46.8	0.9	7.06	5.97	4.81	4.38	0.318	0.269	0.216	0.197
52	1	0	0	0	0	---	---	---	---
					Average	0.381	0.300	0.184	0.134
					St. Dev.	0.031	0.022	0.022	0.031

Truck Run 3, Distribution Factors (Experimental)									
Panel Points		Averages				Distribution Factors			
x (ft)	x/L	G1	G2	G3	G4	G1	G2	G3	G4
0	0	0	0	0	0	---	---	---	---
5.2	0.1	11.50	12.88	12.69	9.95	0.245	0.274	0.270	0.212
10.4	0.2	16.95	24.16	24.59	15.61	0.208	0.297	0.302	0.192
15.6	0.3	21.85	27.11	27.14	20.67	0.226	0.280	0.280	0.214
20.8	0.4	25.67	33.46	32.26	24.15	0.222	0.290	0.279	0.209
26	0.5	26.37	45.65	42.93	26.31	0.187	0.323	0.304	0.186
31.2	0.6	22.54	41.11	37.84	22.85	0.181	0.331	0.304	0.184
36.4	0.7	15.79	21.22	20.05	15.41	0.218	0.293	0.277	0.213
41.6	0.8	8.81	9.57	9.43	10.89	0.228	0.247	0.244	0.281
46.8	0.9	4.13	4.49	4.60	6.74	0.207	0.225	0.230	0.338
52	1	0	0	0	0	---	---	---	---
					Average	0.213	0.284	0.277	0.225
					St. Dev.	0.020	0.033	0.026	0.051

Truck Run 4, Distribution Factors (Experimental)									
Panel Points		Averages				Distribution Factors			
x (ft)	x/L	G1	G2	G3	G4	G1	G2	G3	G4
0	0	0	0	0	0	---	---	---	---
5.2	0.1	6.88	9.32	11.47	11.32	0.176	0.239	0.294	0.290
10.4	0.2	12.29	20.79	25.43	19.99	0.157	0.265	0.324	0.255
15.6	0.3	17.29	24.62	29.00	27.59	0.176	0.250	0.294	0.280
20.8	0.4	19.38	28.11	34.93	31.62	0.170	0.247	0.306	0.277
26	0.5	19.06	35.56	49.00	32.68	0.140	0.261	0.360	0.240
31.2	0.6	15.37	30.77	42.23	27.69	0.132	0.265	0.364	0.239
36.4	0.7	11.69	18.23	22.24	18.97	0.164	0.256	0.313	0.267
41.6	0.8	6.65	8.68	9.59	10.74	0.186	0.243	0.269	0.301
46.8	0.9	-0.23	0.24	1.16	3.45	-0.051	0.052	0.252	0.747
52	1	0	0	0	0	---	---	---	---
					Average	0.139	0.231	0.308	0.322
					St. Dev.	0.073	0.068	0.037	0.161

Truck Run 5, Distribution Factors (Experimental)									
Panel Points		Averages				Distribution Factors			
x (ft)	x/L	G1	G2	G3	G4	G1	G2	G3	G4
0	0	0	0	0	0	---	---	---	---
5.2	0.1	9.55	12.74	16.28	19.40	0.165	0.220	0.281	0.335
10.4	0.2	7.41	14.20	26.91	31.41	0.093	0.178	0.337	0.393
15.6	0.3	11.95	20.02	29.51	32.93	0.127	0.212	0.313	0.349
20.8	0.4	14.23	24.62	36.73	37.21	0.126	0.218	0.326	0.330
26	0.5	15.64	28.97	53.33	42.69	0.111	0.206	0.379	0.304
31.2	0.6	14.93	26.96	48.64	40.32	0.114	0.206	0.372	0.308
36.4	0.7	13.06	20.31	29.41	30.72	0.140	0.217	0.315	0.329
41.6	0.8	7.94	10.15	14.18	20.08	0.152	0.194	0.271	0.384
46.8	0.9	4.12	4.13	6.97	13.35	0.144	0.145	0.244	0.467
52	1	0	0	0	0	---	---	---	---
				Average		0.130	0.200	0.315	0.355
				St. Dev.		0.022	0.025	0.045	0.052

Truck Runs 1 & 4, Distribution Factors (Experimental)									
Panel Points		Averages				Distribution Factors			
x (ft)	x/L	G1	G2	G3	G4	G1	G2	G3	G4
0	0	0	0	0	0	---	---	---	---
5.2	0.1	26.66	22.86	19.92	17.07	0.616	0.529	0.461	0.395
10.4	0.2	48.62	45.12	37.55	27.31	0.613	0.569	0.474	0.344
15.6	0.3	59.58	51.53	43.46	37.83	0.619	0.536	0.452	0.393
20.8	0.4	68.52	57.59	50.64	43.90	0.621	0.522	0.459	0.398
26	0.5	84.16	72.37	65.05	45.38	0.630	0.542	0.487	0.340
31.2	0.6	75.19	63.23	55.61	39.58	0.644	0.541	0.476	0.339
36.4	0.7	44.81	36.88	31.86	28.37	0.631	0.520	0.449	0.400
41.6	0.8	22.19	17.40	15.36	19.90	0.593	0.465	0.410	0.532
46.8	0.9	2.84	1.65	2.09	7.32	0.409	0.238	0.301	1.053
52	1	0	0	0	0	---	---	---	---
				Average		0.597	0.496	0.441	0.466
				St. Dev.		0.072	0.101	0.057	0.228

Truck Runs 2 & 5, Distribution Factors (Experimental)									
Panel Points		Averages				Distribution Factors			
x (ft)	x/L	G1	G2	G3	G4	G1	G2	G3	G4
0	0	0	0	0	0	---	---	---	---
5.2	0.1	26.03	25.73	25.64	26.67	0.500	0.494	0.493	0.513
10.4	0.2	38.85	40.17	41.76	42.42	0.476	0.492	0.512	0.520
15.6	0.3	49.28	49.05	47.63	45.14	0.516	0.513	0.499	0.472
20.8	0.4	57.78	58.69	57.98	51.07	0.512	0.520	0.514	0.453
26	0.5	72.32	74.52	74.48	56.62	0.520	0.536	0.536	0.407
31.2	0.6	67.03	67.43	67.16	52.72	0.527	0.530	0.528	0.415
36.4	0.7	43.70	43.39	43.23	39.29	0.515	0.512	0.510	0.463
41.6	0.8	23.89	22.05	22.86	26.77	0.500	0.461	0.478	0.560
46.8	0.9	11.18	10.11	11.78	17.73	0.440	0.398	0.464	0.698
52	1	0	0	0	0	---	---	---	---
				Average		0.501	0.495	0.504	0.500
				St. Dev.		0.027	0.043	0.023	0.089

Truck Run 1, Bending Stress (Exp)					
Panel Points		Average Stress (ksi)			
x (ft)	x/L	G1	G2	G3	G4
0	0	0	0	0	0
5.2	0.1	0.57	0.39	0.25	0.17
10.4	0.2	1.05	0.71	0.35	0.21
15.6	0.3	1.23	0.78	0.42	0.30
20.8	0.4	1.43	0.85	0.46	0.36
26	0.5	1.89	1.07	0.47	0.37
31.2	0.6	1.73	0.94	0.39	0.34
36.4	0.7	0.96	0.54	0.28	0.27
41.6	0.8	0.45	0.25	0.17	0.27
46.8	0.9	0.09	0.04	0.03	0.11
52	1	0	0	0	0

Truck Run 2, Bending Stress (Exp)					
Panel Points		Average Stress (ksi)			
x (ft)	x/L	G1	G2	G3	G4
0	0	0	0	0	0
5.2	0.1	0.48	0.38	0.27	0.21
10.4	0.2	0.91	0.75	0.43	0.32
15.6	0.3	1.08	0.84	0.53	0.35
20.8	0.4	1.26	0.99	0.62	0.40
26	0.5	1.64	1.32	0.61	0.40
31.2	0.6	1.51	1.17	0.54	0.36
36.4	0.7	0.89	0.67	0.40	0.25
41.6	0.8	0.46	0.35	0.25	0.19
46.8	0.9	0.20	0.17	0.14	0.13
52	1	0	0	0	0

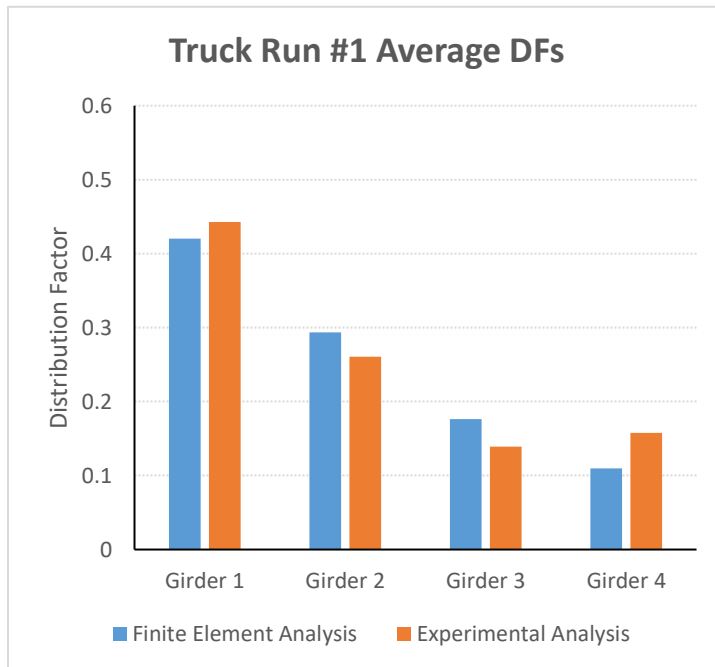
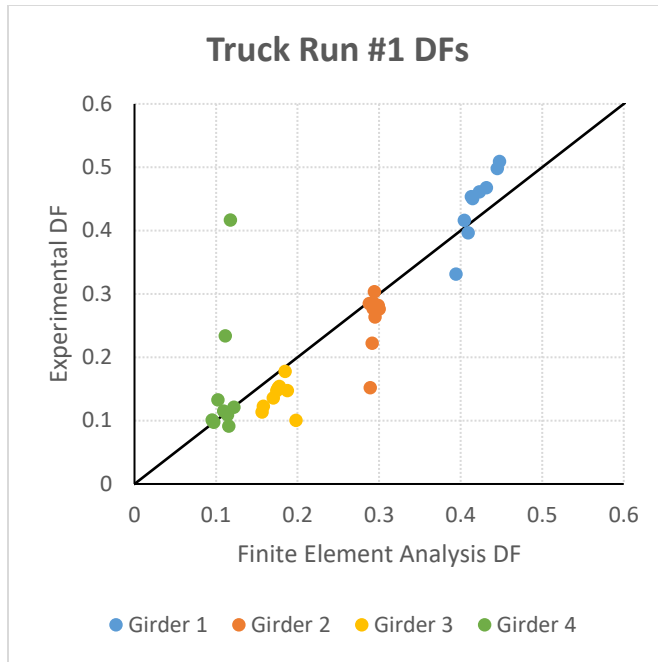
Truck Run 3, Bending Stress (Exp)					
Panel Points		Average Stress (ksi)			
x (ft)	x/L	G1	G2	G3	G4
0	0	0	0	0	0
5.2	0.1	0.33	0.37	0.37	0.29
10.4	0.2	0.49	0.70	0.71	0.45
15.6	0.3	0.63	0.79	0.79	0.60
20.8	0.4	0.74	0.97	0.94	0.70
26	0.5	0.76	1.32	1.25	0.76
31.2	0.6	0.65	1.19	1.10	0.66
36.4	0.7	0.46	0.62	0.58	0.45
41.6	0.8	0.26	0.28	0.27	0.32
46.8	0.9	0.12	0.13	0.13	0.20
52	1	0	0	0	0

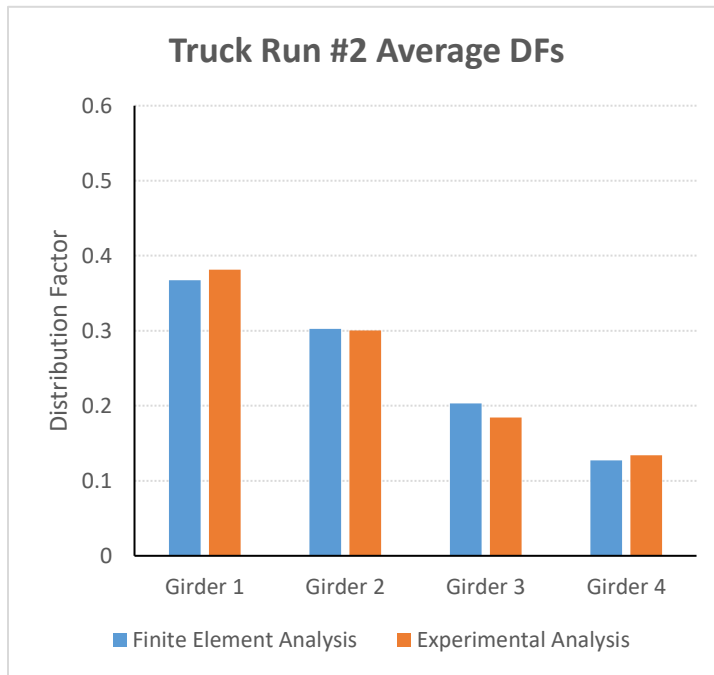
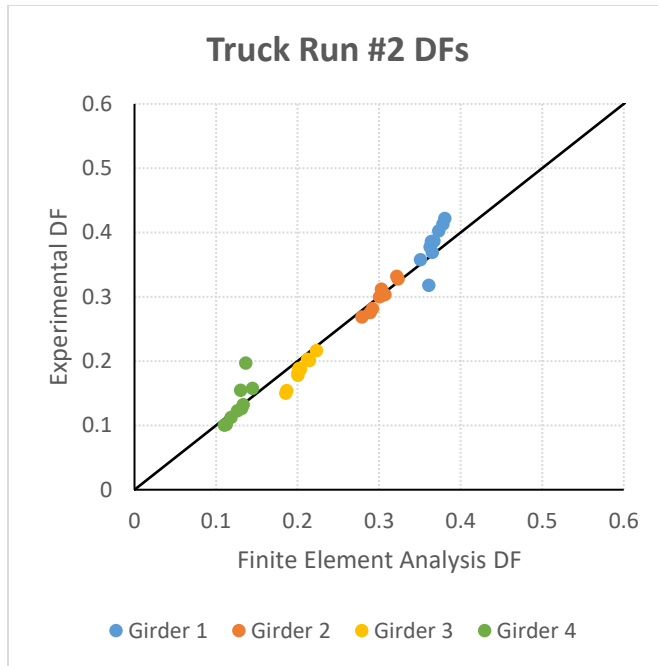
Truck Run 4, Bending Stress (Exp)					
Panel Points		Average Stress (ksi)			
x (ft)	x/L	G1	G2	G3	G4
0	0	0	0	0	0
5.2	0.1	0.20	0.27	0.33	0.33
10.4	0.2	0.36	0.60	0.74	0.58
15.6	0.3	0.50	0.71	0.84	0.80
20.8	0.4	0.56	0.82	1.01	0.92
26	0.5	0.55	1.03	1.42	0.95
31.2	0.6	0.45	0.89	1.22	0.80
36.4	0.7	0.34	0.53	0.64	0.55
41.6	0.8	0.19	0.25	0.28	0.31
46.8	0.9	-0.01	0.01	0.03	0.10
52	1	0	0	0	0

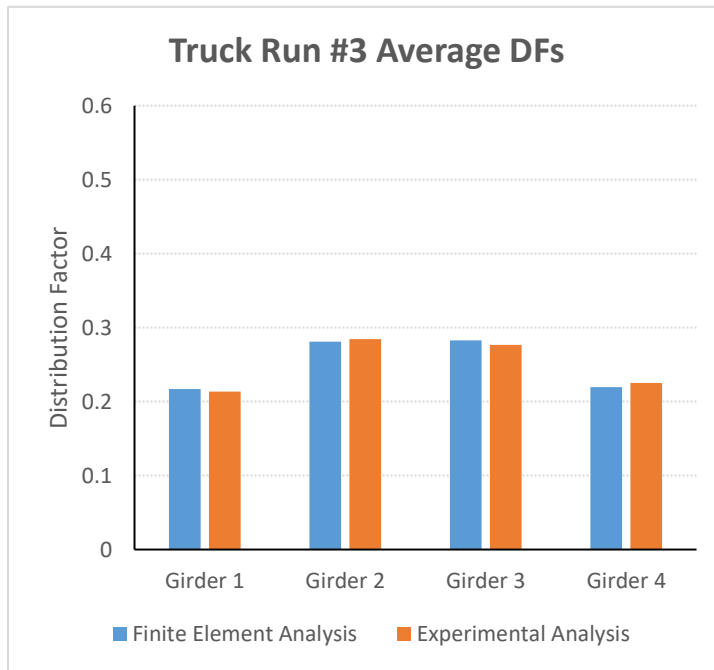
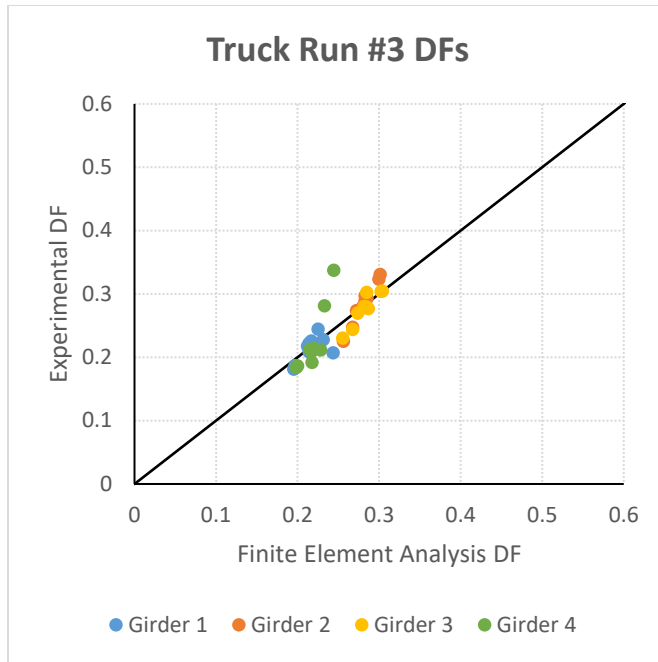
Truck Run 5, Bending Stress (Exp)					
Panel Points		Average Stress (ksi)			
x (ft)	x/L	G1	G2	G3	G4
0	0	0	0	0	0
5.2	0.1	0.28	0.37	0.47	0.56
10.4	0.2	0.21	0.41	0.78	0.91
15.6	0.3	0.35	0.58	0.86	0.95
20.8	0.4	0.41	0.71	1.07	1.08
26	0.5	0.45	0.84	1.55	1.24
31.2	0.6	0.43	0.78	1.41	1.17
36.4	0.7	0.38	0.59	0.85	0.89
41.6	0.8	0.23	0.29	0.41	0.58
46.8	0.9	0.12	0.12	0.20	0.39
52	1	0	0	0	0

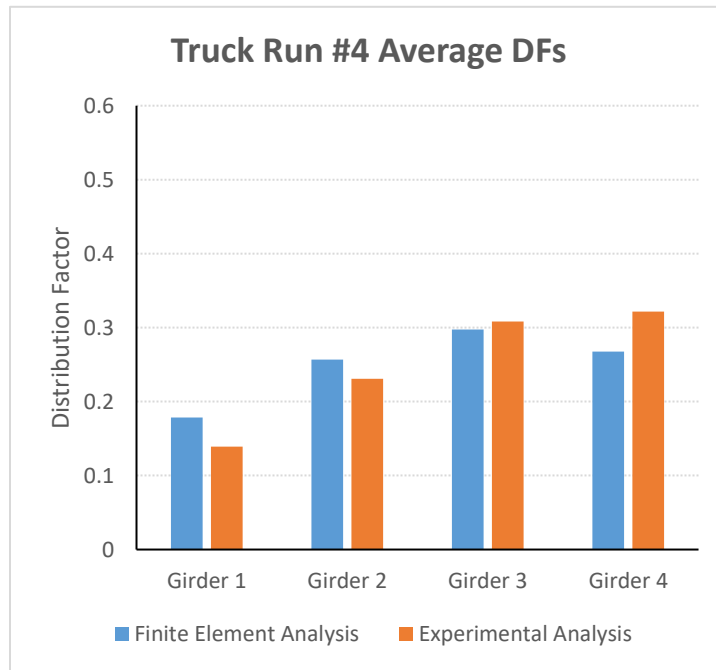
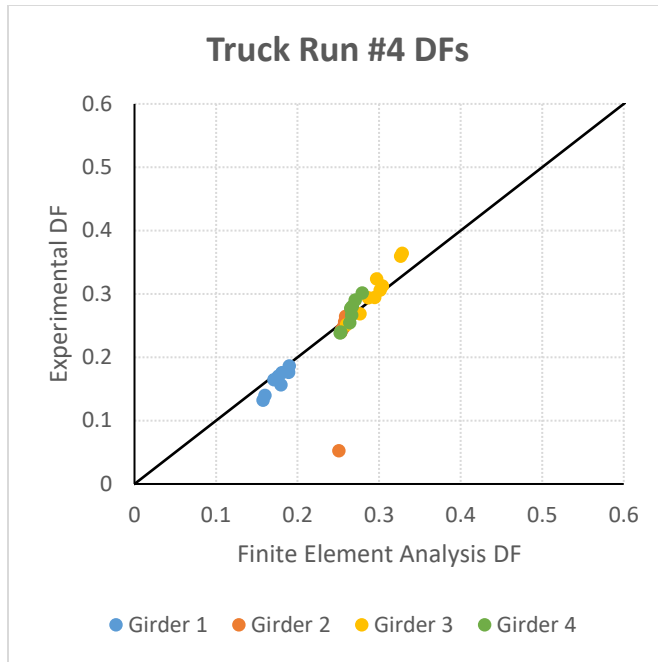
Truck Runs 1 & 4, Bending Stress (Exp)					
Panel Points		Average Stress (ksi)			
x (ft)	x/L	G1	G2	G3	G4
0	0	0	0	0	0
5.2	0.1	0.77	0.66	0.58	0.50
10.4	0.2	1.41	1.31	1.09	0.79
15.6	0.3	1.73	1.49	1.26	1.10
20.8	0.4	1.99	1.67	1.47	1.27
26	0.5	2.44	2.10	1.89	1.32
31.2	0.6	2.18	1.83	1.61	1.15
36.4	0.7	1.30	1.07	0.92	0.82
41.6	0.8	0.64	0.50	0.45	0.58
46.8	0.9	0.08	0.05	0.06	0.21
52	1	0	0	0	0

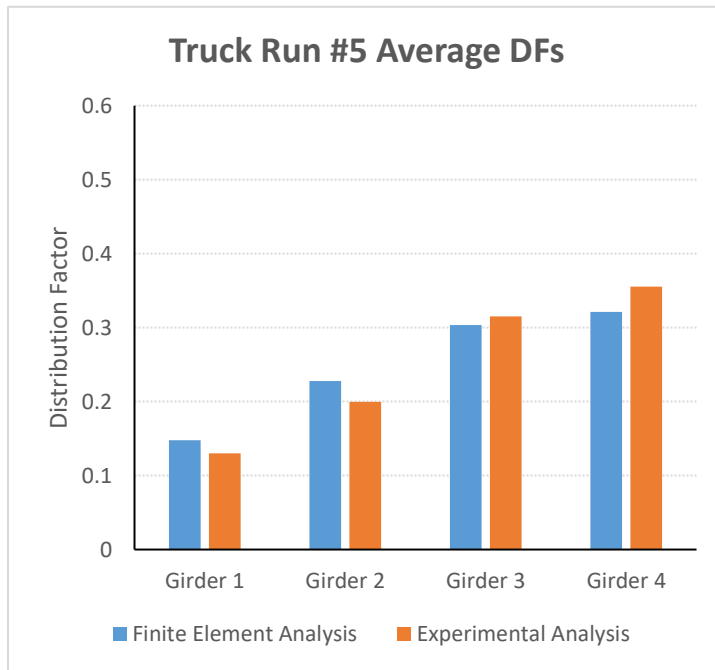
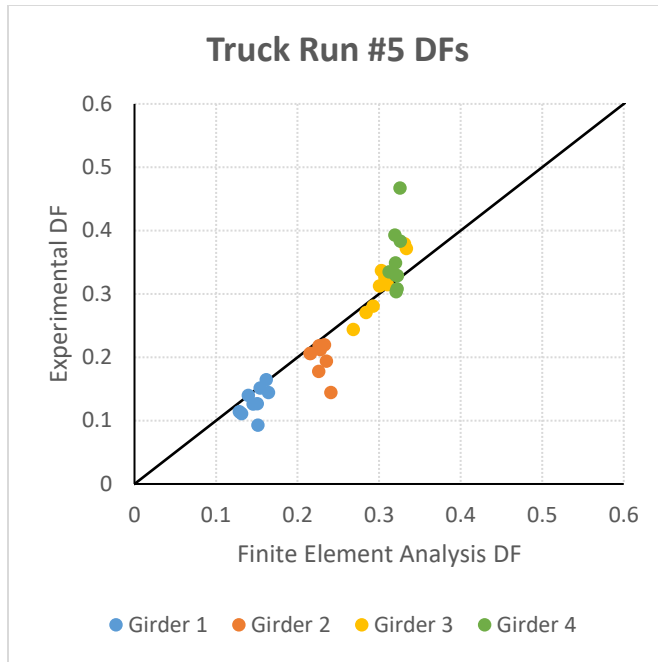
Truck Runs 2 & 5, Bending Stress (Exp)					
Panel Points		Average Stress (ksi)			
x (ft)	x/L	G1	G2	G3	G4
0	0	0	0	0	0
5.2	0.1	0.75	0.75	0.74	0.77
10.4	0.2	1.13	1.16	1.21	1.23
15.6	0.3	1.43	1.42	1.38	1.31
20.8	0.4	1.68	1.70	1.68	1.48
26	0.5	2.10	2.16	2.16	1.64
31.2	0.6	1.94	1.96	1.95	1.53
36.4	0.7	1.27	1.26	1.25	1.14
41.6	0.8	0.69	0.64	0.66	0.78
46.8	0.9	0.32	0.29	0.34	0.51
52	1	0	0	0	0

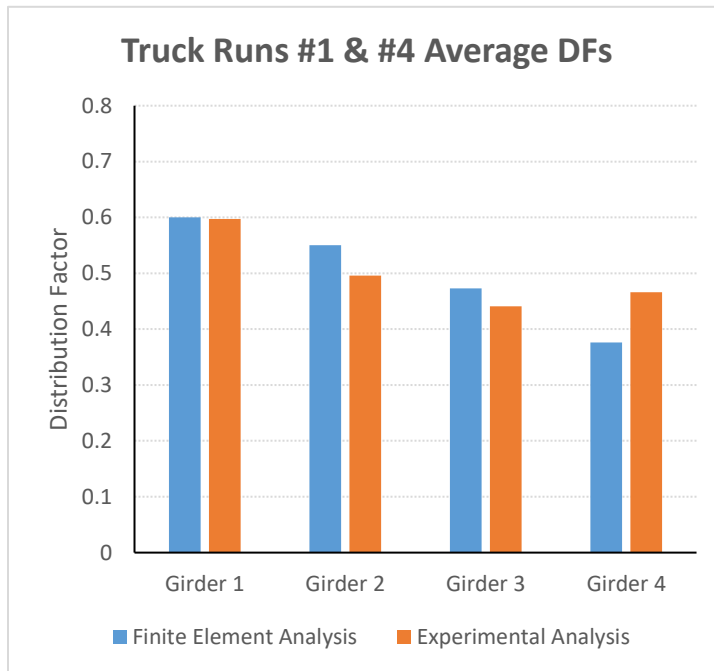


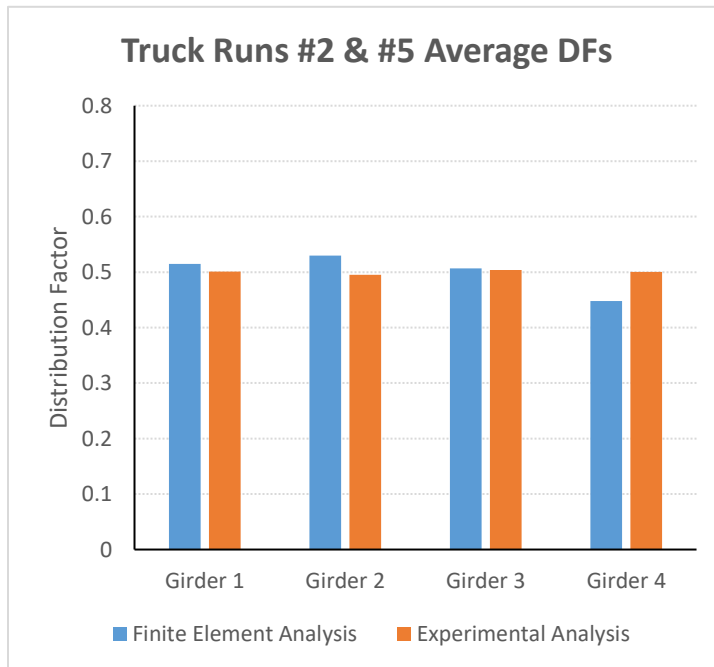


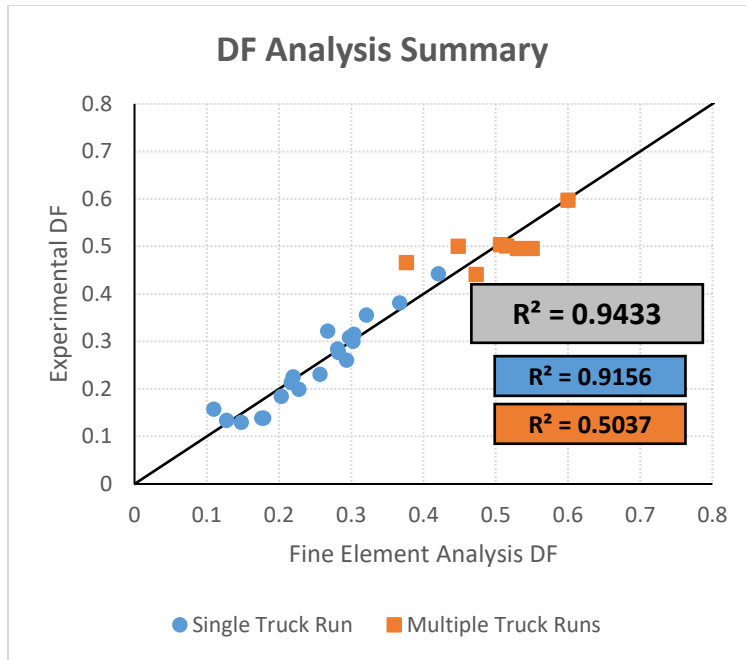




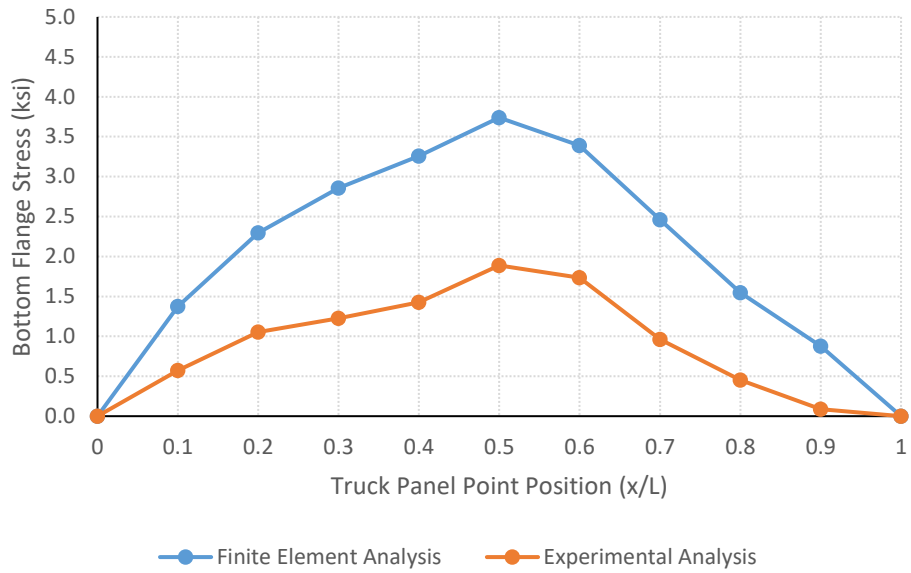




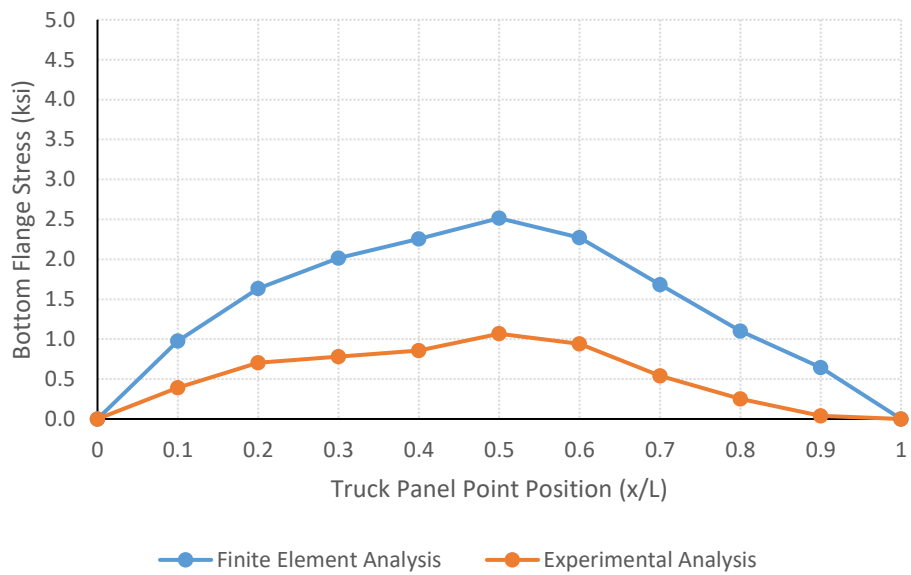




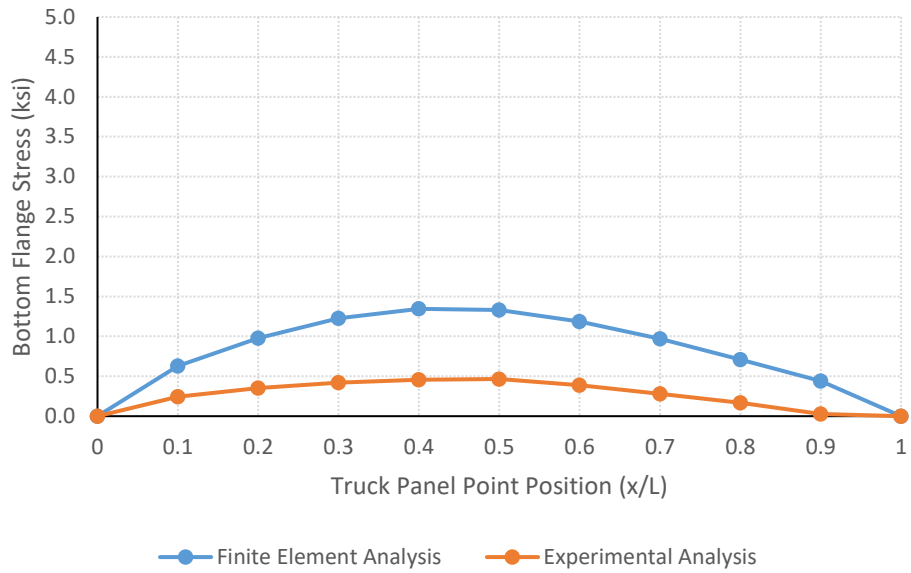
Girder 1, Truck Run #1



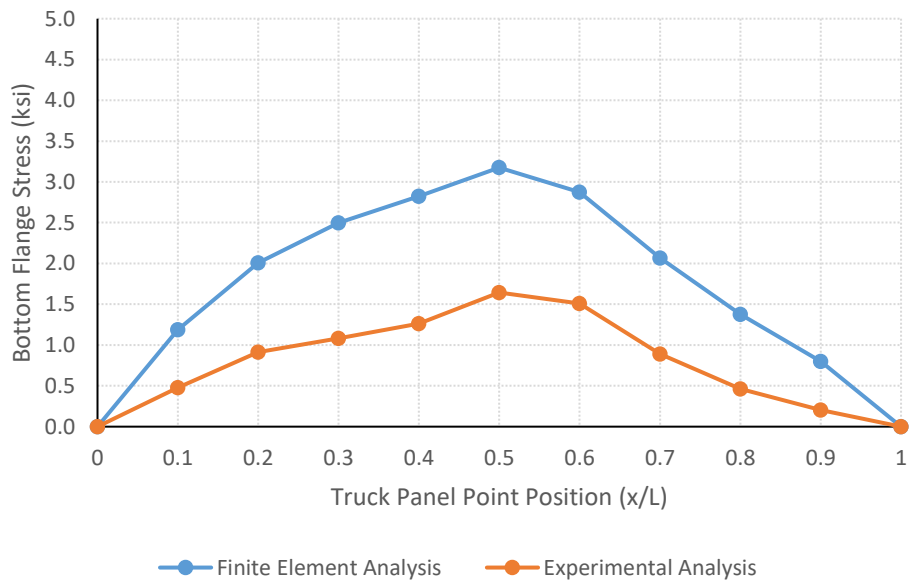
Girder 2, Truck Run #1



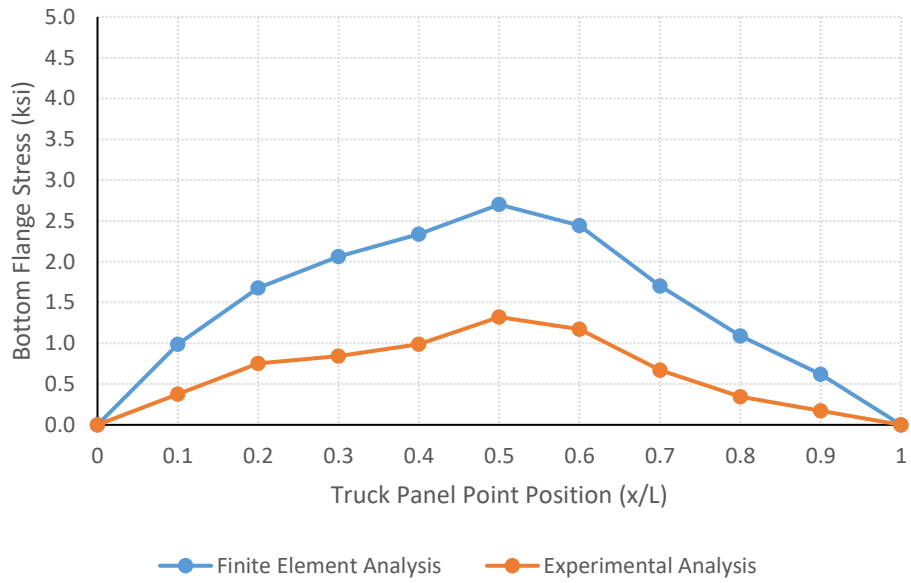
Girder 3, Truck Run #1



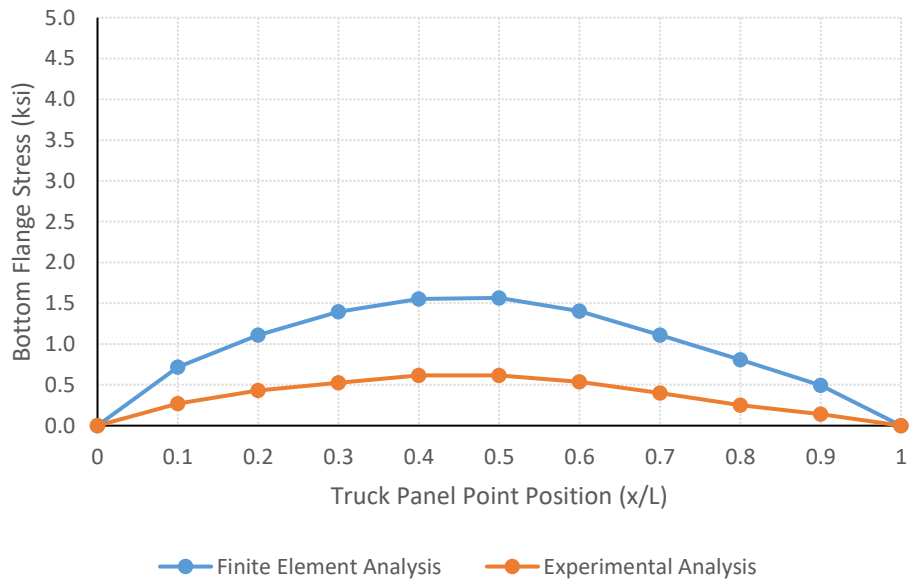
Girder 1, Truck Run #2



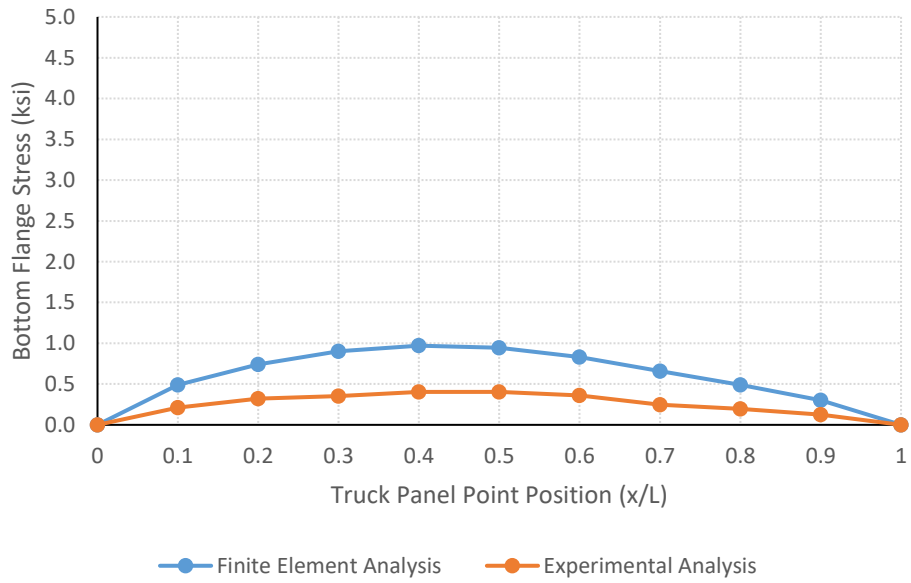
Girder 2, Truck Run #2



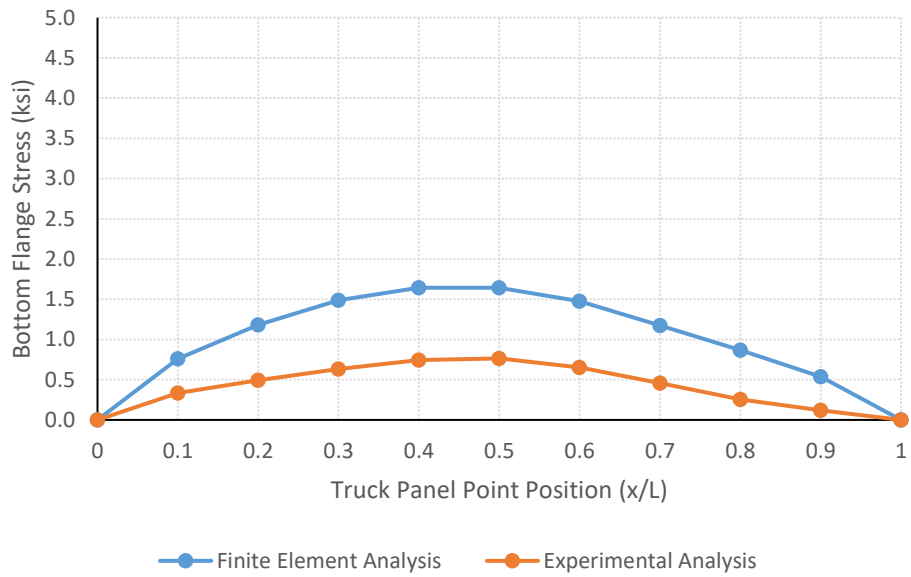
Girder 3, Truck Run #2



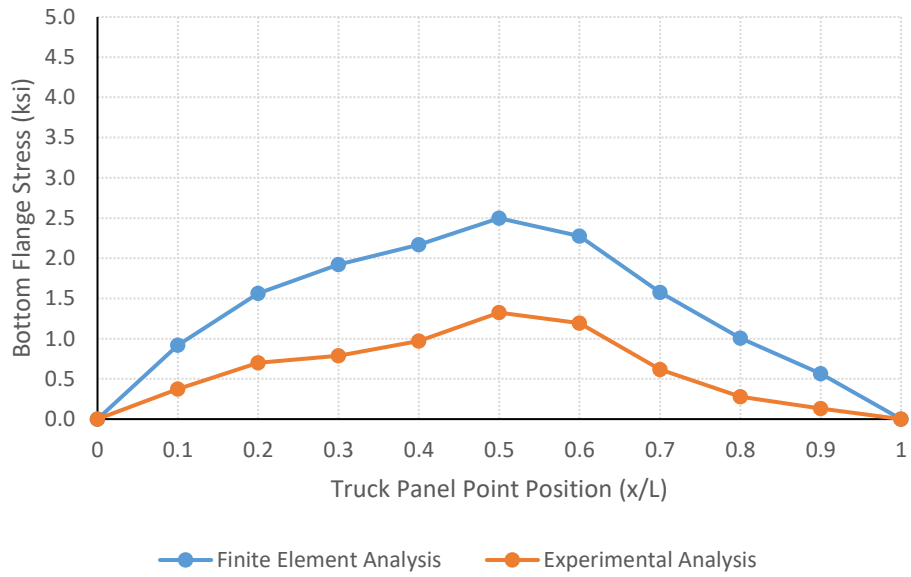
Girder 4, Truck Run #2



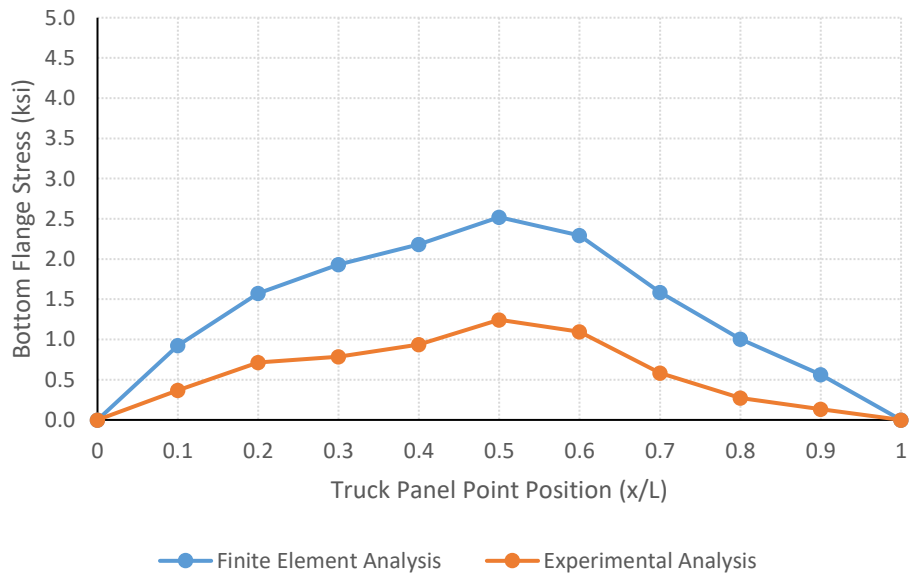
Girder 1, Truck Run #3



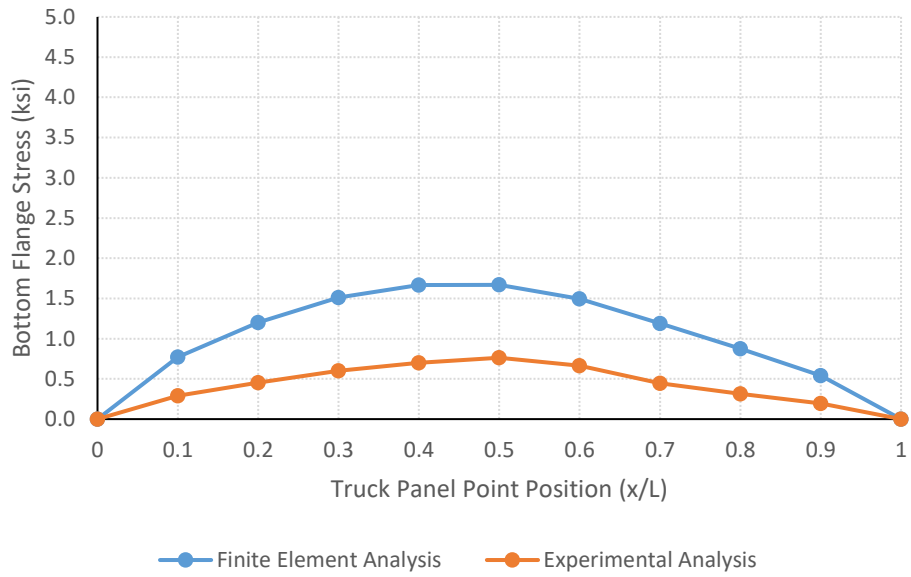
Girder 2, Truck Run #3



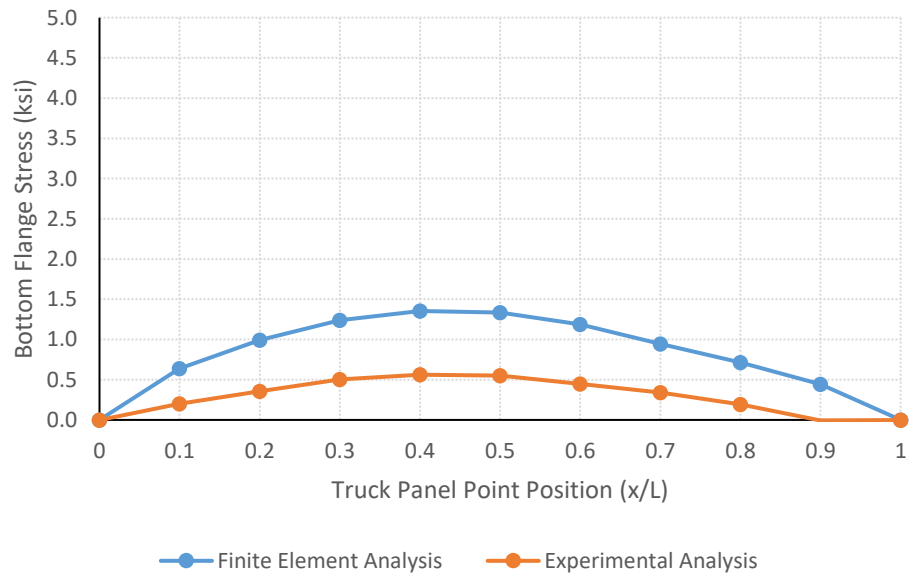
Girder 3, Truck Run #3



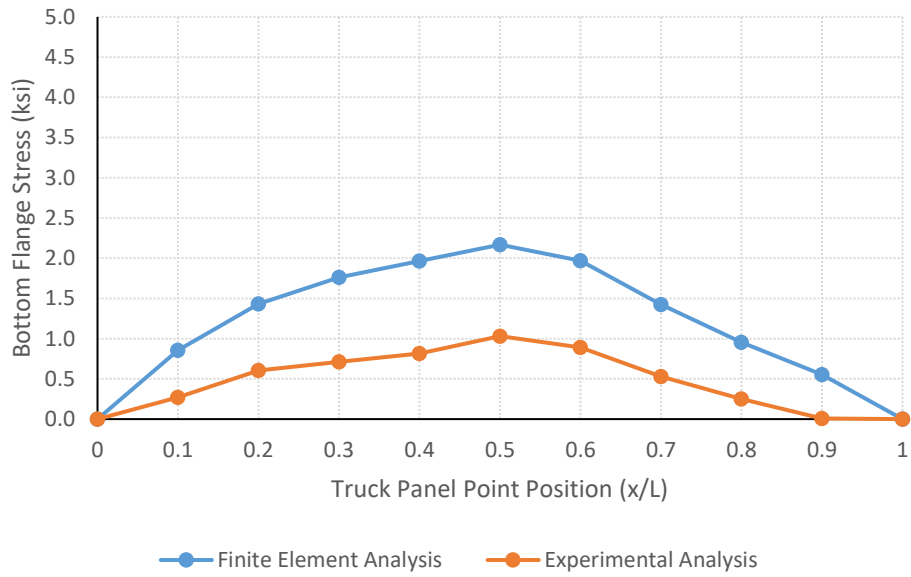
Girder 4, Truck Run #3



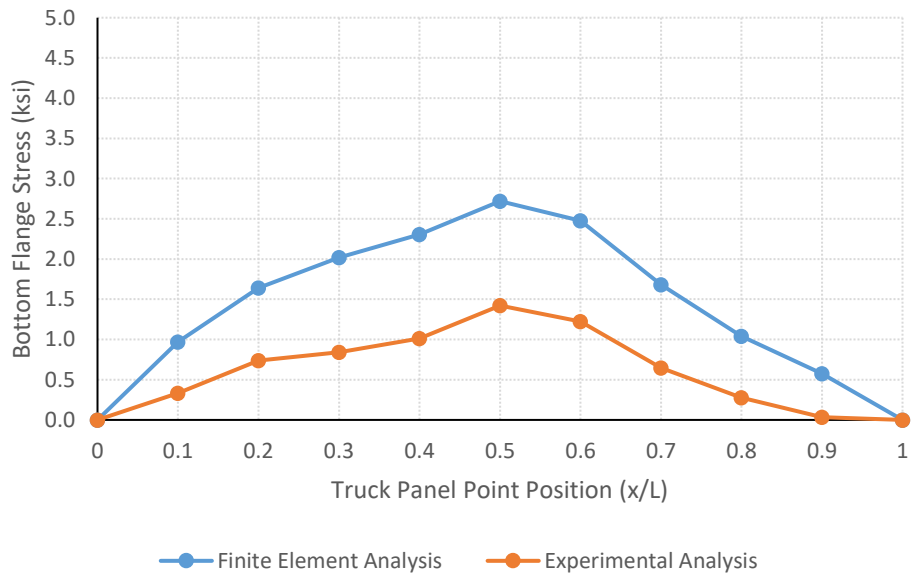
Girder 1, Truck Run #4



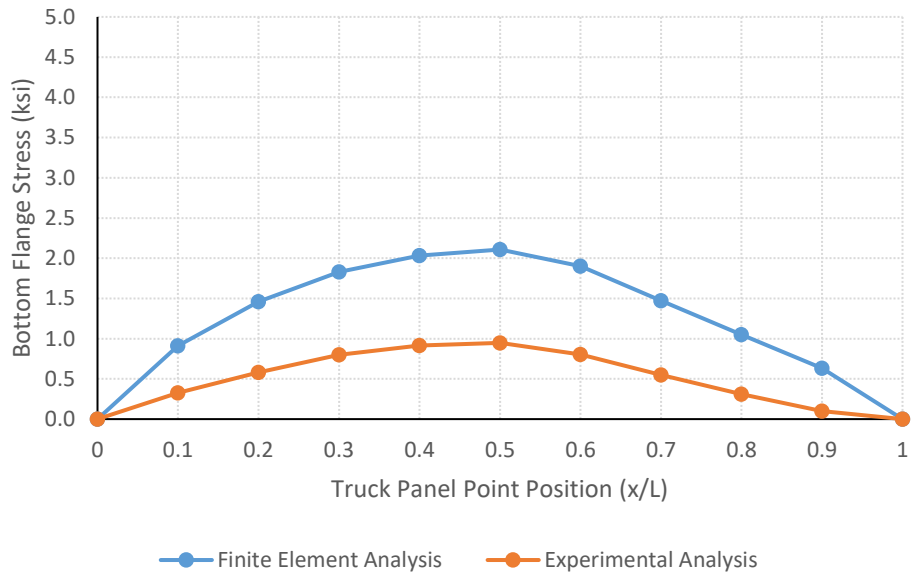
Girder 2, Truck Run #4



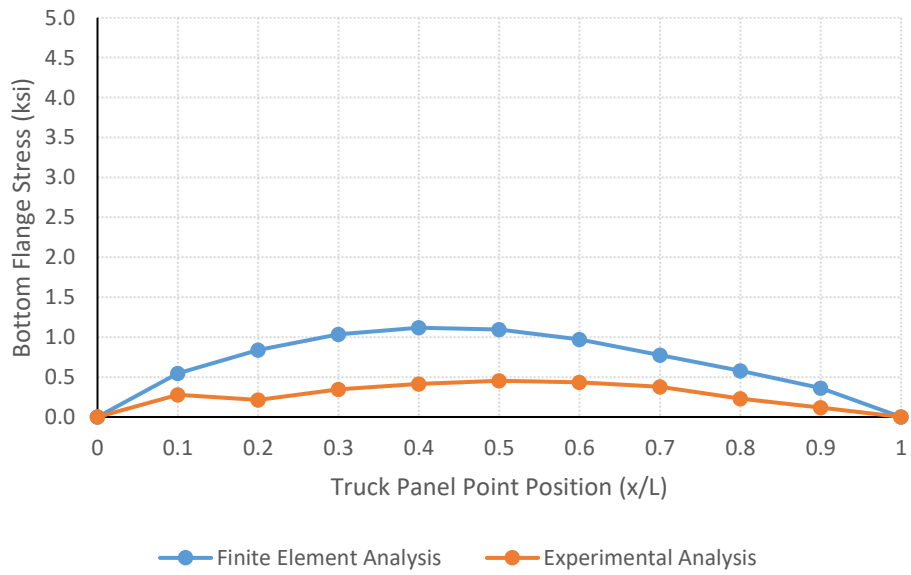
Girder 3, Truck Run #4



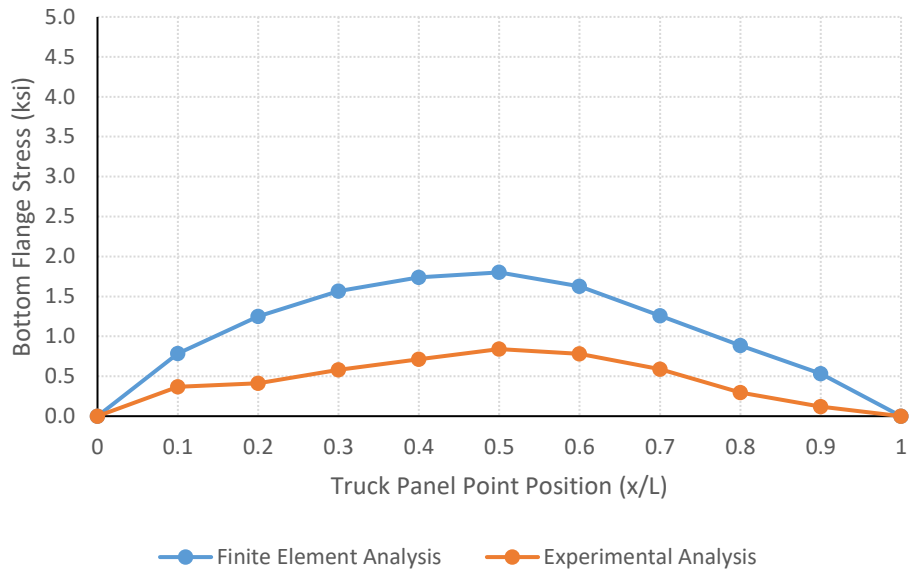
Girder 4, Truck Run #4



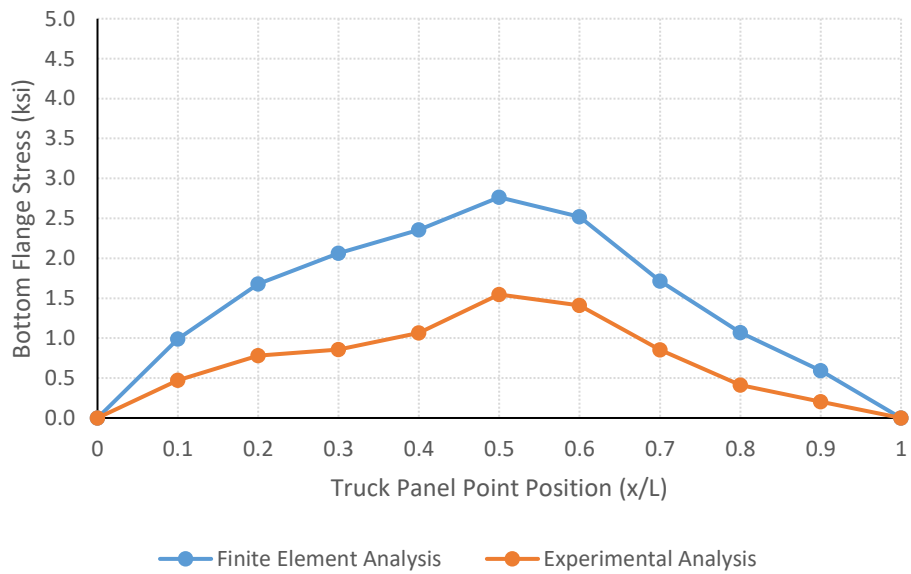
Girder 1, Truck Run #5



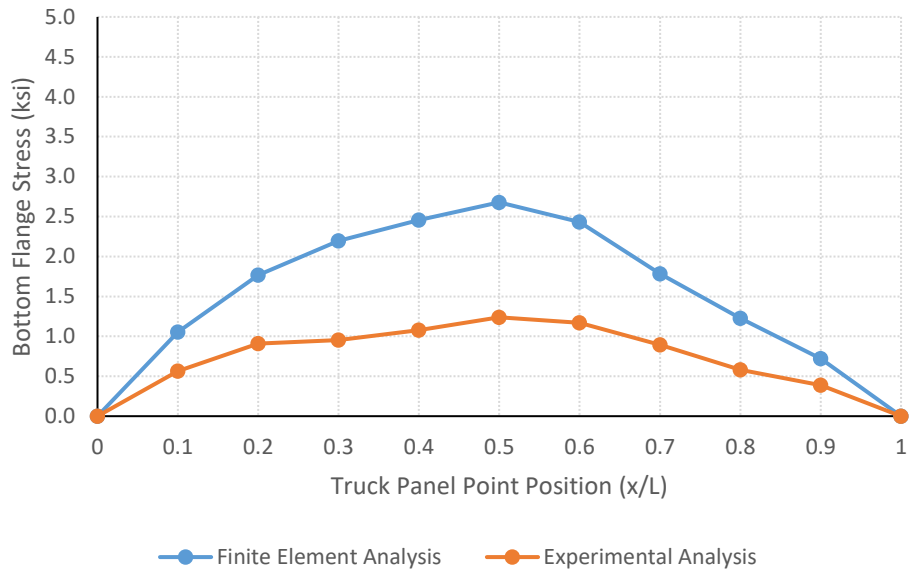
Girder 2, Truck Run #5



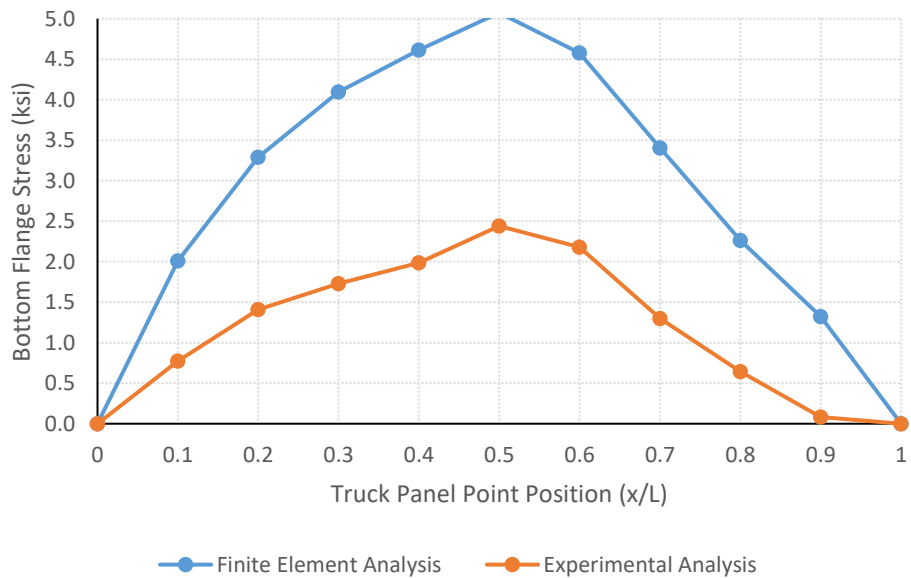
Girder 3, Truck Run #5

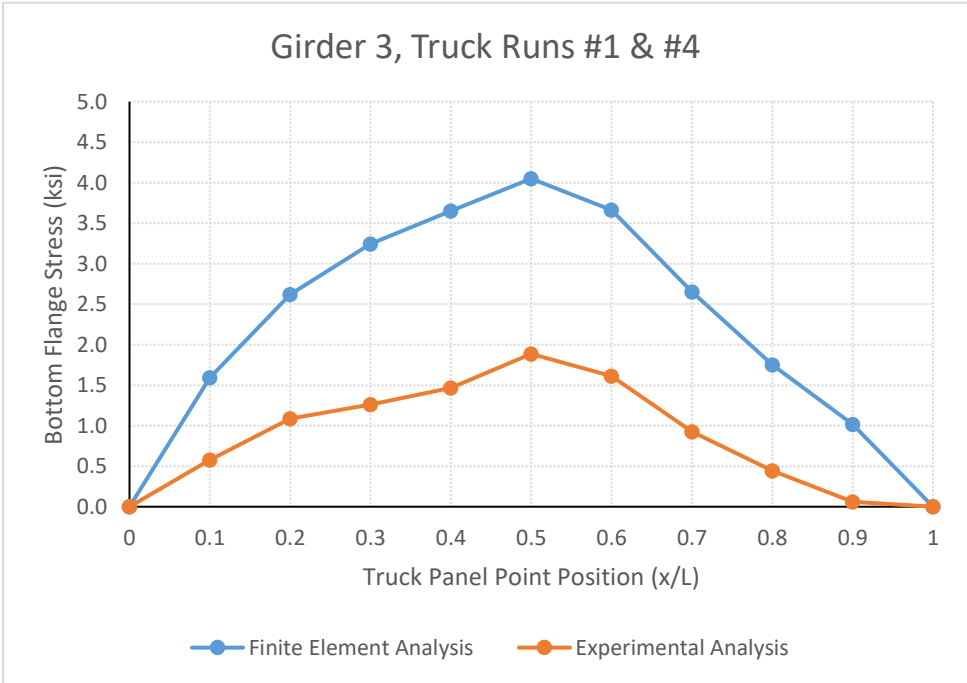
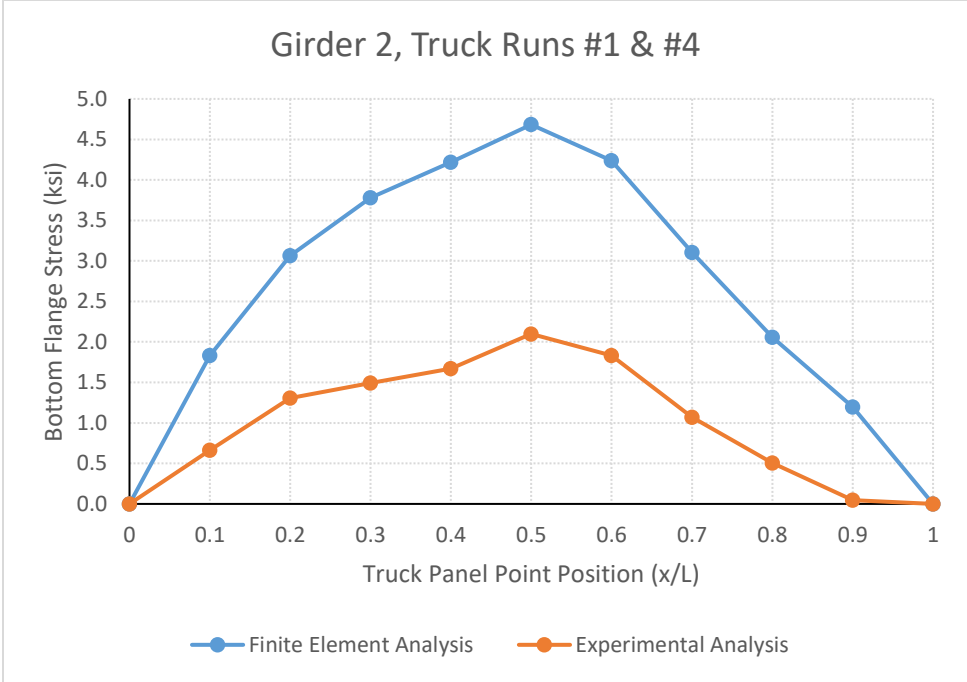


Girder 4, Truck Run #5

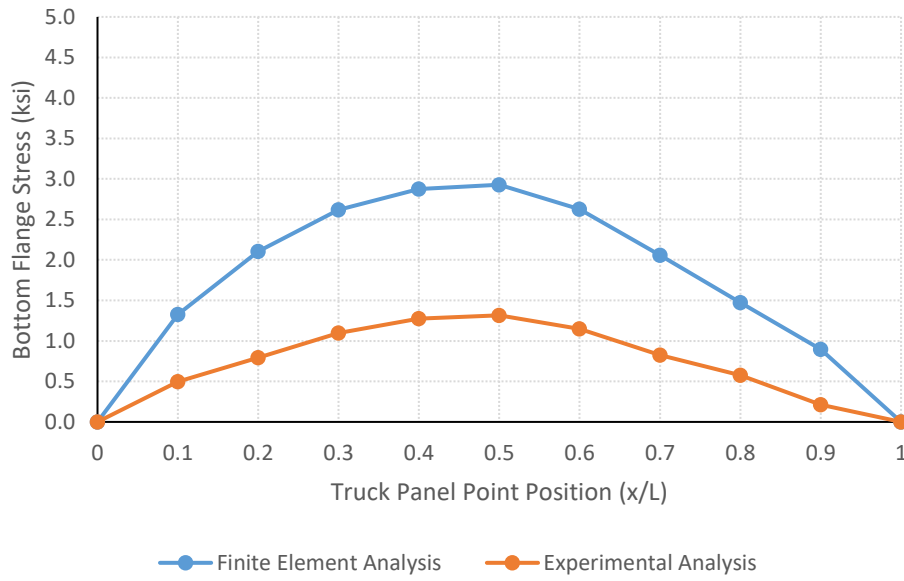


Girder 1, Truck Runs #1 & #4

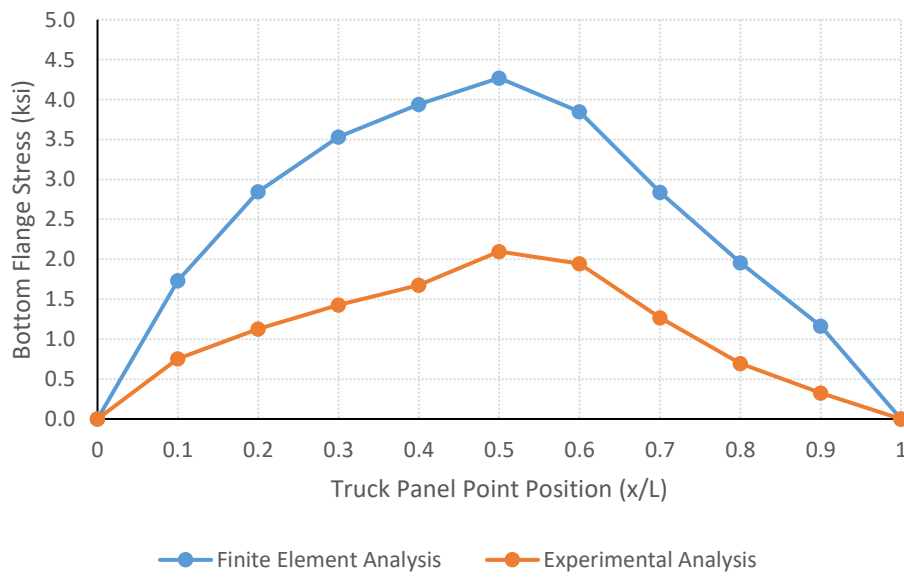


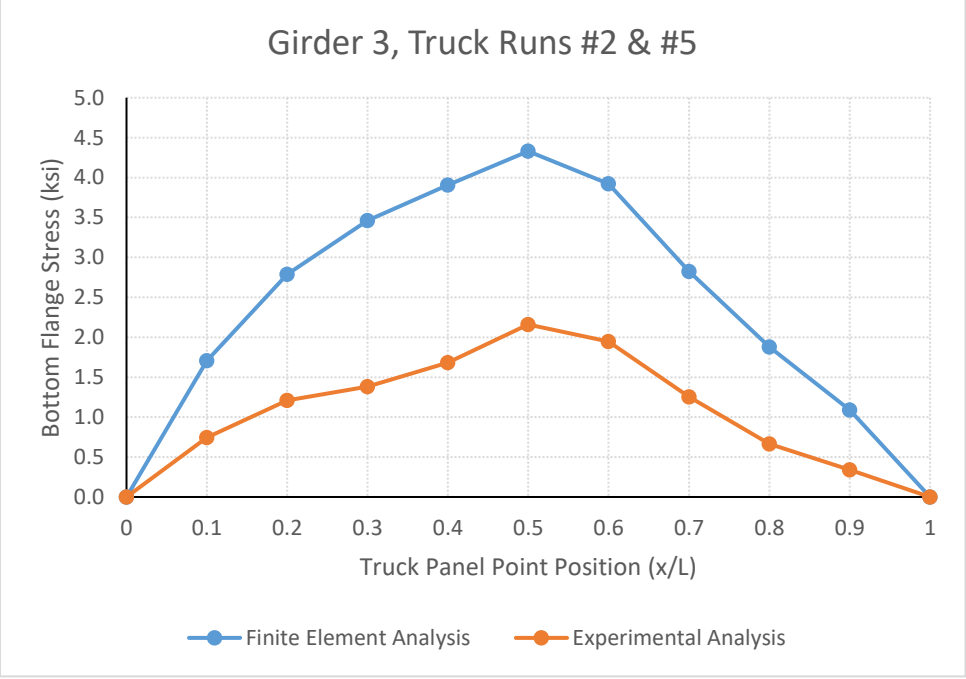
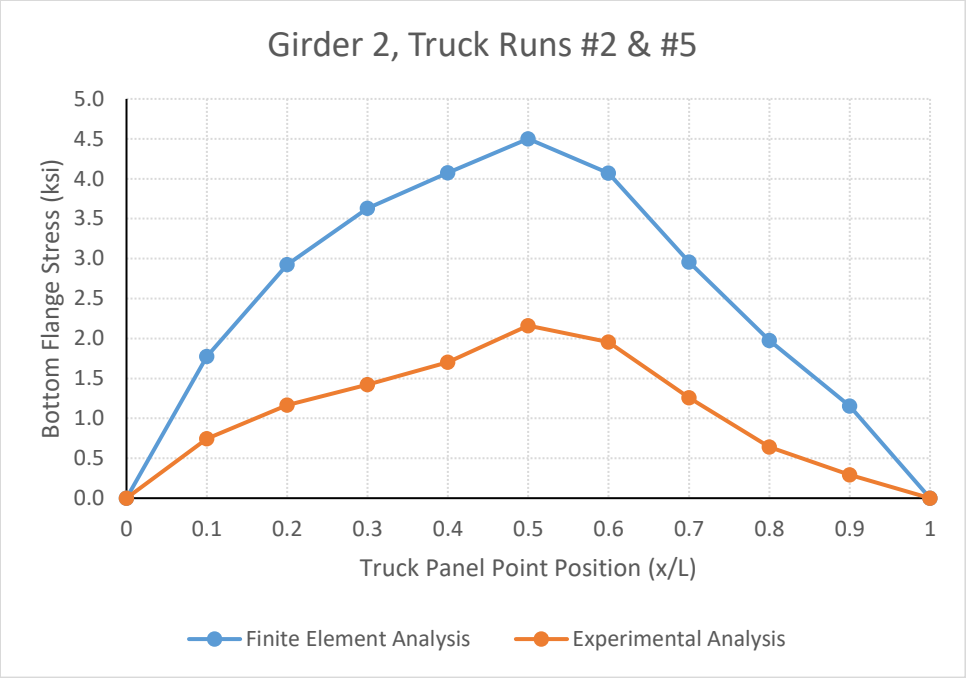


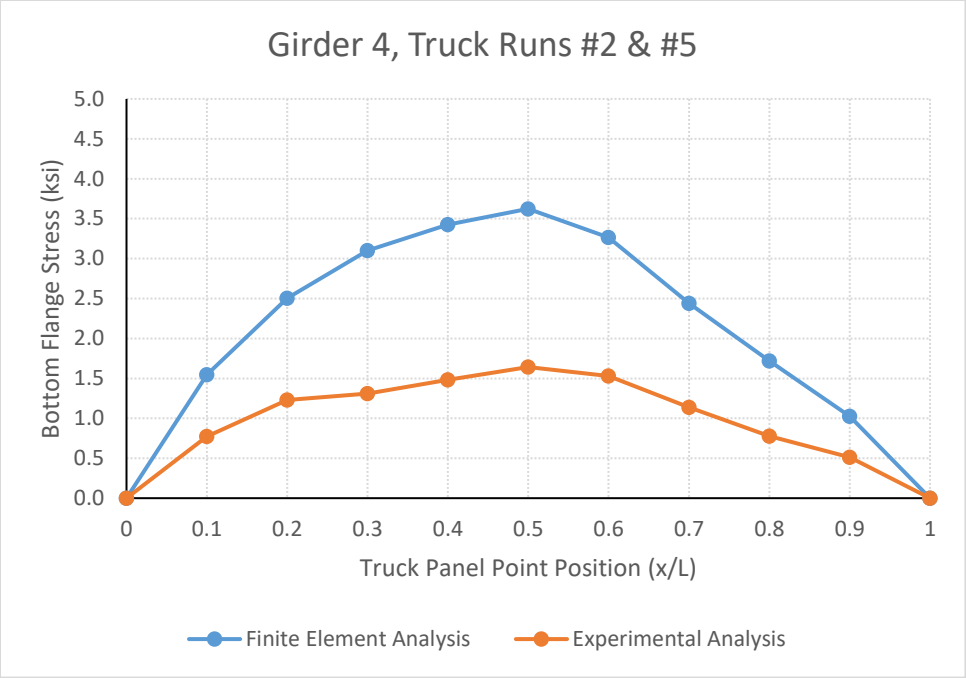
Girder 4, Truck Runs #1 & #4



Girder 1, Truck Runs #2 & #5

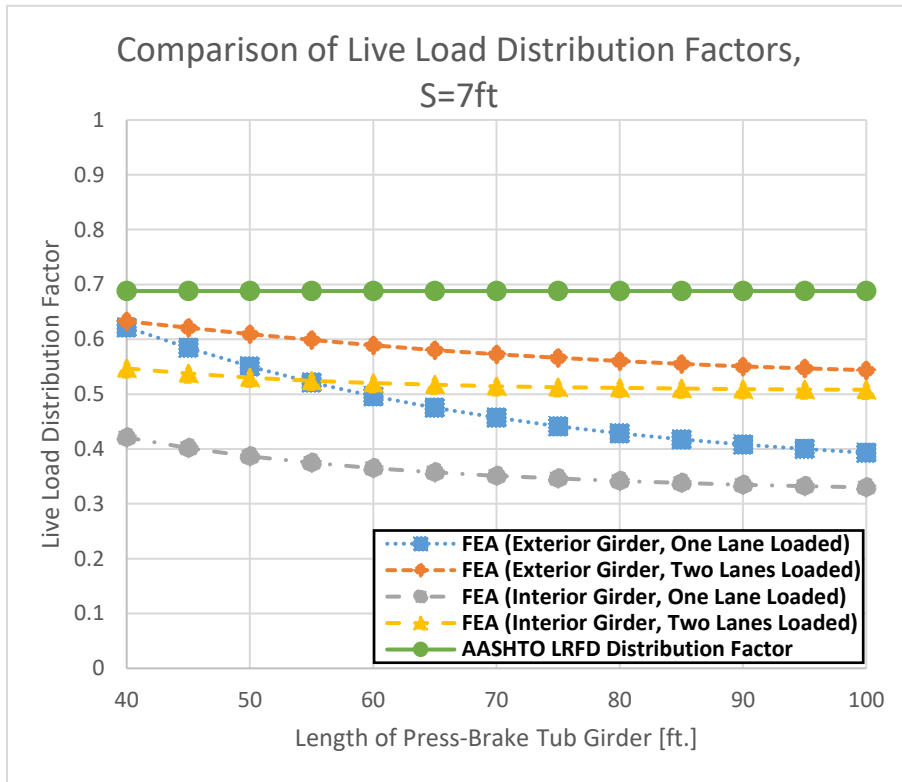
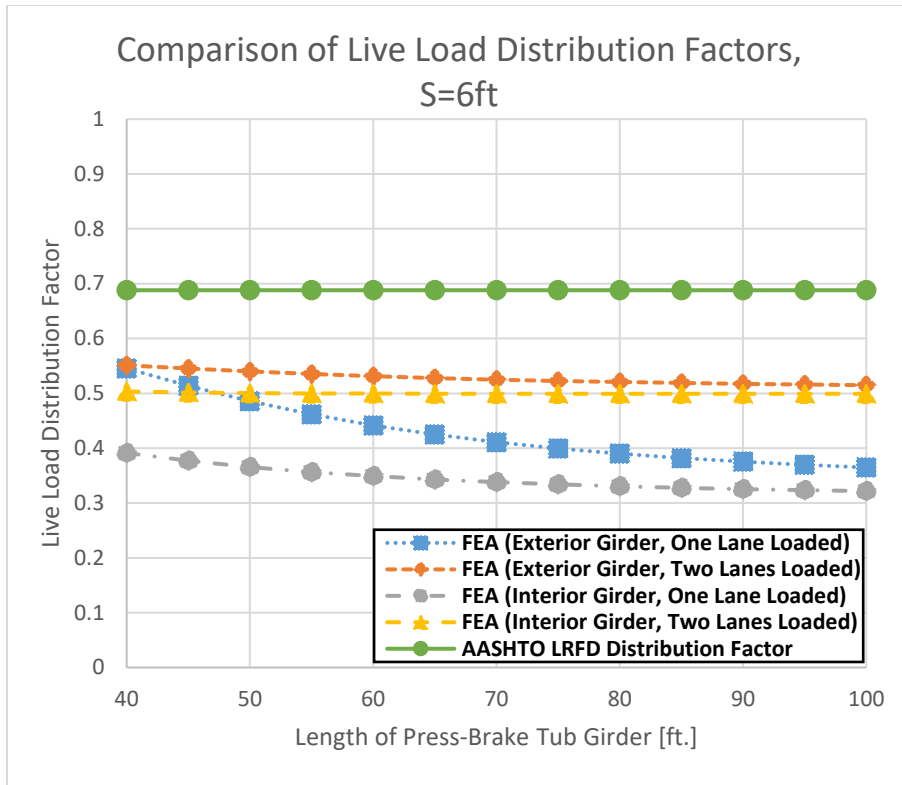


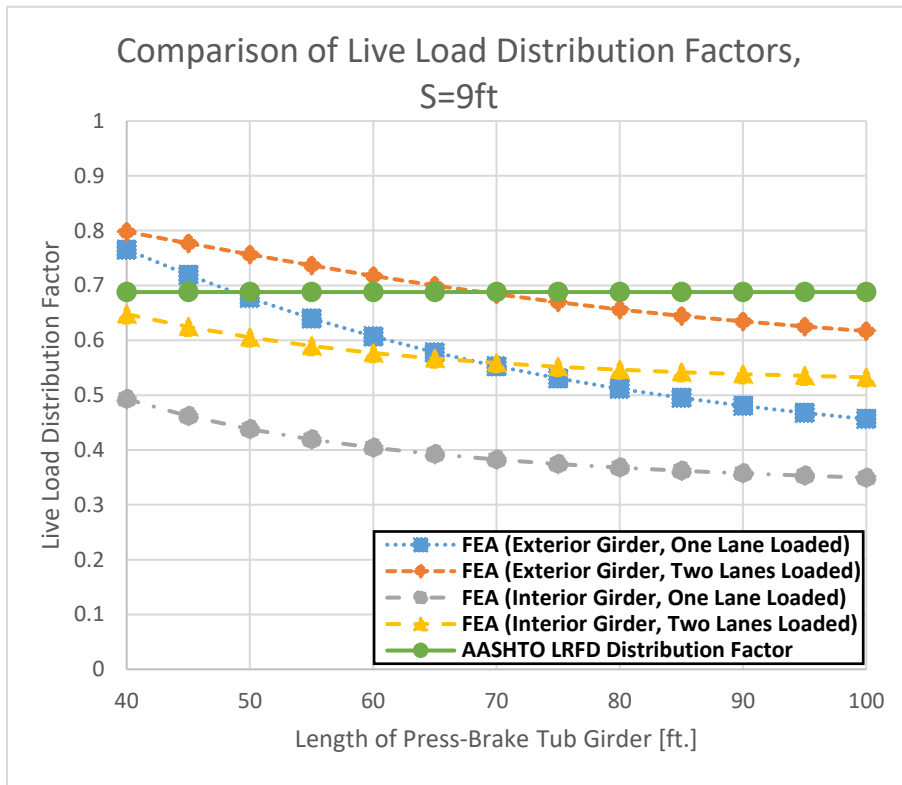
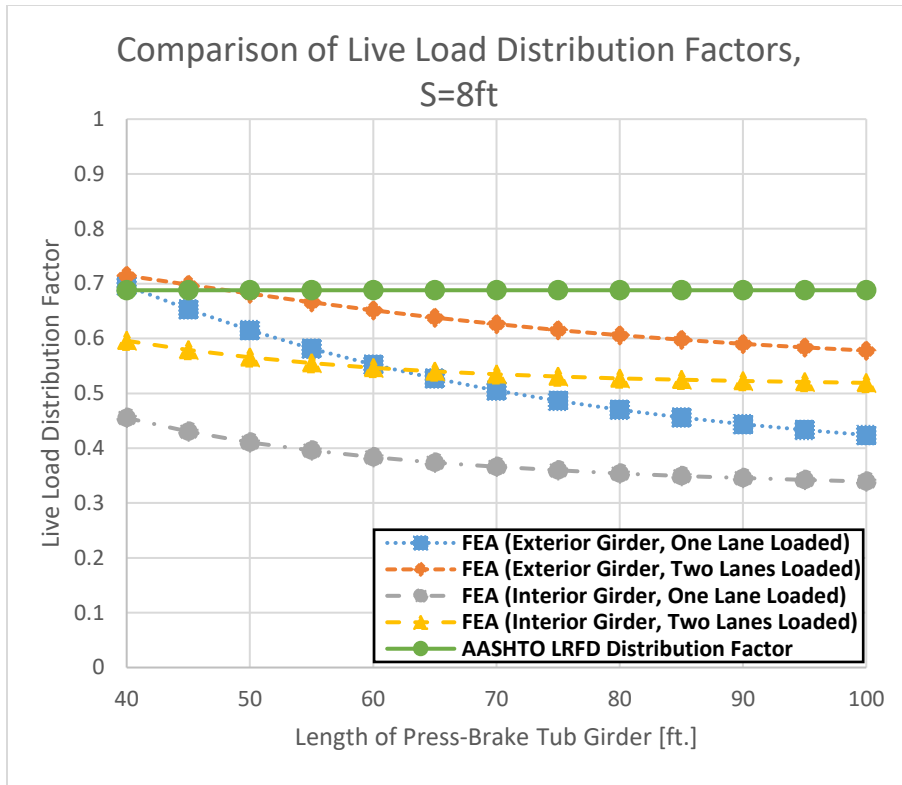


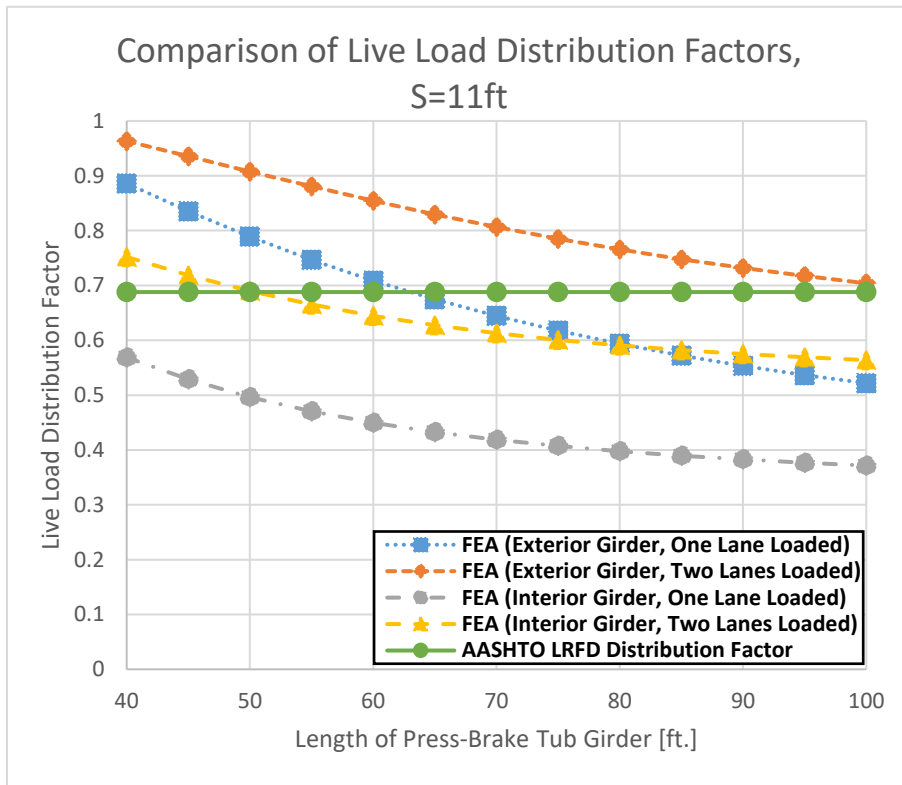
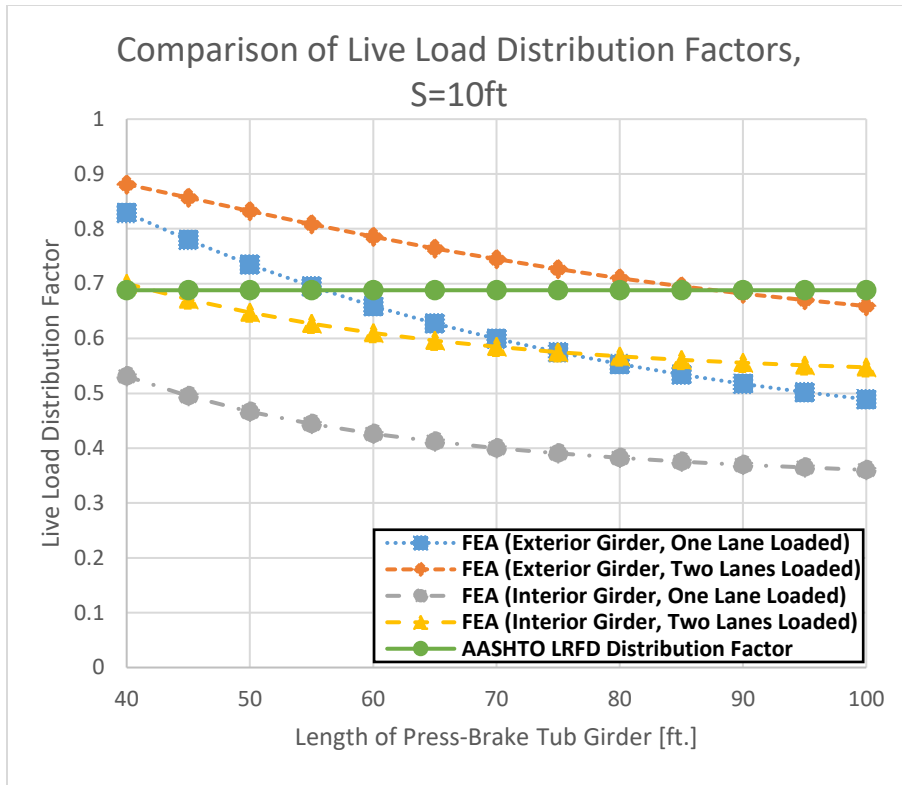


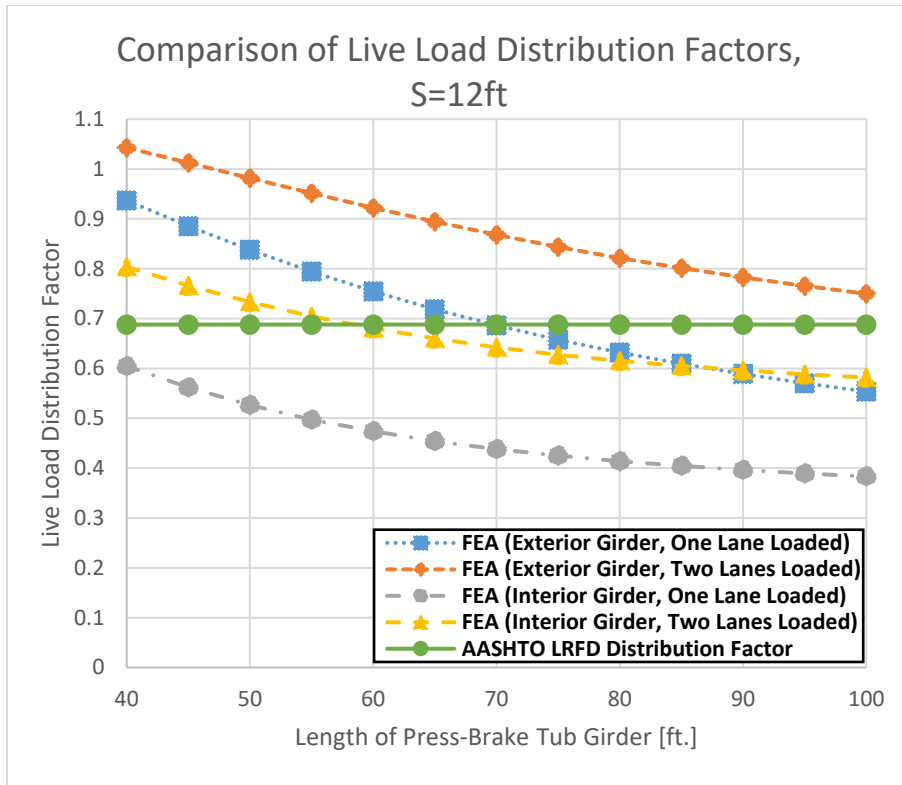
APPENDIX C: RESULTS OF PARAMETRIC ASSESSMENTS

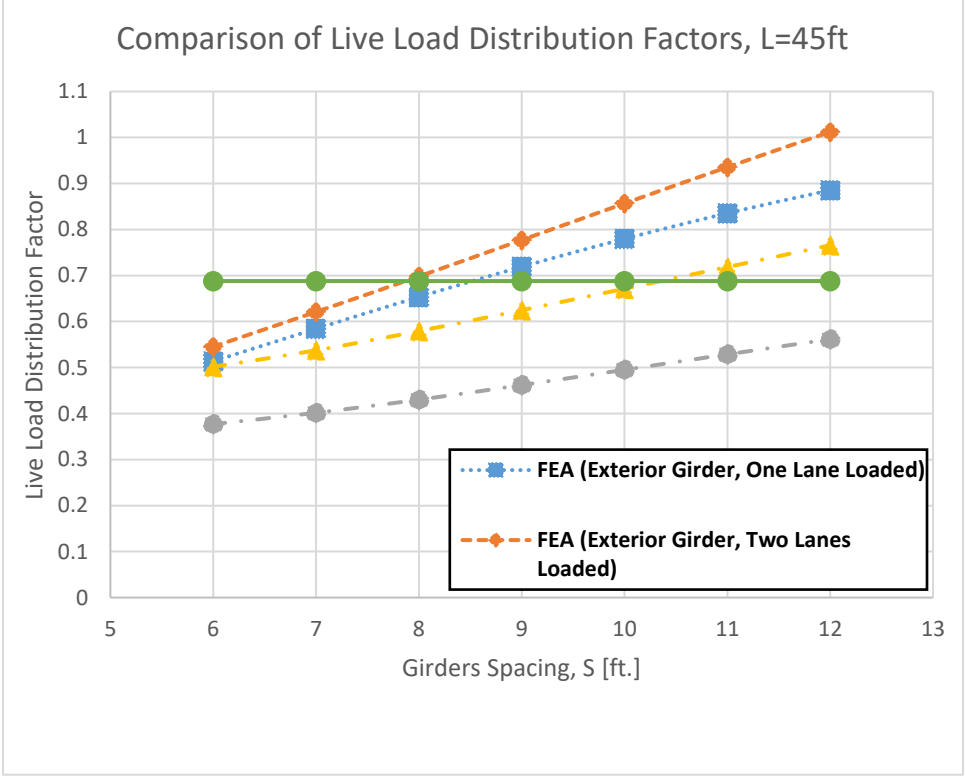
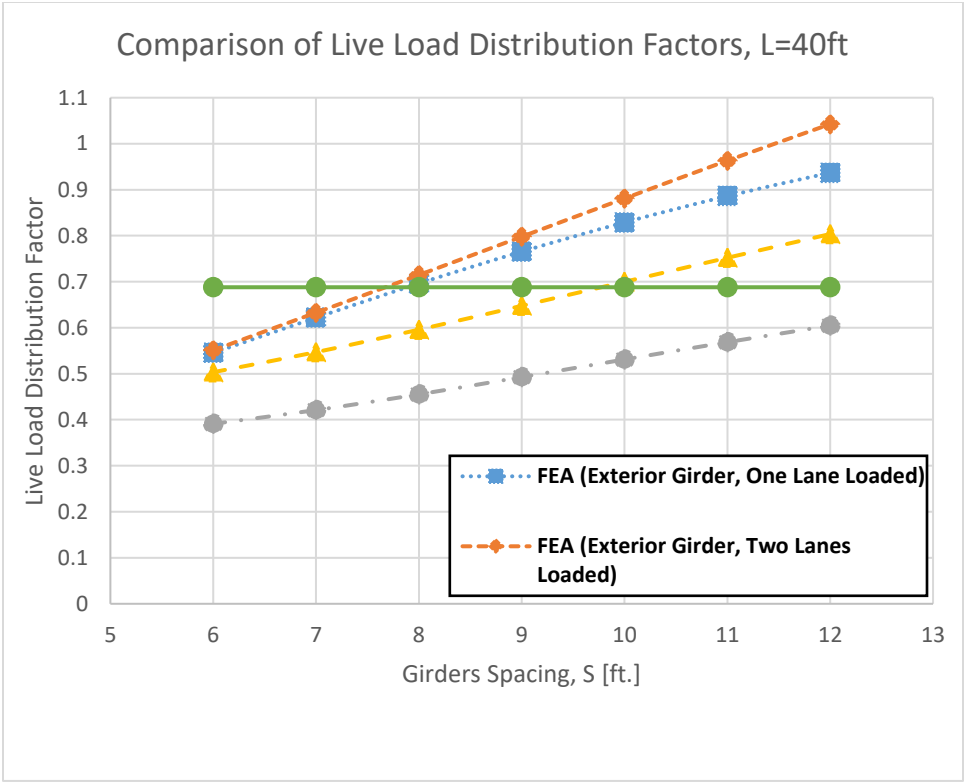
This appendix contains the complete collection of tabulated data, graphs and diagrams utilized for the parametric assessments.

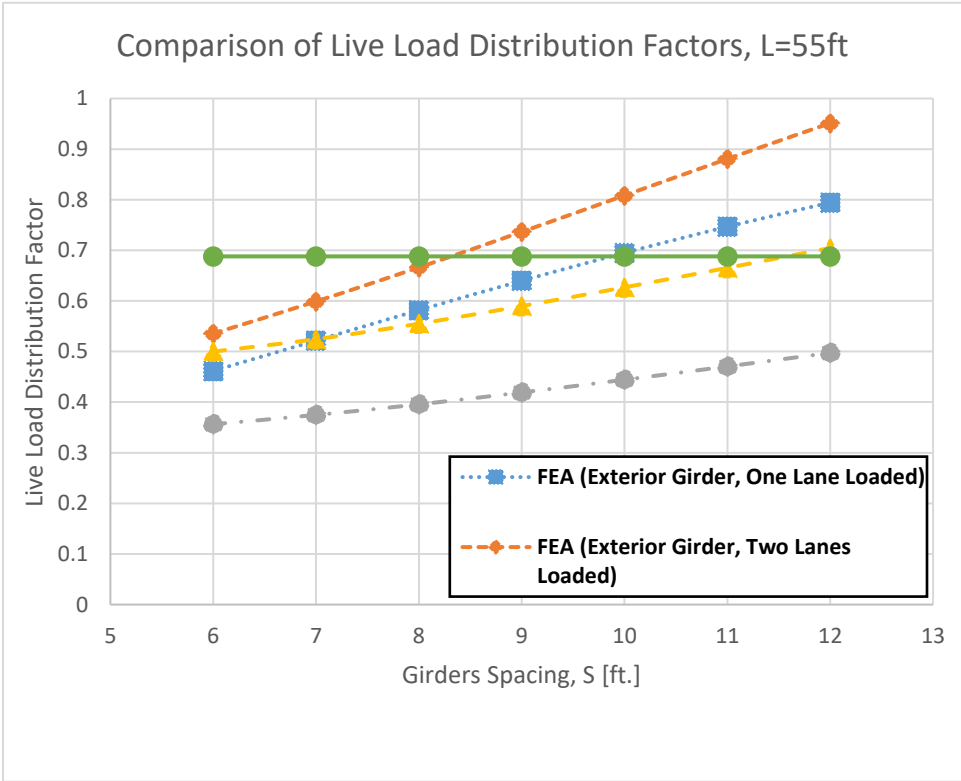
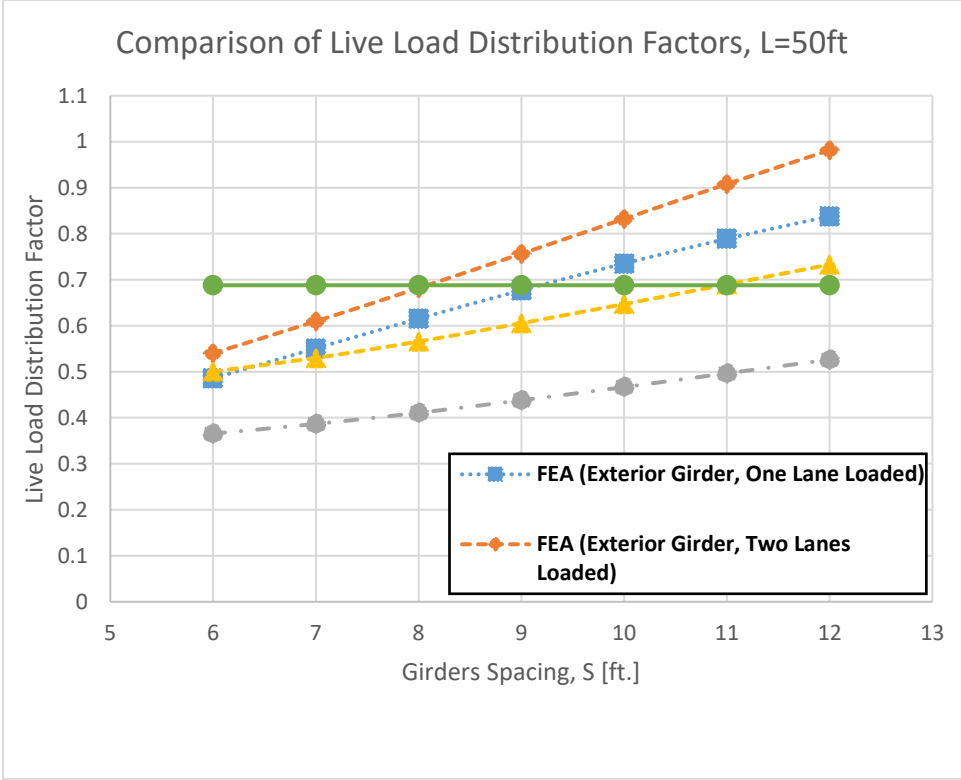


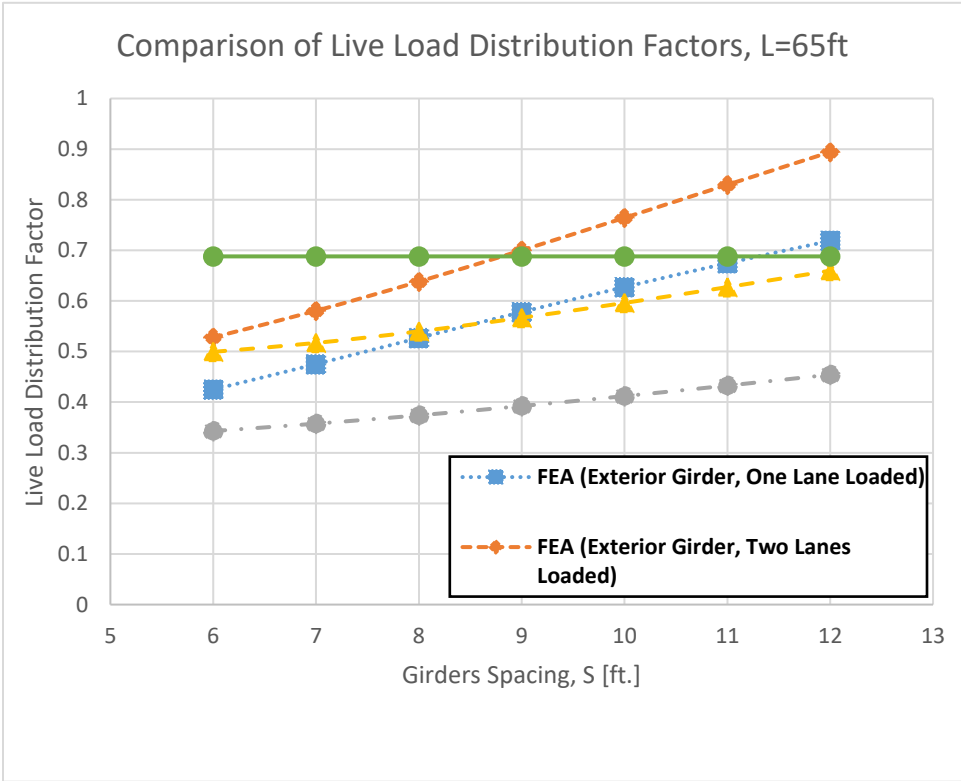
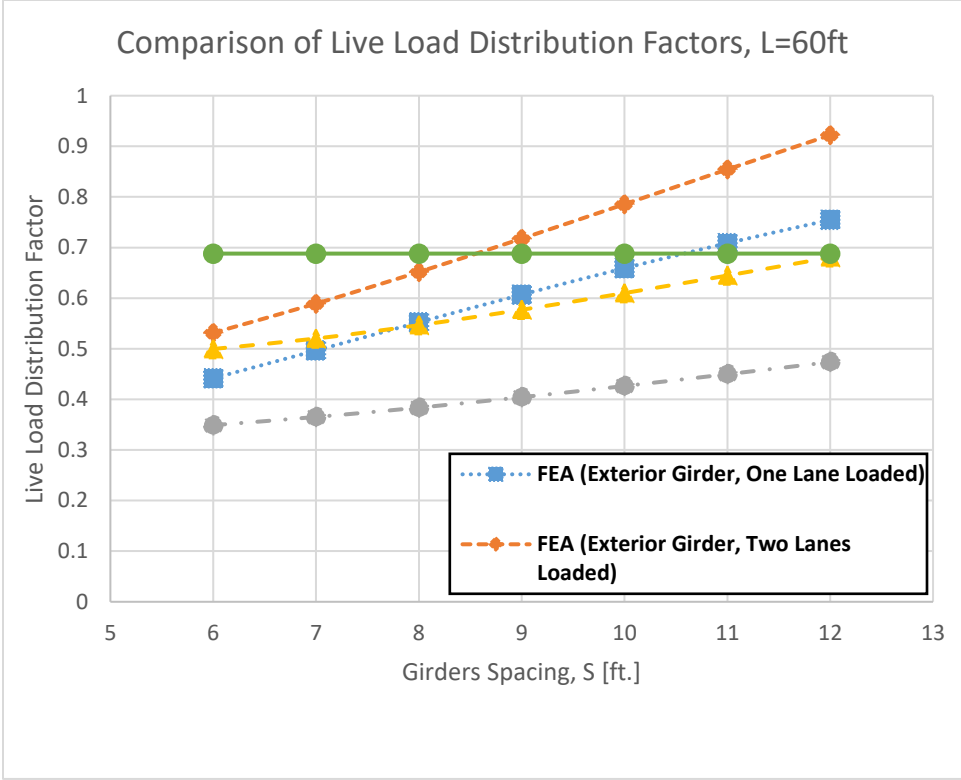


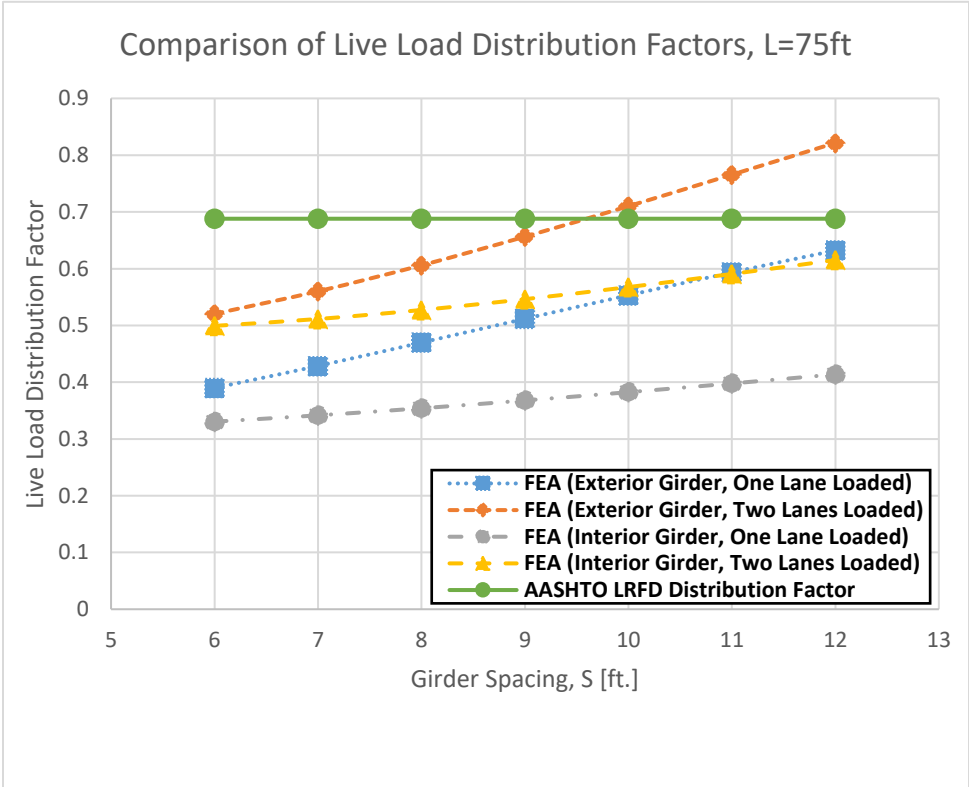
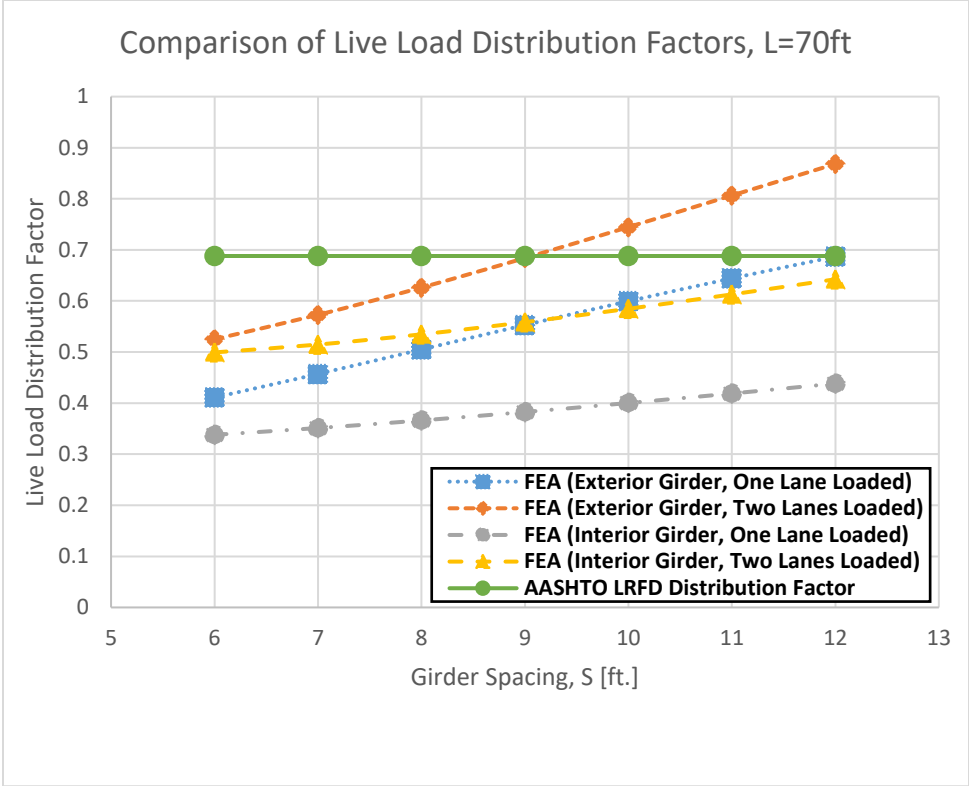


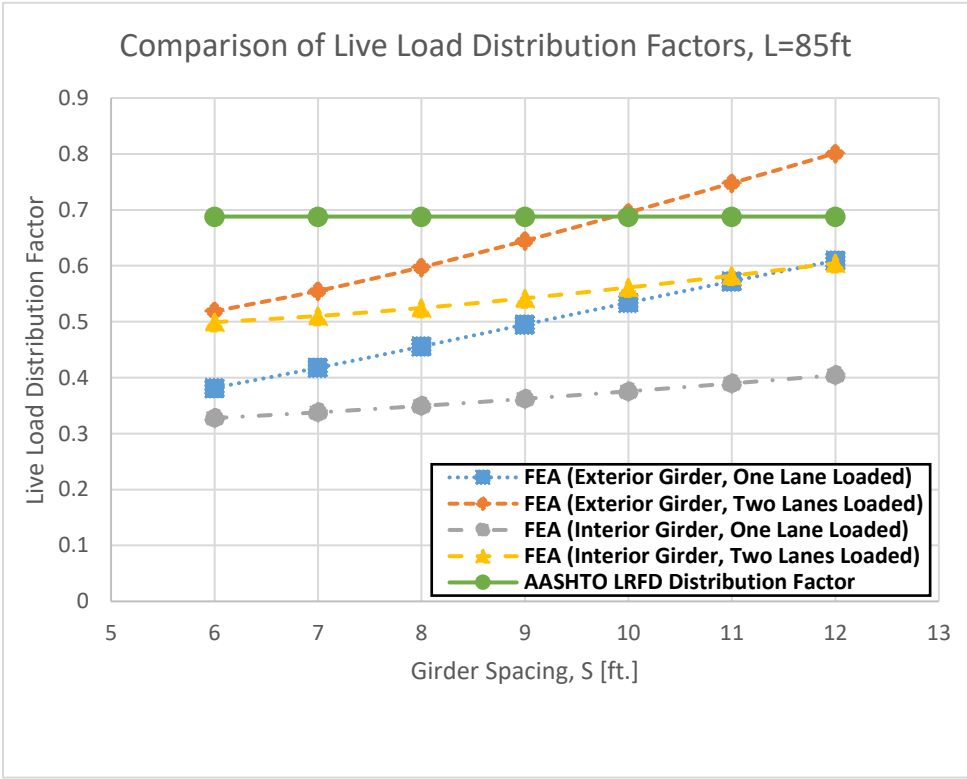
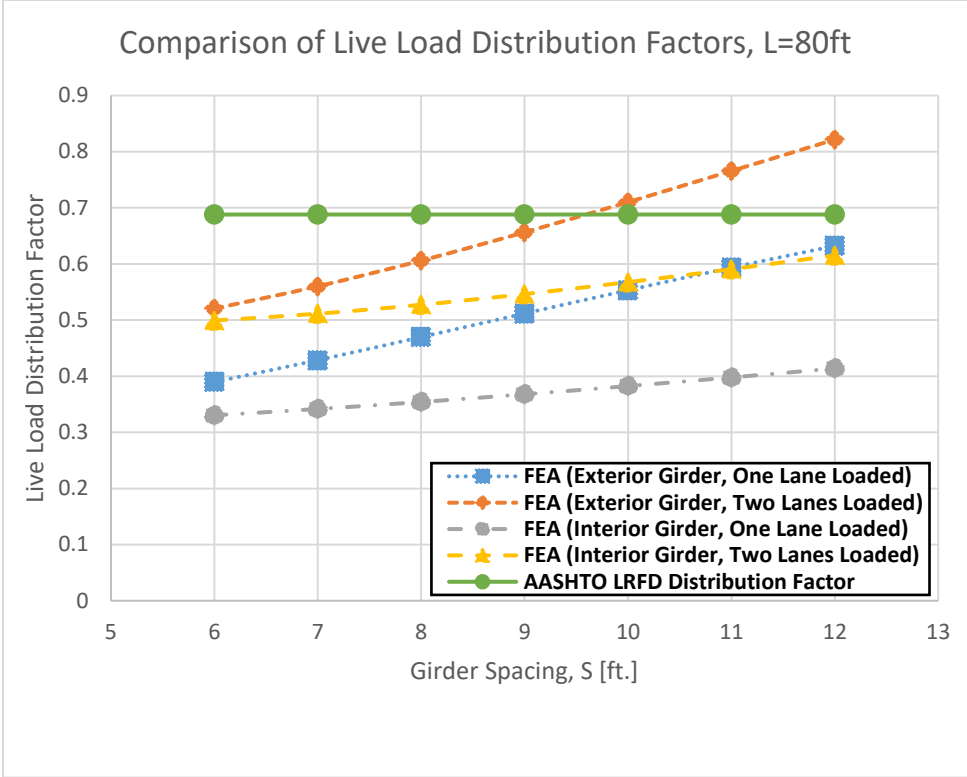


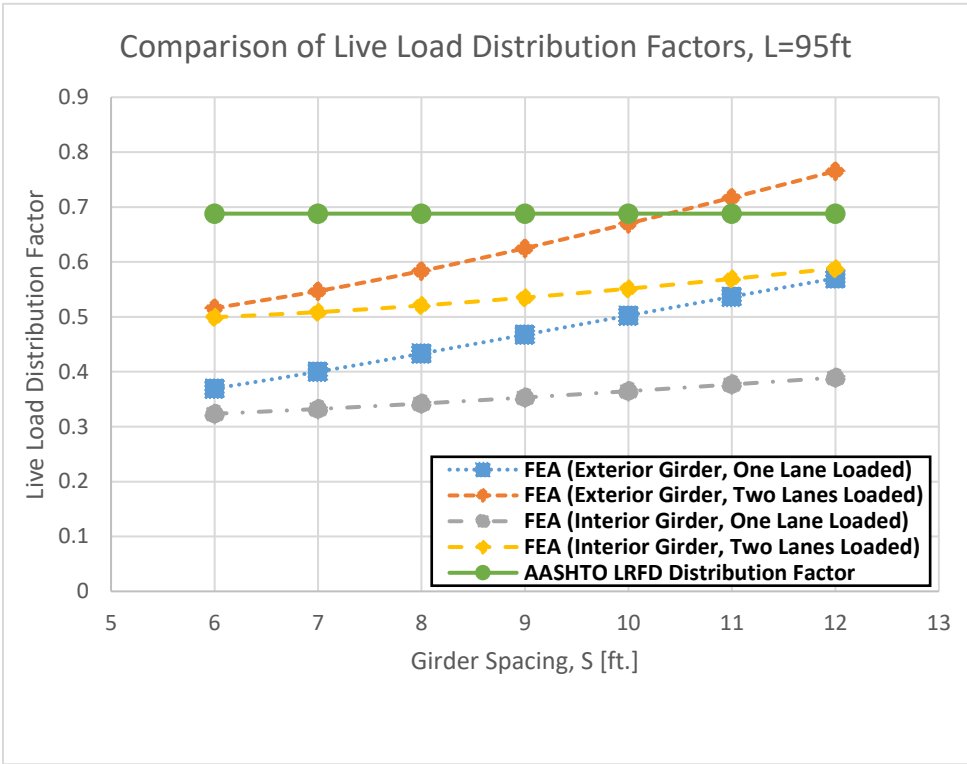
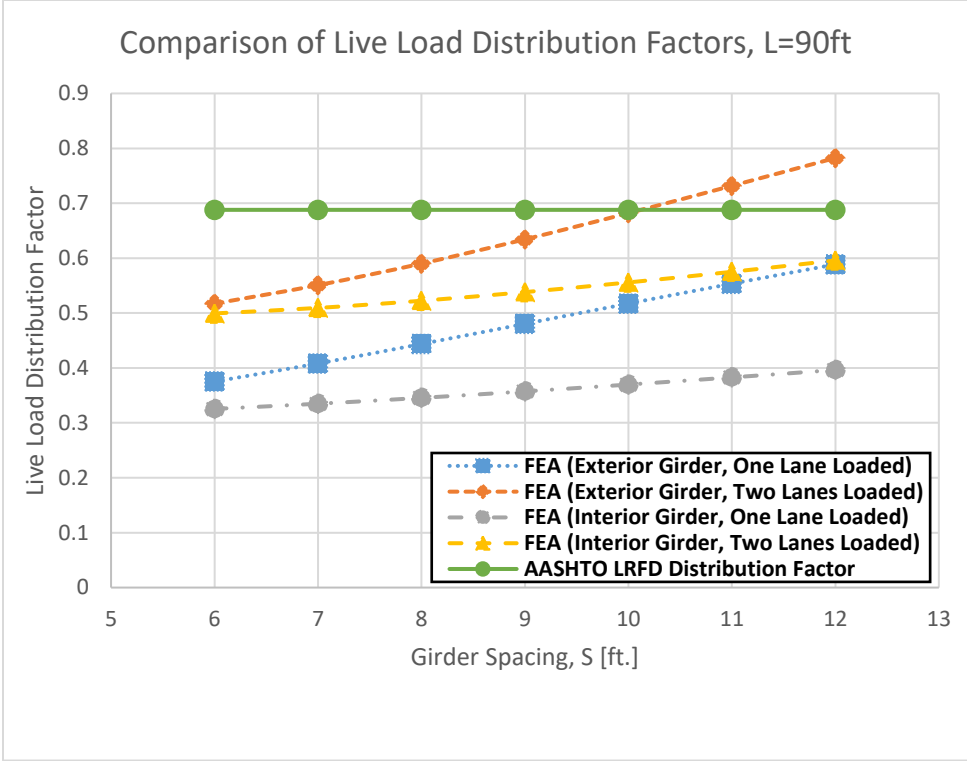












Comparison of Live Load Distribution Factors, L=100ft

